INVESTIGATION OF BEHAVIOUR OF RUBBERISED CONCRETE

A thesis Submitted

in partial fulfilment of the requirements for the award of the degree of

DOCTOR OF PHILOSOPHY

in

CIVIL ENGINEERING

by

RAHUL KUMAR

(En. No. - 2K17/PhD/CE/03)

Under the supervision of

Prof. NIRENDRA DEV

DEPARTMENT OF CIVIL ENGINEERING

DELHI TECHNOLOGICAL UNIVERSITY

SHAHBAD DAULATPUR, BAWANA ROAD, DELHI - 110042 (INDIA).

2024

DELHI TECHNOLOGICAL UNIVERSITY
(Formerly Delhi College of Engineering, Since 1941)
Shahbad Daulatpur, bawana road, Delhi- 110042

DECLARATION

I hereby declare that the research work presented in this thesis entitled "Investigation of Behaviour of Rubberised Concrete" is original and carried out by me under the supervision of Prof. Nirendra Dev, Professor, Department of Civil Engineering, Delhi Technological University, Delhi, and being submitted for the award of PhD degree to Delhi Technological University, Delhi, India. The content of this thesis has not been submitted either in part or whole to any other university or institute for the award of any degree or diploma.

Date: 10/01/2024 (Rahul Kumar)
Place: DTU, Delhi. En. No. – 2K17/PhD/CE/03

DELHI TECHNOLOGICAL UNIVERSITY
(Formerly Delhi College of Engineering, Since 1941)
Shahbad Daulatpur, bawana road, Delhi- 110042

Date: - 10/01/2024

CERTIFICATE

This is to certify that the PhD thesis entitled "Investigation of Behaviour of Rubberised Concrete" is being submitted by Mr Rahul Kumar for the fulfilment of the requirements for the award of the degree of Doctor of Philosophy in Civil Engineering to the Department of Civil Engineering, Delhi Technological University, Delhi, India, is a bonafide record of original research work carried out by him under my guidance and supervision. The results embodied in this thesis have not been submitted to any other university or institution for the award of any degree or diploma.

Prof. Nirendra Dev
Supervisor
Department of Civil Engineering
Delhi Technological University
Delhi – 110042.

ACKNOWLEDGEMENTS

I would like to express my appreciation to the people who have helped me most during my research work. First and foremost, I am deeply grateful to my research supervisor, Prof. Nirendra Dev, for his nonstop guidance, enduring patience, and nurturing support throughout this research, without which successful completion would not have been possible. It has been an honour to be associated with such a great supervisor and learn from his experience.

I want to extend special thanks to the immense contribution made by my family, especially my father, Late Sh. Sher Singh encouraged and supported me, stood by me like a pillar, and gave me constant motivation. All my family members have shown enormous patience during this process and have cheerfully sacrificed the time that rightfully belonged to them. Finally, I extend a profound expression of respect to all elders in the family and especially my parents, who have always showered me with their blessings and made me who I am today.

I accord my heartfelt thanks to Dr Manvendra Verma, assistant professor in the civil engineering department, GLA University, Mathura, U.P who was a source of inspiration for me to take up this research work. At the time of my research work, he was my senior at DTU, Delhi. It would not have been possible without the support of central instrumentation facilities laboratory technicians; I am thankful to them.

I am grateful to Prof. Archana Rani (Chemical Engg. Department, DTU), assistant professor Dr Ritu Raj, assistant professor in DTU and Dr Ibadur Rehman assistant professor in JMI and my colleagues Meghali Deka, Geeta Devi, Dinesh Reddy, Rahul Meena, Abhishek Paswan, Nitin Lamba, Rajat Gautam, Lakhan Kumar, Dr Mrityunjay Kumar Singh for providing me critical comments and suggestions and all those who interacted and exchanged ideas with me in completing the research.

LIST OF PUBLICATIONS

1. Rahul Kumar; Nirendra Dev, "Mechanical and Microstructural Properties of Rubberized Concrete After Surface Modification of Waste Tire Rubber Crumb", Arabian Journal for Science and Engineering. Springer International Publishing 47, 4571–4587 (2022). Impact Factor: 2.807
2. Rahul Kumar; Nirendra Dev, "Assessment of Mechanical and Impact Resistance Properties of Rubberized Concrete After Surface Modification of Rubber Crumb", Iranian Journal of Science and Technology – Transactions of Civil Engineering. Springer International Publishing. vol. 46, no. 4, pp. 2855–2871, Aug. 2022. Impact Factor: 1.461
3. Rahul Kumar; Nirendra Dev, "Effect of acids and freeze-thaw on the durability of modified rubberized concrete with optimum rubber crumb content", Journal of Applied Polymer Science. Wiley Online Library. 139, 52191 (2022). Impact Factor: 3.057
4. Rahul Kumar; Nirendra Dev; Manvendra Verma; Nitin Lamba, "Influence of chloride and sulfate solution on the long-term durability of modified rubberized concrete", Journal of Applied Polymer Science. Wiley Online Library, vol. 139, no. 37, pp. 1–15, Oct. 2022. Impact Factor: 3.057.
5. Rahul Kumar; Nirendra Dev; Shobha Ram; Manvendra Verma, “Investigation of dry-wet cycles effect on the durability of modified rubberised concrete” Forces in Mechanics. Elsevier, 2023.DOI: https://doi.org/10.1016/j.finmec.2023.100168

LIST OF CONFERENCES

1. Assessment of the effect of superplasticizer on the different type of cement-based on marsh cone test, “6th International Conference on Advanced Production and Industrial Engineering (ICAPIE) – 2021”, June 2021
2. Effect of waste tire rubber in the concrete matrix: A Review,” 7th International Conference on Recent Trends in Engineering & Technology (ICRTET 2021)”, November 2021

3. Investigation of fresh, mechanical, and impact resistance properties of rubberised concrete, “International E-Conference on Sustainable Development and Recent Trends in Civil Engineering (ICSDRT-2022)”, January 2022
4. Evaluation of the Effect of Polycarboxylate Superplasticizer on the Different Types of Cement by Marsh Cone Test, "3rd International Conference on Futuristic and Sustainable Aspects in Engineering and Technology (FSAET-2022)” November 2022.

ABSTRACT

High impact resistance and energy-absorbing capability are beneficial properties of rubberised concrete. Rubberised concrete is highly effective in areas where more flexibility is required. Rubberised concrete has greater flexibility, impact resistance, and lower unit weight compared to conventional concrete. In this study, sulfuric acid is used in the surface treatment process of rubber particles to strengthen the bonding property of rubber particles and cement paste. Six waste tire rubber crumb contents (0, 10, 15, 20, 25, and 30%) and particle sizes of 0.6-2.36 mm were used to replace fine aggregate in concrete partially. Microstructural analyses (EDX, TGA, XRD) are conducted on rubber crumbs to examine rubber's compatibility before using it in concrete. The fresh, hardened, microstructural properties (SEM and XRD), stress vs strain behaviour, pull-off strength, impact-resistant, ultrasonic pulse velocity, and electrical resistivity of rubberised concrete are investigated. The durability properties (water absorption, acid attack resistance, and freeze-thaw attack resistance) are evaluated on the optimum mix of rubberised concrete.

The mechanical properties of rubberised concrete reduce by increasing the rubber crumb in the mix; still, the mechanical properties of 90 days of water-cured concrete increase compared to 28 days of water-cured concrete. The results are not much troubling up to 15% replacement level of rubber crumb, and the rubberised concrete has a highly deformable capacity than conventional concrete. The SEM image analysed that the surface treatment technique improves the bonding properties of rubber particles and cement paste compared to untreated rubber particles. Impact resistance and energy absorption capacity of rubberised concrete are increased by 33.33% and 10% up to 15% replacement of rubber crumb. Two correlation equations have been established between the split tensile and compressive strength and flexural and compressive strength of concrete: $f_{st}=0.776\ f_c^{0.39}$ and $f_{fs}=0.652\ f_c^{0.5}$, respectively. The results are not much troubling up to 15% replacement level of rubber crumb. The optimum dosage of rubber crumbs to replace fine aggregates is found to be 15% without significant losses in the properties of rubberised concrete. Structural analyses show that the specimens remain in the crystalline phase after being submerged in H_2SO_4 and HCl acid. When rubberised concrete is immersed in H_2SO_4 and HCl solution with equal concentrations and duration,

specimens immersed in HCl solution have been found to have less surface erosion, less weight loss, and lower compressive strength loss. When the conventional concrete mix is immersed in H_2SO_4 and HCl solution, the losses in compressive strength are 74.56% and 30.34%, but in rubberised concrete, the losses are 60.01% and 24.22% only. No apparent microcracks and no spalling on the surfaces of the specimens are found up to 90 freeze-thaw cycles. Rubberised concrete's ultrasonic velocity decreases slightly up to 90 freeze-thaw cycles, but it still has good concrete quality. Overall, the rubberised concrete is durable, with enough capacity to absorb the impact energy, and has a higher deformable capacity than conventional concrete.

ABBREVIATIONS

RuC	Rubberised Concrete
NaOH	Sodium hydroxide
FA	Fine aggregate
CA	Coarse aggregate
RC	Rubber crumbs
XRD	X-ray diffraction
SEM	Scanning electronic microscope
EDX	Energy-dispersive X-ray spectroscopy
OPC	Ordinary Portland cement
PCE	Poly-carboxylate ether
C-S-H	Calcium silicate hydrate
UPV	Ultrasonic pulse velocity
ASTM	American standard testing materials
IS	Indian Standard
TGA	Thermogravimetric analysis
DTG	Derivative thermogravimetry
UTM	Universal Testing Machine
CTM	Compression Testing Machine

TABLE OF CONTENTS

LIST OF FIGURES

LIST OF TABLES

CHAPTER 1 INTRODUCTION

1.1 Overview

Due to the worldwide increase in vehicles, waste tire disposal has raised serious pollution concerns. India produces 6% of the world's annual waste tyre production of 1.5 billion or more [1]. Every year, between 1 billion and 1.8 billion used tyres are disposed of as waste across the world [2]. A billion or more waste tyres are produced each year, in addition to the more than 1.6 billion new tyres that are produced annually [3]. Two significant aspects that result in tires being a challenging waste source are the large production volume and material durability. A tire decomposes very slowly and can remain in a landfill for up to 100 years. The thermoset properties of tires allow them to resist high temperatures and resist melting; therefore, tires do not separate into their chemical components. Both rubber and plastic are non-biodegradable materials that accumulate and disrupt the surrounding environment. Over the years, the disposal of waste tires increasing the issue continuously for the environment. Waste rubber tires have little scope of being recycled and mostly form a landfill and degrade the environment. There is an excellent potential for the rubber to be used in concrete, thus saving the area from becoming a landfill, which means eco-friendly. Rubber is more flexible and has a lower unit weight than natural rock aggregate; thus, making RuC (Rubberised concrete) with better impact resistance and energy absorption capacity than standard concrete would be advantageous. The rubber crumb and powder rubber results are economical and environmentally friendly to alternative aggregates with higher ductility [4]. The RuC can be used to design earthquake shock-wave absorbers, machinery base foundations, roadway pavement, and airport runways because it has a highly deformable capacity [5]. Under multiple ground motion excitations, reinforced concrete's seismic response is enhanced with different high-strength RuC mixes [6]. Due to the ability to absorb impacts, RuC has a better energy absorption capacity than standard concrete [7]. When used in small amounts, the rubber crumb improves ductility and energy absorption, enhancing the toughness of concrete while having only minor effects on its strength [8]. RuC would thus be beneficial from a recycling point of view and in situations where

greater flexibility is required because it has higher ductility and energy absorption capacity than standard concrete.

Fig. 1.1 Waster rubber tyres [9–11]

The adhesive property of rubber particles and cement paste is the main issue, and another is the strength decrement in rubberised concrete. These are the gaps that this research is attempting to solve. According to previous research, the addition of rubber aggregate proportion and size in concrete increases the microcrack width of RuC [12]. The surface modification of rubber crumbs can improve the adhesion property between cement paste and rubber particles. The compressive strength of RuC after treatment with sodium hydroxide is slightly enhanced compared with ordinary concrete [13]. Mohamed K. Ismail et al. (2018) investigate the fresh and hardened properties of self-consolidating RuC using waste rubber crumb and powder rubber as a partial replacement for sand and supplementary cementing materials. The rubber crumb and powder rubber results are economical and environmentally friendly to alternative aggregates with higher ductility. The inclusion of powder rubber in concrete shows better performance of fresh and mechanical properties of RuC than the inclusion of rubber crumbs [4]. The five methods (cement coating, silica coating on rubber particles, and the other three processes are,

soaking rubber crumbs in NaOH, $KMnO_4$, and H_2SO_4 solutions) enhance the strength of RuC compared to RuC without surface treatment of rubber. The silica fume coating and 10% H_2SO_4 solution treatments give the best result for improving the strength of RuC [14].

According to Trilok Gupta (2018), the compressive strength and MOE are decreased with increasing rubber fibre quantity. The RuC can be used to design earthquake shock-wave absorbers, machinery base foundations, roadway pavement, and airport runways because it has a highly deformable capacity [5]. The flexural strength of RuC decreases with increasing the quantity of rubber ash but increases with the increasing content of rubber fibre. "The reduction in static and dynamic modulus of elasticity indicates higher flexibility, which can be viewed as a positive gain in rubberised concrete mixtures"[15]. For the treatment process, Liang He et al. (2016) investigated after oxidizing the rubber crumb with $KMnO_4$ solution, then sulfonated with $NaHSO_3$ solution, and used the FT-IR for oxidation and sulphonation progression, presenting a large amount of hydroxyl and sulfonate to rubber crumbs. The bonding property of rubber and cement is enhanced by 41.1% after the surface treatment and concluded that the treatment of rubber crumb with $KMnO_4$ and $NaHSO_3$ improves the bonding property with the cement matrix [16]. According to Samar Raffoul et al. (2016), after the surface treatment of rubber crumbs by silica fume, RuC was compared with control concrete and found that rubber with silica fume's surface treatment did not affect RuC's bonding properties. The surface treatment of rubber crumbs can enhance the bonding properties of rubber particles with cement by NaOH [17–21].

RuC would thus be beneficial in situations where greater flexibility is required. Under multiple ground motion excitations, reinforced concrete's seismic response is enhanced with different high-strength RuC mixes [6]. Due to the ability to absorb impacts, RuC has a better energy absorption capacity than standard concrete [7]. When used in small amounts, the rubber crumb improves ductility and energy absorption, enhancing the toughness of concrete while having only minor effects on its strength [8]. The better results in terms of fracture toughness and energy absorption came from pre-coating the rubber with mortar, demonstrating a strong consensus between conclusions drawn at both micro and macro levels [22].

The compressive strength of the RuC is slightly decreased as the percentage of tire rubber particles replaced increased, but there are substantial improvements in impact resistance and fracture toughness [23]. Waste tire rubber fibre can be used to increase the impact resistance and ductility of concrete as a recycled material [24]. Crumb rubber as an FA reduces the concrete's compressive strength and abrasion resistance while greatly increasing its energy-absorbing capacity [25]. The rubber substitution in concrete increases the damping potential and ductile performance and improves the energy absorption of self-compacting RuC compared to normal self-compacting concrete [26]. RuC provides softness to the surface and performs well in abrasion and skid resistance tests; RuC is also useful for producing concrete blocks [27]. The use of rubber shreds in concrete increased the resistance to acid attack but reduced the RuC's compressive strength [28].

1.2 Gaps Found Through Literature Review

- Study on the rubber-cement bonding mechanism to improve the bonding property and increase the strength of the rubberised concrete.
- As the consequences of the surface treatment of rubber crumbs by acid, the durability of rubberised concrete needs to be studied.

1.3 The Objectives of the Research

Following a review of the literature on RuC, we came to the following objectives of the PhD research project:

- To determine the effect of sulphuric acid treatment on rubber particles to improve the adhesion properties between cement and rubber and to study the durability of rubberised concrete due to acid treatment of rubber particles.
- To study the effect of different replacement levels of fine aggregate by rubber particles in rubberised concrete.
- To study the lateral and axial deformation measurement of rubberised concrete.
- To study the energy absorption capacity of rubberised concrete.

1.4 Scope of Work

Making RuC is a good idea because it has a good capability of absorbing impact energy to be used as an energy dissipater. Concrete deformability and ductility might be improved by using recycled RC.

The RuC can be used in Highway barriers, Railway buffers, Pipe bedding, Curbstone, Manholes, Highway Pavements, Runways for the airport, and Harbour structures.

The following applications for the RuC were determined by the author following the experimental research:

- Smart structures
- For residential and commercial buildings
- Pavements

1.5 Thesis Arrangement

Chapter 1 provides a broad overview of the study work area in terms of its purpose and scope. At the beginning of the introduction, generalized data is available about the research area with the usage of the raw materials in the production. It also defined the complete methodology used in this research work.

Chapter 2 offers an extensive and thorough literature review of the RuC research project. This chapter is divided into 2 parts, first section lists a set of papers and in second section a critical analysis of all articles in which multiple properties of RuC are considered.

Chapter 3 discusses the materials utilised in the RuC mix design, including their specific characteristics and testing programme. The test performed on the materials to assess their quality is also explained. It also described the entire experimental setup description of the samples, as well as the operating descriptions of the equipment in accordance with the standard codes.

Chapter 4 provides the results and discussion parts of several experimental investigations on specimens on all RuC mixtures. The mix design of the RuC varies on several parameters to get the optimum point of strength. After the optimum strength mix design, the durability test on the mix design specimens in various test setups is water absorption, acid attack, electrical resistivity, and freeze-thaw conditions.

Chapter 5 discusses regression analysis of experimental data to produce correlation equations between mechanical properties and compares them to other equations given by standard codes and other authors in various countries.

Chapter 6 describes the conclusions of the study of the RuC.

1.6 Methodology

In order to answer the research questions, the procedure followed during the research presented in this thesis can be summarised as follows:

- Reviewed previous studies on RuC to find research gaps in RuC by using rubber crumbs as supplementary material of fine aggregate in concrete.
- Carried out experimental tests on all materials to check the feasibility of materials for use in concrete.
- Studied the bonding properties between rubber crumbs and concrete and assessed the effect of sulphuric acid treatment on rubber particles to improve the adhesion properties between cement and rubber and the mechanical properties of RuC. Surface treatment was done to reduce the hydrophobic nature of rubber crumbs. The detailed surface treatment process is explained in the experimental chapter.
- Various tests are performed to find the concrete hardened properties, such as compressive strength, split tensile strength, workability, density, Poisson's ratio, MOE (modulus of elasticity) and flexural strength after partial replacement of fine aggregate with rubber crumbs and surface treatment of rubber crumbs. SEM (Scanning electron microscope) analysis and pull-off strength tests are done to evaluate the bonding between the concrete matrix and the rubber particle.
- Studied the energy absorption capacity of RuC by impact tests to investigate its utility and importance in structural members.
- Studied the durability properties (water absorption, acid attack, electrical resistivity and freeze-thaw) of RuC due to acid treatment of rubber particles. The optimum mix for RuC is obtained after analyzing the results of the fresh and mechanical properties of all RuC mixes. This is the control sample of the study.
- Further tests for durability are conducted on the optimum mix of RuC and compared with standard concrete. On the other hand, exposure to two distinct kinds of acids, sulfuric and hydrochloric acid, is used to test the acid attack

resistance of RuC. For a 30-day exposure time, visual appearance, differences in weight, and compressive strength of conventional and RuC are recorded and compared with other studies. Apart from that, the resistance to freeze-thaw of RuC is tested by visual appearance, UPVT, differences in weight, and compressive strength test at the interval of 15 cycles.

- After thorough research, the fresh, hardened and durability results are compared to and validated on behalf of earlier literature on RuC investigations without chemical treatment to determine the effect of sulphuric acid treatment on rubber particles and the adhesion properties between cement and rubber crumbs and to meet the objective of this thesis. Moreover, the control sample is also compared with standard concrete to check the chances of the fresh, hardened and durability properties of RuC. On the basis of that, conclusions were made.

Fig. 1.2 shows the flow chart for the methodology utilized in this investigation.

1.6.1 Flow chart of work

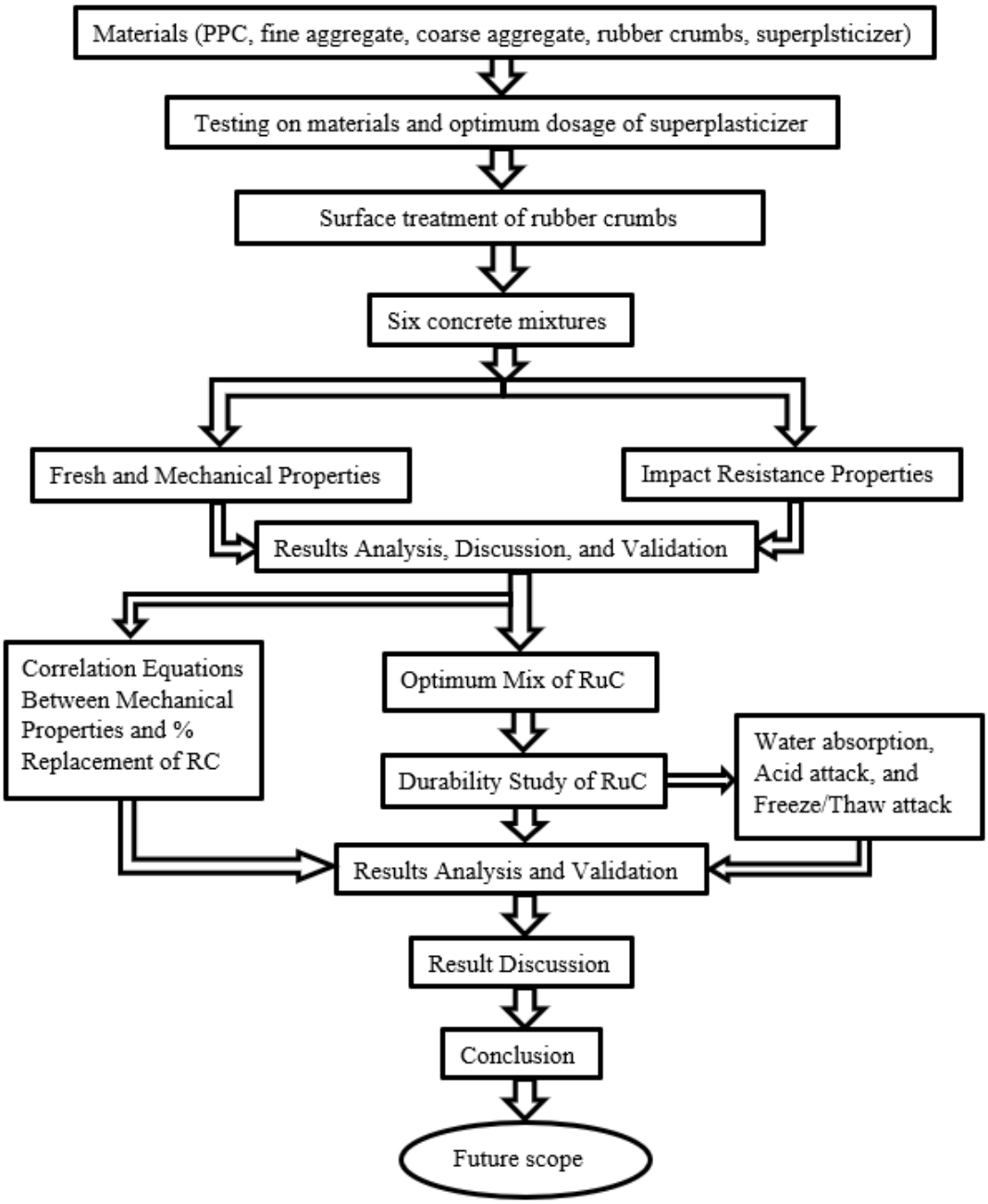

Fig. 1.2 Flow chart of the methodology used in this study

CHAPTER 2 LITERATURE REVIEW

This chapter aims to review the existing knowledge in the literature that relates to the topic of this study. A brief description is presented in addition to some key points that govern concrete properties and behaviour to show a fundamental understanding of the technology of concrete. This chapter presents a comprehensive review of RuC to highlight the main advantages of this material alongside its drawbacks. Due to the differences in the physical properties of the rubber and mineral aggregates, controversial and sometimes contradictory findings have been observed in reviewed literature that relates to RuC. In order to find a solid base of information on materials, fresh, hardened and durability properties in addition to the freeze-thaw and acid attack resistance properties, this section was divided as follows.

a) Deep literature review with the key findings
b) Critical analysis of the literature review

2.1 Deep literature review with the key findings

2.1.1 Effect of replacement level, size and surface modification of rubber crumbs in RuC

1. **(Ayub et al., 2022)** worked on self-compacting rubberised concrete (SCRC) using waste materials such as fly ash, retarded tyres, and polyethene terephthalate (PET) drinking bottles as fibres. The mechanical characteristics of 10 different combinations combining tyre rubber and PET fibres were studied. In SCRC, 35% cement is replaced by fly ash by mass and 0, 5, 10, 15, and 20% FA is replaced by tyre rubber by mass in five mixes. The rest of the five SCRC mixes comprised a fixed 2% volume proportion of PET fibres by concrete volume. The results showed that substituting 15% mass of FA with tyre rubber is optimum without compromising the concrete's strength. Concrete compression and flexure performance were increased using tyre rubber as FA and PET fibres as reinforcement [29].
2. **(Gupta et al., 2021a)** investigates the suitability of utilising rubber tyre particles in concrete as FA. In series I, FA was replaced with rubber ash (by volume of 5%, 10%, 15%, and 20%); however, in series II, rubber fibre was introduced as a replacement for FA (by volume of 5%, 10%, 15%, 20% and 25%) and the quantity of rubber ash

was kept constant at 10%. Mechanical properties, impact resistance, fatigue resistance, water penetration, and shrinkage strain were all tested on the RuC mixtures. It was discovered that adding rubber ash to concrete improves the impact resistance and slightly reduces the mechanical properties of RuC [30].

3. **(Habib et al., 2021)** studies the seismic response of reinforced concrete buildings with various high-strength RuC mixes through a variety of ground motion excitations. They concluded that the seismic performance of the structure was significantly enhanced by the use of RuC jacketing. The use of high-strengths RuC instead of the control material enhanced the damping capacity and slightly lowered the structure's base shear forces [6].
4. **(Karunarathna et al., 2021)** uses a variety of design combinations that include low-level rubber aggregate replacements of FA from tyres rubber. The influence of the size of coarse (15 mm tyre shreds) and small (2-4 mm tyre crumbs) rubber aggregates on the fresh and mechanical characteristics of concrete, particularly its fracture characteristics, was examined. The rubber substitutes in concrete had crack-bridging effects. The results show that adding rubber aggregates at low percentages enhances the ductility, energy absorption capacity, and toughness of concrete while having only a minor negative influence on its strength and other parameters. Overall the modified RuC might be used in earthquake-resistant structural components, integrated bridges, or impact-resistant road barriers [8].
5. **(Khelaifa et al., 2021)** studied the mechanical characteristics of compacted sand concrete after the partial substitution of dune sand with rubber particles. To improve the mechanical properties of compacted sand concrete containing rubber aggregates, four volumetric replacements of sand (10, 30, 40, and 50%) and four compaction energies were utilised. Rubber aggregates reduce the concrete's mechanical properties in the mixtures. They suggested that by increasing the compaction energy, this reduction in mechanical properties might be mitigated [31].
6. The impact of rubber crumb and polyvinyl alcohol fibre (PVA) on the deformation parameters of rubberised engineered cementitious composites (R-ECCs), including drying shrinkage, elastic modulus, and Poisson's ratio, are studied by **(Mohammed et al., 2021)**. The quantity of crumb rubber replacement to FA by volume of 0–5% and PVA fibres from 0 to 2% by volume of cementitious materials were taken into consideration while producing R-ECC mixes. According to experimental results,

rubber crumb reduces the compressive strength and elastic modulus of ECC. The addition of rubber crumbs resulted in a considerable increase in Poisson's ratio and drying shrinkage. According to numerical optimisations, the optimal combination was achieved by mixing 1.92 % crumb rubber with 1.86 % PVA fibres [32].

7. **(Islam et al., 2021)** examines the durability of RuC with various levels of rubber aggregate (RA) (0-30%). They evaluated rubber particle size, quantity, replacement type in RuC, and exposure environments of RuC. In different exposure situations, the slump value, mechanical properties, chloride ion penetration, and water absorption of RuC were investigated. The results show that smaller rubber particles have higher adhesion to cement particles and higher strength than rubber particles. Finer RA included concrete had much-improved durability under continuous wet-dry cycles and chloride ion solution. RuC's porosity rises as RA's amount and particle size increase [33].
8. **(Amiri et al., 2021)** investigated the effects of replacing coarse aggregate with recycled concrete aggregate (RCA) and cement with waste rubber powder (WRP) on concrete's durability and mechanical properties. Coarse aggregate was replaced with 25% and 50% RCA and cement was replaced with WRP 2.5% and 5% by weight of cement to prepare RuC specimens. It was discovered that rising the amounts of RCA and WRP in concrete lowers its mechanical properties. The rate of chloride ion migration in concrete is reduced by raising WRP due to the blocking of micropore connections in the case of durability [34].
9. **(He et al., 2021)** investigated the surface modification of rubber crumbs with different approaches. Contact angle and infrared spectroscopy were used to investigate the surface characteristics of rubber treated with sodium hydroxide, sulfonation, and urea. The modified RuC's mechanical and impact resistance were evaluated and correlated by Scanning electron microscopy (SEM) image investigation. The findings indicate that the rubber crumb modification can increase rubber crumb and cement paste bonding and interaction. The compressive strength of sodium hydroxide-treated RuC was marginally enhanced compared to conventional RuC, while its flexural strength, tensile splitting strength, and impact resistance improved significantly [13].
10. **(Wu et al., 2020)** casted RuC specimens after replacing natural coarse aggregate (NCA) with 0-100% chipped tyre rubber. Before demolding, the RuC was

compressed in a specifically built mould to compress the wet concrete volume for some time. The compressed and uncompressed RuC's stress-strain behaviour was examined and compared to NAC specimens. The results indicate that compressed RuC specimens have greater compressive strength and elastic modulus than uncompressed RuC specimens. In comparison to NAC specimens, compressed RuC specimens with a 20% replacement of chipped rubber exhibit a 35% and 29% improvement in strength and elastic modulus. The suggested technology supports the use of waste tyre rubber in concrete and is simple to implement in the precast sector for the production of concrete components [35].

11. **(Nematzadeh et al., 2020)** investigated the axial compressive behaviour of steel fibre and tyre rubber particles in short concrete-filled steel tube (CFST) columns subjected to extreme temperatures. Tyre rubber particles were added as FA in 5% and 10% replacement ratios to the concrete core, while steel fibres were added in two-volume fractions of 1% and 1.5%. Axial compression tests were performed after CFST columns were subjected to temperatures of 20, 250, 500, and 750°C. The findings of the experimental tests indicate that increasing the exposed temperature to 500°C has no effect on the compressive strength of CFST columns; however, increasing the temperature to 750°C causes a considerable drop (34%) in the compressive strength of the CFST columns [36]**.**
12. According to **(Luo et al., 2020),** the addition of rubber crumb in concrete has two major effects: decreased mechanical strength and increased durability. Steel fibres were added to the concrete to improve the mechanical characteristics of RuC. Steel fibre reinforced RuC was examined for mechanical characteristics, mass loss rate, and dynamic elastic modulus after being exposed to cyclic freezing and thawing. When there were no freeze-thaw effects, adding 2.0% steel fibres increased the compressive strength of RuC by 26.6%, but when there was cyclic freeze-thaw, the compressive strength of RuC was enhanced. Steel fibres have a beneficial influence on mass loss but an adverse influence on dynamic elastic modulus [37].
13. According to **(Chaikaew et al., 2019),** short steel fibres were added to improve the mechanical characteristics of RuC pedestrian blocks. At 0.5 and 1.0% by volume fractions, two hooked end steel fibres with 35 and 65 mm lengths were mixed in RuC. The concrete blocks were tested for density, water absorption, slip resistance, flexural load resistance, and field abrasion resistance. With increasing fibre content,

toughness and abrasion resistance improved considerably. However, the slip resistance was unaffected by the inclusion of fibres [38].

14. **(Gregori et al., 2019)** evaluated the impact of partial substitution of natural FA with tyre rubber on RuC compressive strength. FA, CA, and both aggregate (FA and CA) are simultaneously replaced by percentages of rubber aggregate from 0% to 100%. Many research was taken into account, with around 1,500 tests from various authors, including the current one. On the basis of this vast data set, new analytical equations are established and proposed for analysing the concrete strength decrease factor [39].
15. **(Wang et al., 2019)** study the potential of turning waste tyre rubber aggregates into the RuC. The concrete's mechanical and durability properties are affected by the performance of the ITZ (interface transition zone). The ITZ of conventional and rubber aggregate cement pastes was investigated in terms of rubber particle size and replacement percentage by volume. The ITZ between conventional aggregate and cement paste and rubber crumb and cement paste revealed similar crack width patterns, according to the findings. RuC's ITZ micro-crack structure was enhanced by adding 50–90 mesh rubber powder. The microcrack width of ITZ increased as the rubber content, and particle size increased [12].

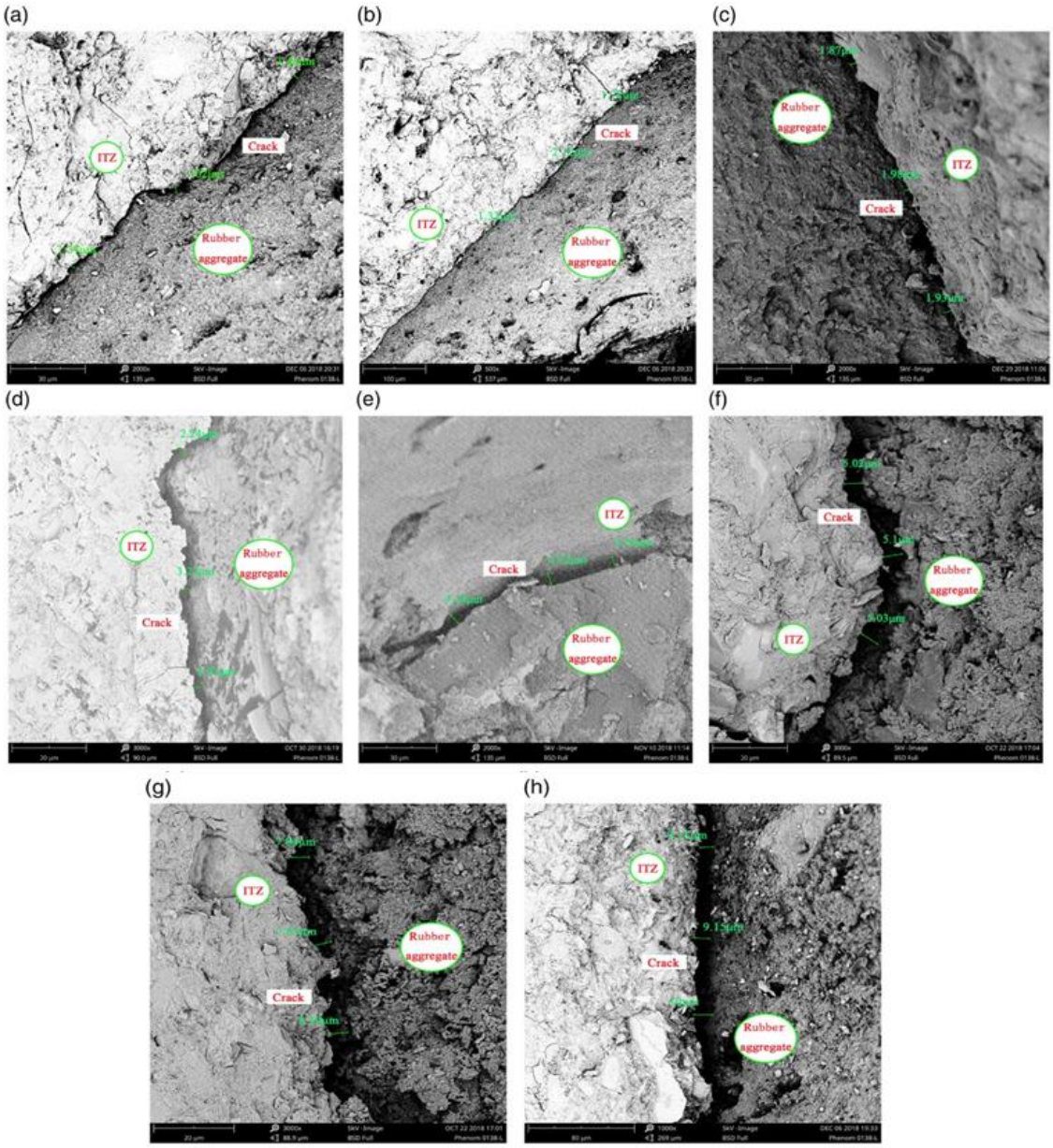

Fig. 2.1 SEM analysis of ITZ between the rubber and cement paste [12]

16. **(Murali et al., 2019)** studied the fibre-reinforced grouted aggregate rubberised concrete (FRGARC) impact strength after replacing the FA 5%, 10%, 15%, 20%, 25% and 30% with rubber crumb and hooked-end steel fibres of 0.5% volume of concrete at three different water/cement ratios (0.45, 0.50 and 0.55). The rubber crumb's surfaces are treated with 10% NaOH solution for 30 minutes to enhance the mechanical properties of RuC. FRGARC's density reduction factor, compressive strength (CS), and the number of impacts that caused a first fracture and failure were investigated. With increasing rubber content, FRGARC shows a decrease in CS and contributes considerably to the improvement of energy absorption capacity [7].

17. **(Fu et al., 2019)** studied the mechanical and toughness properties of steel fibre-reinforced rubberised concrete (FR-RC) after adding the different fibre dosages and replacement of FA with rubber crumb. Both four-point bending and three-point bending of beams were used to examine the toughness of FR- RC. The findings reveal that the rubber content and fibre dosage influence the compressive strength of FR-RC. However, the modulus of elasticity of FR-RC can be increased marginally using steel fibre [40].
18. **(Aslani and Gedeon, 2019)** added waste tyre rubber aggregate, polypropylene (PP) fibres and steel fibres into the concrete mix to make self-compacting RuC. Crumb rubber diameters of 2–5 mm were used to replace 20% of FA. Steel fibres 0.25, 0.5, 0.75, and 1% are used whereas PP fibres 0.1, 0.15, 0.2, and 0.25% are used by the total volume of the concrete. The findings show that the rheological properties of the self-compacting RuC are negatively impacted when a more quantity of fibre is added. Steel fibres have a substantially greater negative impact on the rheological characteristics of self-compacting RuC than PP fibres. Because a larger proportion of PP fibre was added to the RuC, the compressive strength of the RuC was decreased [41].
19. **(Gurunandan et al., 2019)** investigates the mechanical, ductility and damping characteristics of RuC by using shredded waste rubber as a partial substitute for FA by mass in concrete. Reusing discarded rubber and polymeric fibre reduces the mechanical properties of RuC; however, both enhance the ductility and damping ratio of RuC. The reduction in strength percentage is within permissible limits in both "plain rubberised" and "fibre-reinforced rubberised concrete" at a maximum of 7.5% replacement level of rubber aggregate. Both RuC's damping ratios were enhanced so both can be used as vibration absorbers and may be used in road curbs and barriers, paving blocks and machine foundations structures [42].
20. **(Ismail et al., 2018)** investigate the fresh and hardened properties of self-consolidating RuC after using supplementary cementing materials such as fly ash, ground-granulated blast-furnace slag, silica fume, metakaolin, and percentage replacement of rubber (0–50%), with different rubber sizes. According to the findings, both crumb rubber (CR) and powder rubber (PR) have the potential to be more cost-effective and ecologically friendly alternatives for developing ductile self-consolidating RuC. The CR had a detrimental impact on RuC's fresh and mechanical

characteristics. The compressive strength of RuC for M40 grade can be achieved by 30% CR replacement. PR had greater fresh and mechanical performance than CR, allowing up to 40% rubber replacement to be utilised safely [4].

21. **(Zhu et al., 2018)** investigate the "floating problem" of rubber crumb particles in RuC through several experiments. The results reveal that when the slump test value of concrete is low, the floating rubber particles are not visible. The floating effect is more noticeable when the slump value is high and continues to increase. The floating of rubber particles occurs rapidly once the slump value exceeds a particular value of approximately 18 cm. The floating becomes more noticeable with longer vibrating times of RuC in the mould when placing concrete. It was also found that the floating of rubber particles in RuC can be seen if the sand ratios are too high or too low [43].
22. **(Fernández-Ruiz et al., 2018)** uses epoxy resin and tyre powder as a cement replacement for the compressive behaviour of RuC mixes. Mechanical and durability tests are conducted to investigate the characterisation of RuC mixes. Chloride penetration into the concrete matrix was investigated to determine the durability properties of RuC. The findings suggest that polymer-cement concrete improves the stress-strain curve's post-peak slope, resulting in increased ductility, which is particularly important in earthquake engineering [44].
23. To minimise strength loss in RuC, **(Kashani et al., 2018)** utilised five surface treatment techniques (cement coating, sulphuric acid soaking, sodium hydroxide soaking, potassium permanganate soaking, and silica fume coating). Silica fume coating and sulphuric acid soaking had the maximum substantial improvement in rubber crumbs and cement bonding, and strength gains of 27 to 56% were achieved using all five approaches. Silica fume coating is a cost-effective alternative to chemical treatments since it has a lesser amount of safety and environmental issues [14].
24. The impact response of RuC columns exposed to lateral impact was studied experimentally by **(Pham et al., 2018)**. The concrete columns were made with two rubber crumb replacement levels of 15%, and 30% and particle sizes of 2–5 mm and 5–7 mm were used to replace FA and CA, respectively. All concrete columns were tested using pendulum impact testing equipment. The RuC columns greatly lower the peak impact force (27-40%) according to the test findings. Furthermore, more flexibility was found in the RuC columns compared to standard concrete columns.

Before failing, the RuC columns were able to deflect twice as many reference conventional concrete columns. In comparison to the reference conventional concrete columns, the columns containing 15% and 30% crumb rubber enhanced impact energy absorption by 58 and 63%, respectively [45].

25. **(Li et al., 2018)** presented the study on the stress and strain behaviour of RuC with waste tyre crumb rubber replacement level percentages of 6%, 12%, and 18%. The energy dissipation capacity, modulus of elasticity, peak stress, and strain at peak stress of RuC under uniaxial compression are investigated. They concluded that the axial compressive strength of RuC decreases by the addition of waste tyre crumb rubber into concrete mixes. Rubber crumbs enhance the ductility of RuC and its capacity to absorb energy [46].
26. In the study of **(Gerges et al., 2018),** the partial replacement of natural FA was done by 5%, 10%, 15%, and 20% rubber crumbs. RuC's fresh and hardened characteristics, as well as its impact load capacity, are investigated. The compressive strength of concrete RuC cylinders containing different proportions of rubber was found to be reduced. The rubber particles included in the concrete positively affect the dynamic performance of RuC. RuC possesses several desirable properties, such as lower density, higher toughness, and higher impact resistance compared to conventional concrete [47].
27. **(Raffoul et al., 2017)** used waste tyre rubber to make RuC cylinders by replacing (a) 0-100% of FA or CA volume or (b) 40-60% of total aggregate volume. High-strength, highly deformable FRP Confined RuC was developed using externally bonded fibre-reinforced polymer (FRP) jackets (CRuC). According to the findings, high rubber content in concrete causes early microcracking and lateral movement. To get rid of this issue, externally bonded FRP confinement was applied to RuC cylinders, and after that, greater confinement efficacy was obtained. Engineers will benefit greatly from this unique high-strength, highly deformable CRuC, which may be utilised in structural applications requiring considerable deformability [48].
28. **(Gupta et al., 2017)** replacing FA with tyre rubber powder (0, 5, 10, 15, and 20%) in one mix design, and for another mix design, FA was replaced by rubber waste (10% constant rubber ash along with 0, 5, 10, 15, 20, and 25% of rubber fibre). A drop-weight test, flexural loading test, and rebound test were used to evaluate the impact characteristics of the produced concrete. According to the results, the

resilience properties of RuC toward impact and fatigue loading were enhanced by adding rubber ash and rubber fibre to the concrete [49].

29. An experimental examination was conducted on the ductility and strength of short steel tubes filled with RuC according to **(Duarte et al., 2016)**. The impact of several characteristics on short column ductility and strength is investigated and addressed, including cross-section form (square, rectangular, circular), steel grade, and concrete mix. The study's key finding is that RuC short columns are more ductile than conventional concrete short columns, despite their lower strength. Columns with circular sections have better ductility than those with square or rectangular cross-sections. Structures in seismic zones that require energy dissipation may benefit from this research [50].
30. **(He et al., 2016)** use a rubber surface modification technique to create a strong interaction between the rubber and the cement. In this method, the rubber was oxidised with $KMnO_4$ solution before being sulfonated with $NaHSO_3$ solution. The bonding strength of the cement paste and rubber was enhanced by 41.1% after the surface modification of the rubber. Mechanical testing also revealed that the rubber surface modification effectively improved the compressive strength and impact resistance properties of RuC. The concrete's compressive strength was 48.7% greater with 4% modified rubber powder compared with normal rubber powder [16].
31. **(Su et al., 2015)** replaces 20% of the natural FA by volume with three single-size rubber crumbs (3, 0.5, and 0.3 mm) and one set of mixing all three single-size rubber particles. The findings of the experiments showed that the particle size of rubber crumbs has a more significant impact on the concrete's workability and water permeability than the fresh density and mechanical properties. The concrete, which was made with large rubber crumbs, has better workability and density than the concrete made with small-sized rubber crumb particles. Nevertheless, the RuC shows higher strengths and lower water permeability for smaller or single-size rubber crumbs [51].
32. **(Gupta et al., 2015)** investigated the impact resistance of concrete when waste rubber fibres replaced 5%, 10%, 15%, 20% and 25% of FA, and cement was replaced by 5% and 10% silica fume. Drop weight, flexural loading, and rebound were the three techniques used to conduct impact testing on concrete. The research shows that

discarded tyre rubber fibre may be used as a renewable source to increase concrete's ductility and impact resistance [24].

33. The experimental study was carried out by **(Youssf et al., 2015)** to see if Crumb rubber concrete (CRC) might be used for structural columns. Under axial compressive loading and increasing reversed cyclic loading, three reinforced concrete columns with a diameter of 240 mm were evaluated. The first column was made of CRC, whereas the other two were made of standard concrete and were exposed to differing axial stresses. To assess the damping qualities of each column, a snap-back test was performed. Compared to a standard concrete column, the CRC enhanced the hysteretic damping ratio and energy absorption capacity of the columns by 13% and 150%, respectively [52].
34. The purpose of the study of **(Jusli et al., 2014)** is to investigate the chemical characteristics of waste rubber tyre crumbs. The chemical properties of rubber crumbs were determined using X-ray fluorescence (XRF). The relation between temperature and the weight loss of rubber crumbs was investigated using thermogravimetry and differential thermogravimetry to establish its potential as an aggregate substitute in concrete. The physical characteristics of rubber crumb particles were investigated using SEM, as well as the bonding between cement and rubber crumb particles in concrete mixtures. According to the SEM examination, the principal components of rubber crumbs are carbon, zinc, magnesium, and calcium [53].
35. **(Youssf et al., 2014)** tested the usage of fibre-reinforced polymer (FRP) confinement on the outer layer of the column to mitigate the compressive strength loss while using RuC for columns. The findings showed that using FRP to confine RuC successfully minimises the strength loss while retaining the benefits of enhanced ductility that come with RuC. The RuC structural columns have a great future, mainly in seismic zones where greater ductile structural members are required [54].
36. According to **(Xue and Shinozuka, 2013),** column models were made using RuC with different amounts of waster tyre crumb rubber to investigate the damping ratios and dynamic structural responses to earthquake ground motion using seismic shaking table tests. Meanwhile, the compressive strength and modulus of elasticity were determined using RuC cylinders. The results show that the seismic acceleration

of the structure was reduced by 27%, and the damping coefficient of the RuC was enhanced by 62% compared to conventional concrete [55].

37. According to **(Ma and Yue, 2013),** the particles of waste tyre rubber were soaked in NaOH solution to remove the effect of zinc stearate, which was used during the manufacturing of rubber tyres. RuC specimens were made using tyre rubber with various particle sizes and replacement quantities. The experimental findings revealed that as the quantity of rubber crumbs increased, the mechanical characteristics and elastic modulus reduced. After immersing rubber particles in NaOH solution, the ultimate strain raised slightly, and RuC's toughness and deformation abilities were significantly improved [56].
38. According to **(Ozbay and Lachemi, 2011),** the energy absorption capacity, compressive strength, and abrasion resistance of RuC, including or excluding ground granulated blast furnace slag (GGBFS), were determined by an experimental programme. Three replacement levels of crumb rubber (CR) (5, 15, and 25% of FA by volume) and two levels of GGBFS content (20 and 40%) were examined using a water–binder ratio of 0.4. Energy absorption capability, abrasion resistance, and compressive strength of 12 concrete mixes were examined through experiments. According to test results, the inclusion of CR reduces the compressive strength and abrasion resistance of RuC; however, it enhances the energy absorption capacity of RuC significantly [25].
39. Using the varied sizes and content of tyre rubber particles, **(Son et al., 2011)** evaluated the effectiveness of waste tyre rubber-filled concrete to increase the deformability and energy absorption capacity of RuC columns. 0.6 and 1 mm rubber crumbs were used to examine twelve-column specimens. The compressive strength and modulus of elasticity were marginally reduced when rubber crumbs-filled concrete was used, but ductility can be increased by up to 90%. This kind of RuC was found to have strong energy absorption capability and ductility, making it appropriate for seismic applications. [57].
40. **(Uygunoğlu and Topçu, 2010)**, discusses the findings of experiments that looked at the impact of replacing FA in the self-consolidating mortar (SCM) with tyre rubber crumbs. The dynamic modulus of elasticity, apparent porosity, water absorption, compressive and flexural strength, and drying shrinkage were all

assessed in this investigation. The inclusion of waste tyre rubber reduced the drying shrinkage of SCMs by 10% to 40% made at low water/powder ratios [58].

41. **(Ganjian et al., 2009)** tested RuC for permeability and water absorption as well as durability. With up to 5% replacement by rubber aggregate in each concrete batch, the results indicated no significant changes in RuC properties [17].
42. **(Taha et al., 2009)** replaces CA and FA with varying volume replacement levels using tyre rubber chipped and rubber crumb particles. The effect of adding tyre rubber particles on the fracture performance of RuC is studied using quasi-brittle fracture mechanics models. It was determined that selecting the optimum rubber crumb particle replacement ratio might result in concretes that fulfilled the desired strength and fracture toughness requirements [23].
43. According to **(Ganjian et al., 2009),** different proportions of rubber chipped by weight were utilised to replace CA in the first set, and in the second set, the cement was replaced by scrap-tyre powder. The results were studied after selecting and performing some standard durability tests (permeability and water absorption). With up to 5% FA replacement by rubber aggregate in each batch, the findings demonstrated no significant changes in concrete properties. Nevertheless, considerable changes were observed with a further increase in replacement ratios [17].

2.1.2 Effect of freeze/thaw

44. **(Yao et al., 2020)** examines the impacts of two freeze-thaw conditions on concrete's durability (a) maintenance freeze-thaw (MFT) and (b) immersion freeze-thaw (IFT). The concrete specimens in the MFT environment were initially cured in a conventional curing condition for 28 days before freezing and thawing. Simultaneously, the concrete specimens in IFT condition were initially cured for 90 days in the salt environment ($NaHCO_3$, NaCl, and Na_2SO_4) before being tested in a freeze-thaw atmosphere. The findings suggest that the concrete's relative dynamic young's modulus and erosion-resistance coefficients are 14.3% and 21.0% greater in the IFT environment than in the MFT environment. Therefore, in the MFT environment, concrete deterioration is more severe than in the IFT environment [59].
45. According to **(Xue and Pei, 2018)**, the axial compressive characteristics of RuC were evaluated at temperatures of -30 and 20°C, using rubber crumbs with a size of

2-4 mm. RuC has a lot higher stress and strains at -30°C, and its responsive deformation capacity is better than conventional concrete [60].

46. **(Richardson et al., 2016)** investigated the optimal particle size for rubber crumb, which is utilised as a FA replacement in RuC to give the most significant freeze-thaw protection and minimise the loss in the compressive strength. According to the investigation, the air entrainment was greater when the rubber crumb particle size was less than 0.5 mm. The findings revealed that crumb rubber concrete had better freeze-thaw resistance than ordinary concrete [61].
47. The impact of rubber crumb additive, particle size, and volume on the freeze-thaw resistance of RuC was investigated by **(Zhu et al., 2012).** The findings suggest that the size of rubber crumbs that is either too thick or too thin is not suitable for concrete's freeze-thaw protection. Furthermore, excessive replacement levels of rubber crumbs might compromise concrete's freeze-thaw resilience [62].
48. According to **(Richardson et al., 2012),** to achieve maximum freeze-thaw protection and strength of RuC, an optimum quantity of rubber crumb was utilised in concrete. According to the research finding, the optimum replacement of FA with rubber crumbs to the concrete should be 0.6% by weight. The usage of rubber crumbs to provide freeze-thaw protection for the concrete mix was studied in the test results. It was found that rubber crumbs effectively provided freeze/thaw protection to RuC with the optimum dosage of rubber crumbs [20].

2.1.3 Effect of acid attack

49. **(Gupta et al., 2021b)** uses fibre-type rubber shreds to replace FA and silica fume as a replacement for cement to investigate the durability properties of reinforced RuC. The acid resistance (durability property) of RuC was evaluated by submerging the concrete in acid (H_2SO_4 and HCl) solutions for 90 and 180 days, respectively. Both macrocell current and half-cell potential techniques were used to measure corrosion in samples for 18 months. According to the results, rubber shreds in concrete improve the acid attack resistance of RuC. The addition of silica fume improved the mechanical and durability characteristics of RuC while also lowering the risk of corrosion [28].
50. **(Bisht and Ramana, 2019)** investigates the behaviour of RuC in an aggressive acidic (sulphuric acid) condition after replacing FA with rubber crumb at different

replacement levels (4, 4.5, 5, and 5.5%). Changes in weight, compressive strength, and microstructure were used to evaluate the performance of RuC. The results suggest that adding rubber crumbs to concrete minimises material separation, preventing rupture and deterioration. X-ray diffraction, Fourier transforms infrared spectroscopy, thermogravimetric analysis, and field emission scanning electron microscopy experiments were used to confirm these results. Hence, crumb rubber replacing fine aggregate by up to 4% prevents a significant fall in performance under such an aggressive condition. As a result, substituting FA with rubber crumbs up to 4% prevents a considerable drop in the quality of RuC under such aggressive environments (acid conditions). This technique of making RuC will minimise the requirement for natural FA in the production of structural or non-structural concrete elements [63].

2.2 Critical analysis of the literature review

2.2.1 Effect of rubber crumbs on fresh properties of RuC

After the critical reviews of the literature, it was found that the fresh properties of RuC were slightly influenced by incorporating rubber crumbs in concrete. The particle size of rubber crumbs has a more significant impact on the concrete's workability than the fresh density and mechanical properties. The concrete, which was made with large rubber crumbs, has better workability than the concrete made with small-sized rubber crumb particles. Nevertheless, the RuC shows higher strengths and lower water permeability for smaller or single-size rubber crumbs, so the selection of the size of rubber crumbs is essential [51]. In comparison to conventional concrete, the RuC with large-size rubber particles exhibited better workability than small-size particles [64]. Muñoz-Sánchez et al. suggested that the upto 10 % replacement of rubber crumbs doesn’t much influence the workability of RuC [65]. In comparison to conventional concrete, the RuC showed lower unit weight and sufficient workability up to 15% replacement level, after 15% replacement the slump value starts to decrease [66]. Crumb rubber had an adverse effect on the fresh property of RuC, however effective mixture with up to 30% crumb rubber could be created [4]. Rubber particles in the mixture have little impact on concrete's workability, and marginally decrease the value of slump [8]. Adding fibres (polypropylene, steel) also lowers are rheological properties of RuC and decrease the workability [41]. After carefully reading some review papers, it was discovered that the

workability decreased as the grades (size) and amounts of crumb rubber increased [67–73].

2.2.2 Effect of rubber crumbs on mechanical properties of RuC

After the critical reviews of the literature, it was found that the mechanical properties of RuC decrease by replacing the fine aggregate by rubber crumbs. Rubber aggregates reduce the concrete's mechanical properties in the mixtures [31]. According to Mohammed et al., (2021), rubber crumb reduces the compressive strength and elastic modulus of RuC. The addition of rubber crumbs resulted in a considerable increase in Poisson's ratio and drying shrinkage [32]. Islam et al., (2021) found that the smaller rubber particles have higher adhesion to cement particles which gives higher strength of RuC than the RuC which is made by large rubber particles [33]. Rising the amounts of recycled concrete aggregate and waste rubber powder in concrete lowers the mechanical properties of RuC [34, 47]. Adding 2.0% steel fibres increased the compressive strength of RuC by 26.6% [37]. Reusing discarded rubber and polymeric fibre reduces the mechanical properties of RuC. The reduction in strength percentage is within permissible limits in both "plain rubberised" and "fibre-reinforced rubberised concrete" at a maximum of 7.5% replacement level of rubber aggregate [42]. Li et al., (2018) concluded that the axial compressive strength of RuC decreases by the addition of waste tyre crumb rubber into concrete mixes [46]. With up to 5% FA replacement by rubber aggregate in concrete, no significant changes in concrete properties were found. Nevertheless, considerable changes were observed with a further increase in replacement ratios [17]. It was also found that selecting the optimum rubber crumb particle replacement ratio might result in concretes that fulfilled the desired strength and fracture toughness requirements [23]. However, the rubber crumb modification by sodium hydroxide can increase rubber crumb and cement paste bonding and interaction. The compressive strength of sodium hydroxide-treated RuC was marginally enhanced compared to conventional RuC [7, 13]. The bonding strength of the cement paste and rubber was enhanced by 41.1% after the surface modification of the rubber. The rubber crumbs were oxidised with $KMnO_4$ solution before being sulfonated with $NaHSO_3$ solution. The rubber surface modification effectively improved the compressive strength and impact resistance properties of RuC. The concrete's compressive strength was 48.7% greater with 4% modified rubber powder compared with normal rubber powder [16]. Kashani et al., 2018 suggested that the silica

fume coating and sulphuric acid soaking of rubber crumbs gives an improvement in rubber crumbs and cement bonding, and strength gains of 27 to 56% were achieved [14].

2.2.3 Effect of rubber crumbs on impact resistance and damping properties of RuC

Rubber is an elastic material and it can absorb the impact of external force. Incorporating rubber crumbs in concrete can enhance the impact resistance property of RuC. After partially adding rubber crumbs in place of fine aggregate it was discovered that adding rubber ash to concrete improves the impact resistance and slightly reduces the mechanical properties of RuC [30]. The seismic performance of the structure was significantly enhanced by the use of RuC jacketing. The use of high-strength RuC instead of the control material enhanced the damping capacity and slightly lowered the structure's base shear forces [6]. Adding rubber aggregates at low percentages enhances the ductility, energy absorption capacity, and toughness of concrete while having only a minor negative influence on its strength and other parameters. Overall the modified RuC might be used in earthquake-resistant structural components, integrated bridges, or impact-resistant road barriers [8]. With increasing rubber content, fibre-reinforced grouted aggregate RuC contributes considerably to the improvement of energy absorption capacity [7]. Reusing discarded rubber and polymeric fibre both enhances the ductility and damping ratio of RuC [42]. In comparison to the conventional concrete columns, the columns containing 15% and 30% crumb rubber enhanced impact energy absorption by 58 and 63%, respectively. Furthermore, more flexibility was found in the RuC columns compared to standard concrete columns [45]. Li et al., (2018) concluded that the rubber crumbs enhance the ductility of RuC and its capacity to absorb energy [46]. RuC possesses several desirable properties, such as higher toughness, and higher impact resistance compared to conventional concrete [47]. According to Gupta et al., (2017), the resilience properties of RuC toward impact and fatigue loading were enhanced by adding rubber ash and rubber fibre to the concrete [49]. RuC short columns are more ductile than conventional concrete short columns. RuC’s columns with circular sections have better ductility than those with square or rectangular cross-sections. Structures in seismic zones that require energy dissipation may benefit from this research [50]. According to Gupta et al., discarded tyre rubber fibre may be used as a renewable source to increase concrete's ductility and impact resistance [24]. Compared to a standard concrete column, the crumb

rubber concrete enhanced the damping ratio and energy absorption capacity of the columns by 13% and 150%, respectively [52]. Using FRP to confine RuC successfully minimises the strength loss while retaining the benefits of enhanced ductility that come with RuC. The RuC structural columns have a great future, mainly in seismic zones where greater ductile structural members are required [54].

2.2.4 Effect of rubber crumbs on durability properties of RuC

With up to 5% replacement by rubber aggregate in concrete batches there are no significant changes in permeability and water absorption as well as durability properties of RuC [17]. According to Xue and Pei, (2018), the axial compressive characteristics of RuC were evaluated at temperatures of -30 and 20°C, using rubber crumbs with a size of 2-4 mm. RuC has a lot higher stress and strains at -30°C, and its responsive deformation capacity is better than conventional concrete [60]. The air entrainment was greater when the rubber crumb particle size was less than 0.5 mm. The crumb rubber concrete had better freeze-thaw resistance than ordinary concrete [61]. The size of rubber crumbs that is either too thick or too thin is not suitable for concrete's freeze-thaw protection. Furthermore, excessive replacement levels of rubber crumbs might compromise concrete's freeze-thaw resilience [62]. According to Richardson et al., (2012), the optimum replacement of FA with rubber crumbs to the concrete should be 0.6% by weight. According to their study, rubber crumbs effectively provided freeze/thaw protection to RuC with the optimum dosage of rubber crumbs [20]. The RuC exposed to freeze-thaw cycles doesn't present visible microcracks on the surfaces of samples and any spalling of cement paste, RC, and aggregates. So the RuC can give good performance without significant loss in compressive strength and without spalling of the concrete surface after exposure to freeze/thaw cycles. Adding rubber shreds in concrete improves the acid (H_2SO_4 and HCl) attack resistance of RuC. The addition of silica fume improved the durability characteristics of RuC while also lowering the risk of corrosion [28]. Bisht and Ramana, (2019) also investigate the behaviour of RuC in an aggressive acidic (sulphuric acid) condition. Changes in weight, compressive strength, and microstructure were used to evaluate the performance of RuC. according to their results adding rubber crumbs to concrete minimises material separation, preventing rupture and deterioration. Hence, crumb rubber replacing fine aggregate by up to 4% prevents a significant fall in performance under such an aggressive condition. This technique of making RuC will

minimise the requirement for natural FA in the production of structural or non-structural concrete elements [63].

2.3 Summary

This chapter reviews research published that is relevant to the scope of this thesis. The following points summarise the main conclusions from this literature:

a) Using rubber in concrete negatively affected its workability, compressive strength and tensile strength of RuC. On the other hand, using rubber in concrete enhanced its toughness, ductility, and damping ratio.
b) Pre-treatment of rubber particles using 10% sodium hydroxide solution before mixing with concrete was able to decrease the RuC strength losses. In addition, replacing part of concrete cement by silica fume increased RuC strength as a result of the good adhesion between silica fume particles and rubber.
c) Confining concrete using fibre-reinforced polymer (FRP) increased the concrete ductility, toughness, axial strength, and axial and hoop strains, and prevented concrete cover spalling.
d) The available analytical and empirical methods predicting RuC characteristics are limited and their predictions need improvements by using large experimental database results.
e) No previous studies have so far been carried out to investigate the behaviour of RuC in a structural application. Limited research on structures constructed using RuC has been carried out. More research is required to explore the possibility of using scrap rubber in structural applications.
f) No previous studies have so far been carried out to enhance the bonding property between rubber crumbs and cement particles. Limited researches are available on the surface treatment of rubber crumbs. Only NaOH treatment and supplementary cementing material coating on rubber particles are available. Some more advanced techniques should be explored.

CHAPTER 3 MATERIALS AND EXPERIMENTAL PROGRAM

This chapter aims to present the methodology including materials types and descriptions used to implement the experimental work, specimen types and numbers, mixing procedure, casting, compaction and curing process. Additionally, the tests that have been carried out to assess fresh and hardened properties including mechanical and durability properties of the studied concrete will be also explained.

For this purpose, this chapter will be divided into the following sections.

a) In the first step, all the materials are to be tested to assess their properties and reliability before using in the concrete. All tests on materials are done by the specified IS codes and ASTM codes. The test results on materials give information about their properties and compatibility for using in the concrete. All tests which are used in this study are listed below.

b) In the second part, the fresh and hardened properties of RuC are tested. RuC is prepared by 10%, 15%, 20% 25% and 30% weight replacement of fine aggregate with rubber crumbs. These replacements are done after surface treatment of rubber crumbs with 15% sulphuric acid solution. In fresh properties, the slump test on concrete mixes is done to check the workability of RuC. In hardened properties, the compressive, split tensile and flexural strength tests on standard and RuC mixes are done to check the strength parameters of standard and RuC. The proposed concrete is based on incorporating rubber crumbs as a partial replacement of fine aggregate so the mechanical properties of RuC may be reduced to certain amounts. Hence these tests are carried out to see whether the mechanical properties of the RuC are within the design limits or not. The impact resistance tests are also done to check the impact resistance properties of RuC. Because rubber is elastic material and can absorb the impact energy, so due to his reason this test is performed. The rubber crumb is hydrophobic material and due to this reason, it makes a weak bond with the cement matrix. Due to this issue, the pull-off test is done to check the bonding strength of RuC. SEM analysis is also done to check the bonding properties between rubber crumbs and cement. Moreover, a non-destructive test ultrasonic pulse velocity test is done to check the quality of RuC after incorporating

rubber crumbs. After analysing all these properties the optimum replacement level of rubber crumbs is found to be 15%. After thorough research, the fresh and hardened properties results are compared and validated on behalf of earlier literature on RuC investigations without chemical treatment to determine the effect of sulphuric acid treatment on rubber particles. Moreover, the optimum dosage of rubber crumbs samples are also compared with standard concrete to check the changes in the fresh and hardened properties of RuC.

c) In the third part based on the result from the previous section, the durability tests are done on the optimum mix of RuC. To assess the durability properties of RuC various tests are performed such as water absorption, resistance to acid and freeze-thaw attack. The water absorption test is used to measure the increase in concrete sample mass caused by water absorption when the specimen is exposed to water. The water absorption rate (sorptivity) is assessed using the water absorption test. The acid and freeze-thaw attack test gives information on how the RuC reacts/resists due to exposure to acid and freeze-thaw cycles. The tests include under acid and freeze-thaw attack attacks such as visual inspection, mass loss and compressive strength loss. Visual examination can provide an extensive amount of information that could help positively identify the source of any suffering (cracks, spalling) that is being experienced. Mass loss and compressive strength tests provide information about their losses due to acid and freeze-thaw attacks. Some non-destructive tests are done on RuC such as four-probe resistivity and UPV. These tests are used for assessing the quality or durability of RuC.

3.1 Materials

3.1.1 Cement

In this study, PPC JK Laxmi pro+, up to 30% replacement by fly ash-based, is used. To find the properties of cement preliminary quality tests are done, such as initial and final setting time, specific gravity, soundness and particle fineness before using it in the concrete. All testing of cement is done as tests as per the Indian standard codes [74–80] and this cement passes all preliminary tests. The cement sample shows excellent properties as per the Indian standard codes. Table 3.1 illustrates the preliminary test results conducted on the sample cement.

The XRD (X-ray diffraction) analysis is done to identify the crystalline phases of cement powder passing through an 850 µm size sieve, according to ASTM (American society for testing and materials) [81]. The results of XRD are analyzed by the software X'Pert HighScore Plus. The XRD data of PPC is shown in Fig. 3.1, and peaks are found for calcium silicate, tricalcium aluminate, and silica. The chemical composition of PPC is seen from the XRF (X-Ray Fluorescence), which is presented in Table 3.2.

Table 3.1 Cement characteristics

S. No.	Test	Result
1	Normal consistency	33%
2	Initial setting time	90 min
3	Final setting time	1 hr 55 min
4	Specific gravity	2.97
5	Fineness	2.9%
6	Soundness	3 mm
7	Compressive strength at 28 days	44 MPa

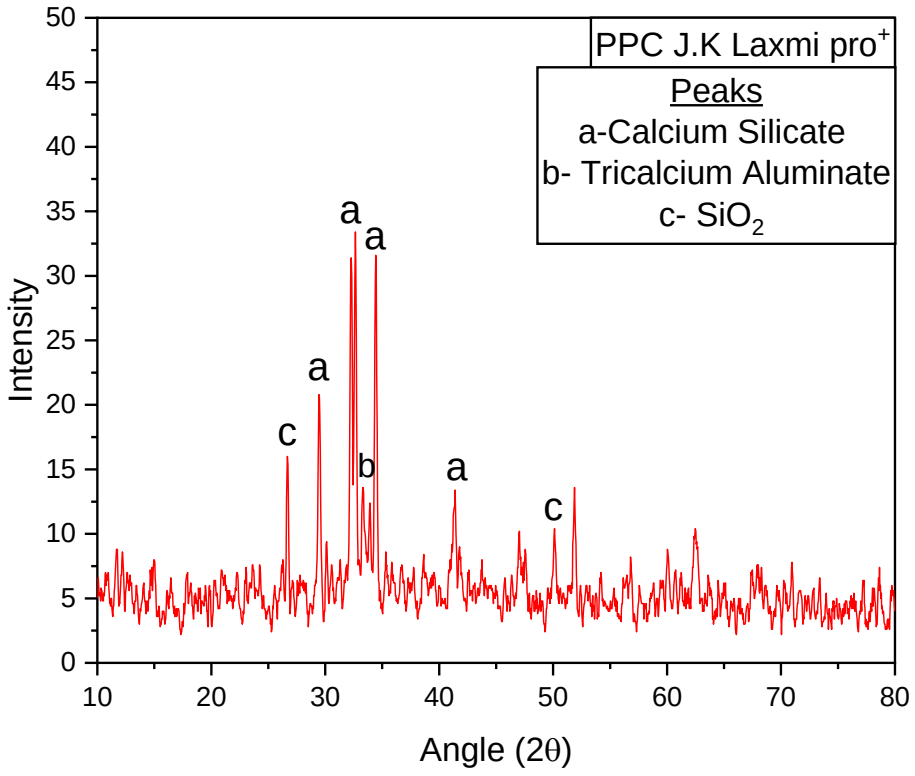

Fig. 3.1 XRD Pattern of PPC (JK Laxmi Pro+)

Table 3.2 Chemical composition of PPC cement (J.K Laxmi pro+ cement)

Component	CaO	SiO_2	Al_2O_3	Fe_2O_3	SO_3	MgO	Na_2O	K_2O
J.K Laxmi pro+ (PPC)	65.80	22.64	3.80	3.10	1.40	1.20	0.31	1.21

3.1.2 Fine Aggregate

To find the properties of fine aggregate preliminary quality tests are done, such as sieve analysis, zone, grade, fineness modulus, specific gravity, water absorption, silt content and bulk density. Fine aggregate in the form of stone dust is procured from a local material shop in Delhi. When aggregate size is less than 4.75mm it is called fine aggregate, and above 4.75 mm is called coarse aggregate. In the fine aggregate, stone dust is used in the concrete mix. The gradation of the aggregates, zone and other physical properties of the fine aggregate samples are examined in the preliminary test according to IS codes [82–90] which are presented in Table 3.4. The semi-logarithmic graph in Fig. 3.2 depicts the grain size distribution of the dust samples in an accurate manner. Table 3.3 lists the varied sizes of particles discovered in the samples along with the particle size retained on the sieve size and passing sieve number with percentages. According to IS code, the particle size distribution of the stone dust sample is in zone II, medium, and well-graded form.

Table 3.3 Sieve Analysis of Sand/Stone Dust

Sieve Size	**Weight Retained (gm)**	**% Weight Retained**	**Cumulated % Weight Retained**	**% Finer**	**Remarks**
4.75 mm	0	0	0	100	Sand falls in zone II
2.36 mm	107	10.7	10.7	89.3	
1.18 mm	298	29.8	40.5	59.5	
600 µm	214	21.4	61.9	38.1	
300 µm	130	13	74.9	25.1	
150 µm	127	12.7	87.6	12.4	
75 µm	38	3.8	91.4	8.6	
pan	86	8.6	100	0	

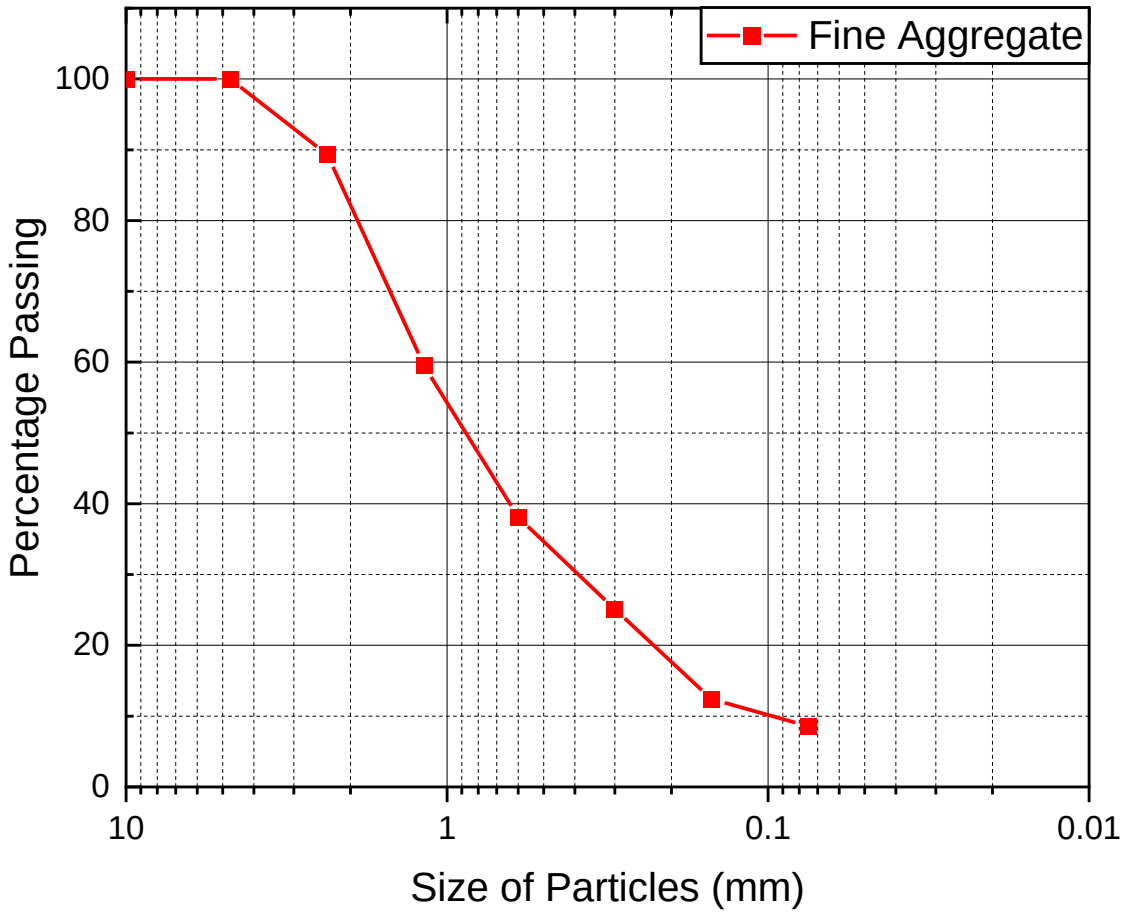

Fig. 3.2 Grain size distribution curve of fine aggregate

The stone dust sand is classified as grade II. D_{10}=0.1, D_{30}=0.4, and D_{60}=1.2 are determined by the gradation curve.

$$C_u = \frac{D_{60}}{D_{10}}$$

$$C_u = \frac{1.2}{0.1} = 12 > 6$$

$$C_c = \frac{D_{30}{}^2}{(D_{10} \text{ X } D_{60})} = \frac{0.4^2}{(0.1\text{X}1.2)} = 1.33 \text{ (Range 1-3)}$$

Thus, the sand is well-graded sand.

Table 3.4 Characteristics of fine aggregate

S. No.	Test	Result
1	Grade	Well graded
2	Zone	Zone II
3	Fineness modulus	2.75 (medium sand)
4	Specific gravity	2.62
5	Water absorption	1.21 %
6	Silt content	6 %
7	Bulk density	1610 kg/m^3

3.1.3 Coarse Aggregate

To find the properties of coarse aggregate preliminary quality tests are done, such as fineness modulus, specific gravity, water absorption, crushing value, impact value, flakiness index, elongation index and los angeles abrasion value. Crushed rock as CA (Coarse aggregate) is also procured from a local material shop in Delhi. In the CA, two types of aggregate used are 10 mm and 20 mm in the design mix. In the different mix designs, the locally accessible CA sample material is utilised. All of the particle size aggregates present in the sample are listed in Table 3.5 along with their percentages and the CA's fineness modulus. Table 3.6 describes the properties of the CA [82, 83, 91–96]. Before the raw materials were utilised in the study project, all the necessary tests were carried out to evaluate their quality.

Table 3.5 Sieve analysis of coarse aggregate

Sieve size	Weight retained (gm)	Cumulative wt. retained	Cumulative % wt. retained	% Cumulative passing	% Passing of nominal size
80mm	0	0	0	100	85-100
40mm	0	0	0	100	-
20mm	264	264	13.2	86.8	-
16mm	573	837	41.85	58.15	-
12.5mm	732	1569	78.45	21.55	-
10mm	334	1903	95.15	4.85	0-20
4.75mm	89	1992	99.6	0.4	0-5
PAN	8	2000	100	0	-

Fineness modulus $= \frac{(13.2+41.85+78.45+95.15+99.6+5X100)}{100} = 7.29$

Table 3.6 Properties of coarse aggregate

S. No.	Test	Result
1.	Fineness modulus	7.29
2.	Specific gravity	2.79
3.	Water absorption	0.2%
4.	Crushing value	23%
5.	Impact value	26.3%
6.	Flakiness index	24%
7.	Elongation index	30%
8.	Los Angeles Abrasion Value	36%

3.1.4 Superplasticiser

In order to improve the performance of the concrete, a superplasticizer is used to decrease the demand for water content in the mix design and increase the workability of the fresh concrete mixtures. To determine the optimum dosage and water-reducing capacity of SP and compatibility of SP with cement, marsh cone and efficiency test are done with PPC (JK Laxmi pro+). Auramix 400 SP (Superplasticizer) based on polycarboxylate ether-based is used in the mix design of concrete obtained from Fosroc Chemical (India). Table 3.7 describes the properties of the superplasticizer sample. The process for determining the SP's optimum dosage and efficiency is obtained from concrete technology by M.S. Shetty [97].

Table 3.7 Superplasticiser specifications

S. No.	Test	Results
1	Specific gravity	1.09@ 25°C
2	pH Value	6
3	Appearance	Brown liquid
4	Air entrainment	Less than 2% additional air entrained at usual dosages

3.1.4.1 The optimum dosage of superplasticizer

The optimum dosage and efficiency of SP are determined from the marsh cone apparatus with a nozzle aperture diameter of 8 mm. There are many aperture sizes available, say 5 mm, 6 mm, 8 mm, and 11 mm, to perform this test; however, the selection of the appropriate nozzle is based on cement paste fluidity. Other attachments with a bigger diameter aperture can be used according to different slurry types and w/c ratios. In this test, w/c is taken 0.38 according to the prescribed mix design of concrete. The dosage of SP is taken 0.2% in the first test, then increased with an interval of 0.2% until the flow time becomes almost constant. Mix them thoroughly in the Hobart mixer for 2 min to avoid the lumps in the mixture. If hand mixing is done, then the slurry should pass through a 1.18 mm sieve before the marsh cone test to prevent lumps in the slurry. The SP's optimum dosage is selected when the slurry takes minimum time to complete out from the marsh cone. After the SP's optimum dosage (saturation point), the slurry's outcome time becomes almost constant for the particular cement and specified w/c ratio. After the saturation point, the addition of SP doesn't influence the fluidity of the cement paste. The testing setup for determining the optimum dosage of SP is shown in Fig. 3.3. The flow time of slurry with different dosages is shown in Fig. 3.4. The optimum dosage of SP is found to be 1.4% for PPC. Experimental data for finding the optimum dosage of SP is shown in Table 3.8.

Fig. 3.3 Testing setup of marsh cone apparatus

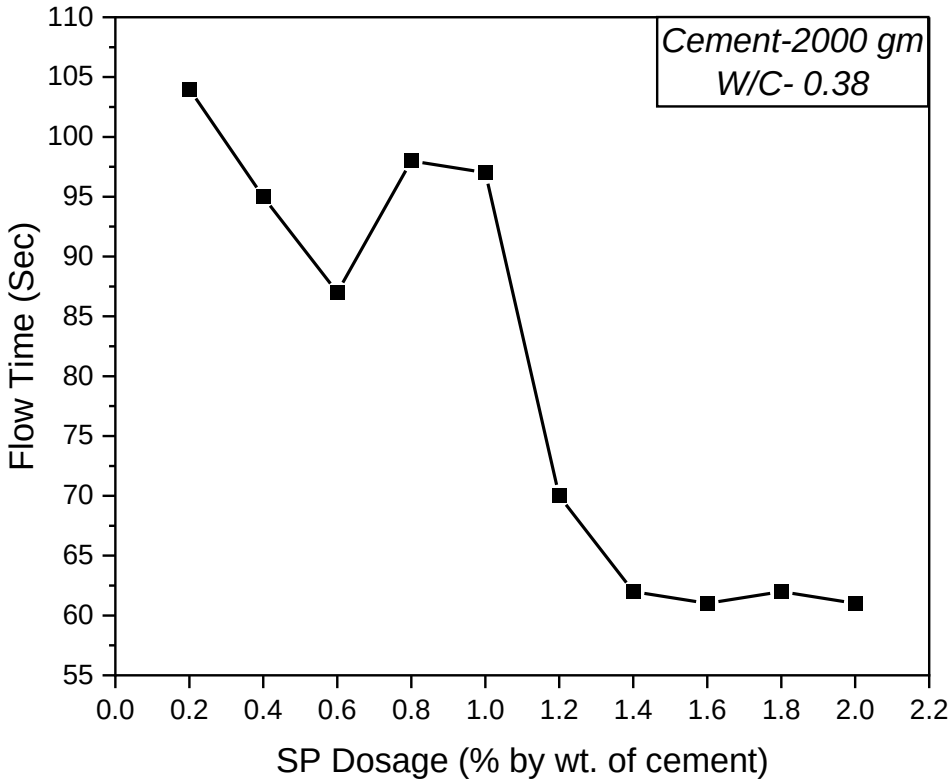

Fig. 3.4 The flow time of slurry with SP dosage

Table 3.8 Experimental data for finding the optimum dosage of SP

Cement (gm)	Dosage (%)	Quantity (ml)	Time (Sec)
2000	0.2	3.66	104
2000	0.4	7.3	95
2000	0.6	11	87
2000	0.8	15	98
2000	1	19	97
2000	1.2	22	70
2000	1.4	26	62
2000	1.6	30	61
2000	1.8	33	62
2000	2	37	61

3.1.4.2 Efficiency of superplasticizer

The marsh cone apparatus is used for finding the SP's efficiency with a nozzle aperture diameter of 8 mm. The efficiency of the SP is essential for making the mix design of desired strength. SP's efficiency indicates that the required amount of water for the concrete design mix can be reduced up to a specific limit. The process for determining the SP's efficiency is obtained from concrete technology (theory and practice) by M.S.Shetty [97]. The cement quantity remains constant in this process, but the water amount changes in all the tests. The flow time of the slurry without SP, having 1100 gm of water should be the same as another slurry with 1% of SP dosage with less water, as shown in Fig. 3.5. The efficiency of the auramix-400 SP for PPC allows the reduction of 22.73% of water. Different kinds of SP may be used for the same nature of cement, and the SP efficiency will be dissimilar. To find the efficiency of the SP flow table test can be used in place of the marsh cone apparatus. Experimental data for finding the efficiency of SP is shown in Table 3.9.

$$The\ efficiency\ of\ \ SP = \frac{The\ difference\ in\ water\ content}{Original\ \ water\ content} \text{X}100 = 22.73\%$$

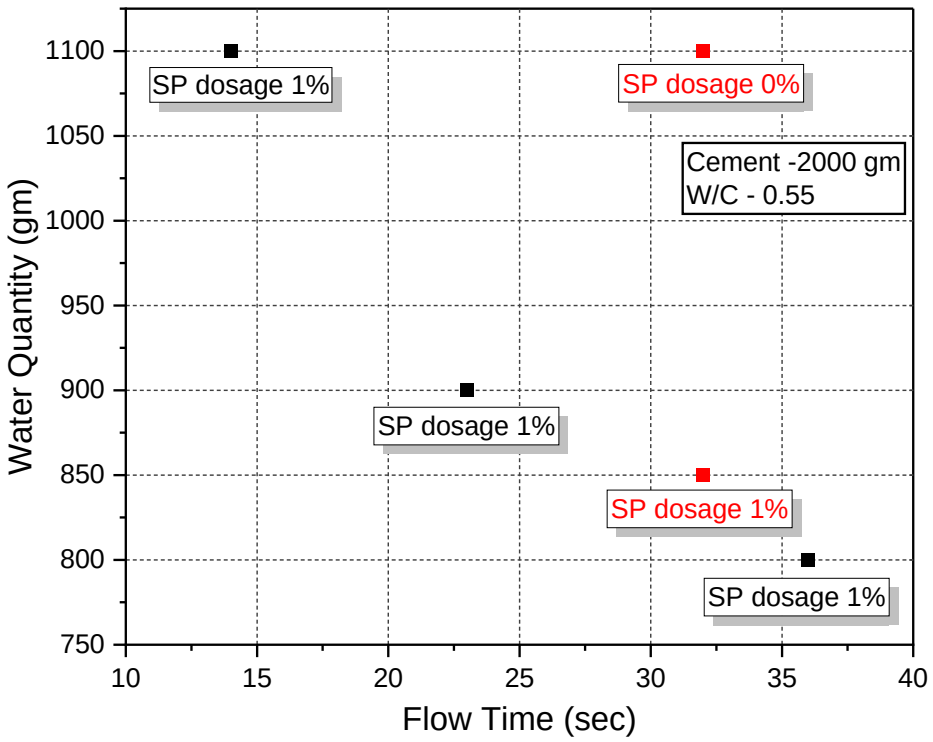

Fig. 3.5 The graph for finding the efficiency of SP

Table 3.9 Experimental data for finding efficiency of SP

Cement (gm)	W/C ratio	Quantity of water (gm)	Dosage (%)	Marsh Cone Time (Sec)
2000	0.55	1100	0	32
2000	0.55	1100	1	14
2000	0.55	900	1	23
2000	0.55	800	1	36
2000	0.55	850	1	32

3.1.5 H_2SO_4 Solution

H_2SO_4 is procured from RANKEM (avantor) (UN1830) with 36.4 normality with 98% purity [98].

3.1.6 Waste Tire Rubber Crumb

Rubber is obtained from a local waste tire rubber factory with a particle size of 0.6 mm-2.36 mm. Rubber is a lightweight material because it's Sp. Gr. is 1.07. Rubber crumb is used as a partial replacement of FA. The particle size distribution curve of rubber crumbs is shown in Fig. 3.6. Table 3.10 describes the sieve analysis conducted on the rubber

crumbs sample to determine the particle size distribution. An optical microscope is used to capture a microscopic image of small-size, medium-size, and large-size particles of rubber crumbs shown in Fig. 3.7-3.9. Rubber crumb particles are gained from the waste rubber tire after grinding in a mechanical grinder. Rubber crumb is a waste material, and it is necessary to find compatibility with concrete; some physical and microstructural analysis is essential before use in concrete. EDX (Energy Dispersive X-Ray Analysis) and XRD analysis have been done to evaluate the chemical elements and mineralogical properties present in waste tire rubber. A high amount of carbon is detected from the rubber crumb sample results, which may be responsible for the loss in strength. EDX results of rubber crumbs also show the zinc element present in rubber, which is also accountable for the strength loss of concrete according to previous research [13, 14, 99], and it should be clean from the rubber crumb. Because of this significant issue, surface treatment of rubber is necessary before adding it to the concrete.

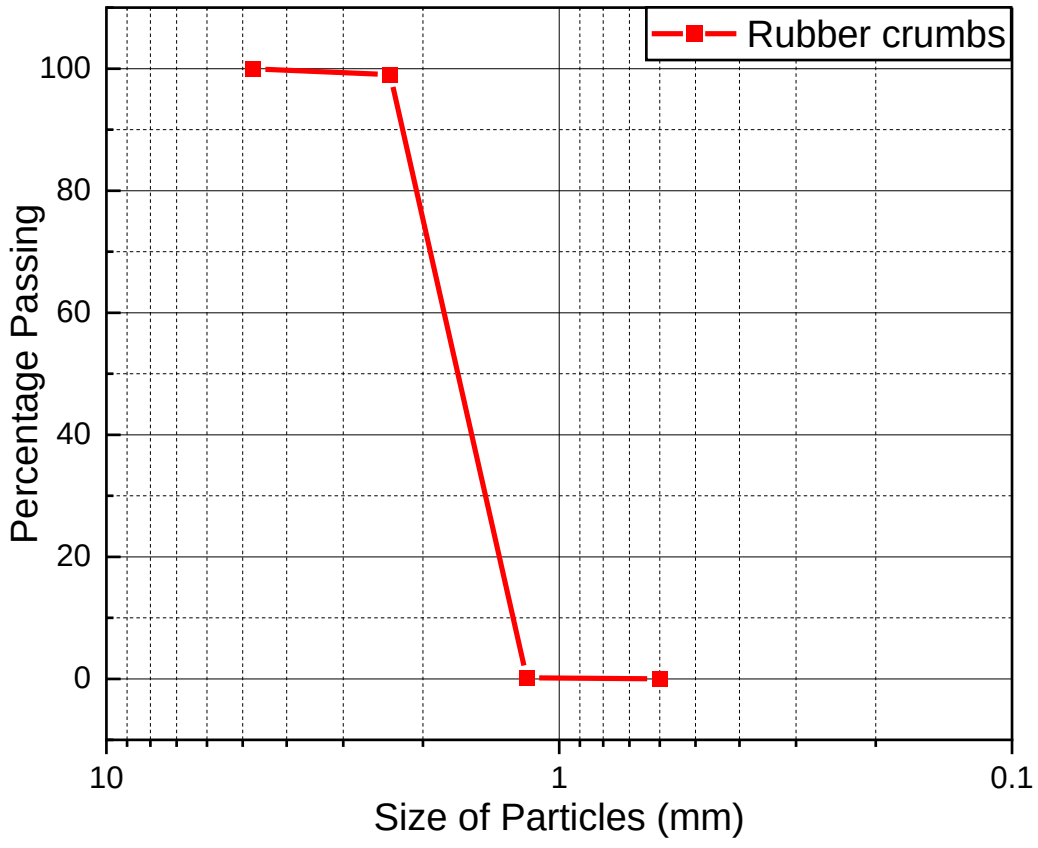

Fig. 3.6 Grain size distribution curve of rubber crumbs

Table 3.10 Sieve Analysis of rubber crumbs

Sieve Size	Weight Retained (gm)	Cumulated Weight Retained	Cumulated % Weight Retained	Cumulated % passing
4.75mm	0	0	0	100
2.36mm	0	0	0	100
1.18mm	10	1	1	99
600µm	988	98.8	99.8	0.2
300µm	2	0.2	100	0
150µm	0	0	100	0
75 µm	0	0	100	0
pan	0	0	100	0

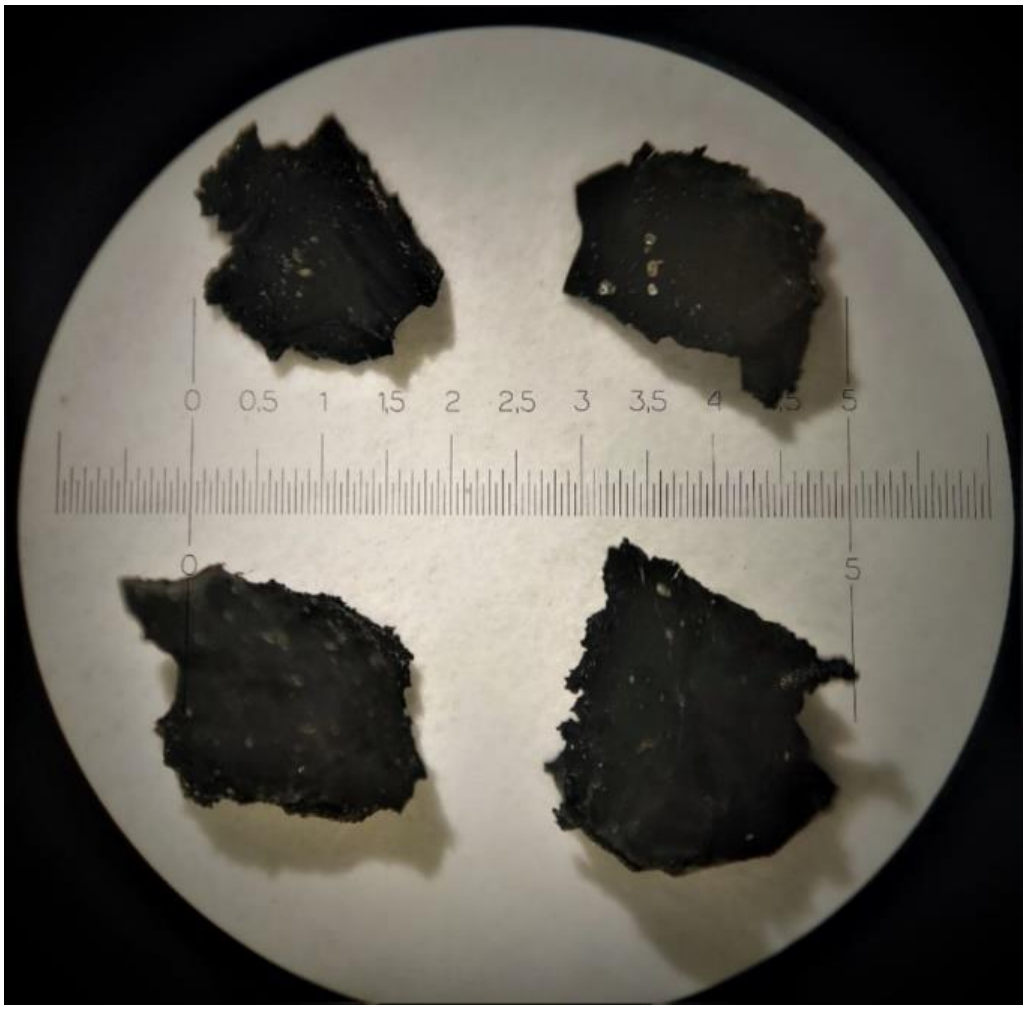

Fig. 3.7 Optical image of rubber crumbs (small size particles)

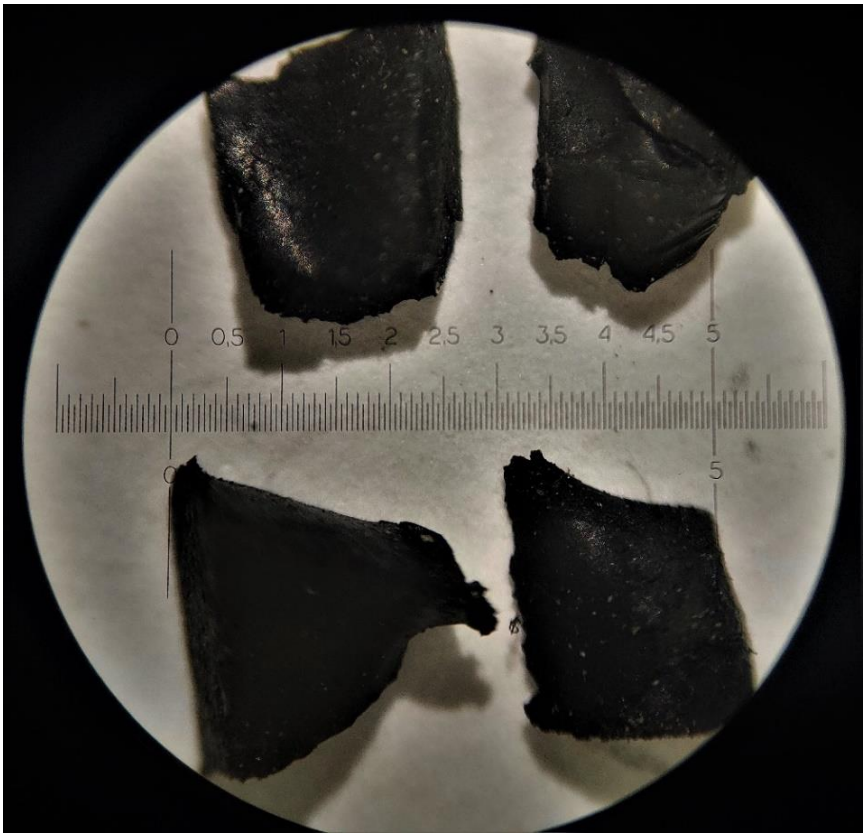

Fig. 3.8 Optical images of rubber crumb (medium size particles)

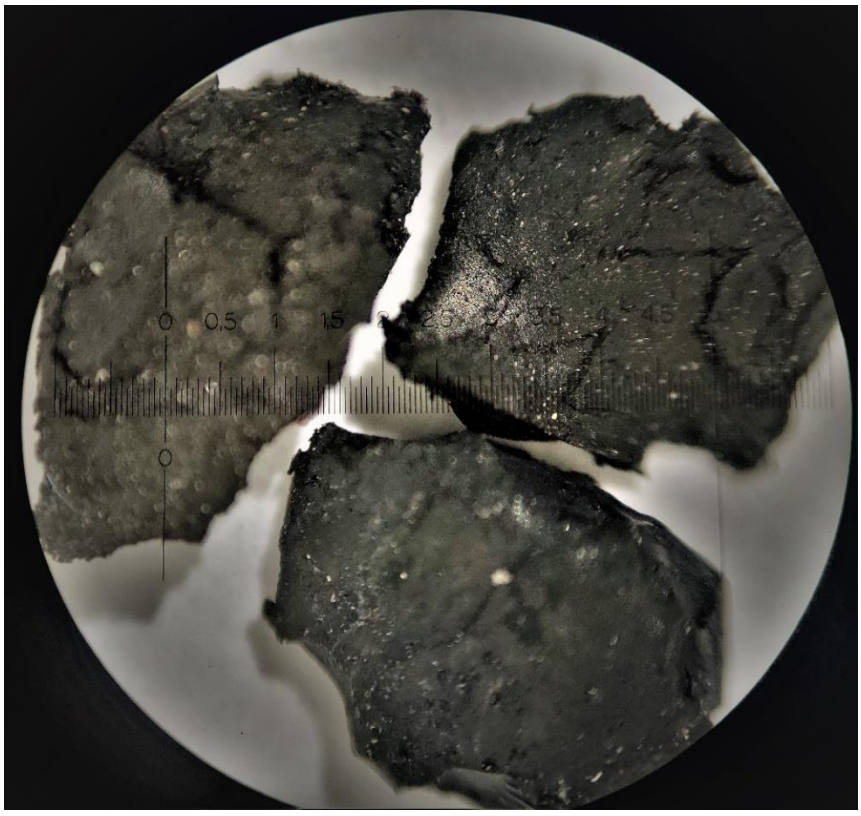

Fig. 3.9 Optical image of rubber crumbs (large size particles)

3.1.6.1 Surface treatment of rubber

Purpose of surface treatment of rubber - Strength reduction is the major drawback of the topic of RuC. Many researchers use untreated rubber crumbs, and they found significant losses in RuC's mechanical properties. The mechanical strength of RuC decreases by increasing the quantity of rubber in concrete due to the weak bonding between the rubber and the cement matrix. Zinc stearate ($C_{36}H_{70}O_4Zn$) is widely used as a release agent for rubber, polyester processing systems, and polyurethane [13, 14, 99]. These applications take advantage of their "nonstick" properties. It is a lubricant and thickening agent and is also used to improve texture. Stearic acid and zinc are component compounds for making Zinc stearate. Zinc stearate is present in the rubber tire, which shows hydrophobic properties and tends to repel water. Due to this property of rubber, particles make a weak bond with the cement matrix. Due to this significant issue, rubber particles should be treated before mixing them in concrete to enhance RuC's compressive strength. Two rubber crumb samples are being treated, one with 10 wt% H_2SO_4 solution and another with 15 wt% H_2SO_4 solution. However, after getting the results from the EDX analysis of both samples (Section 3.1.6.2 EDX analysis of rubber), 15 wt% H_2SO_4 solution is selected for treating rubber tire particles, because in this sample after treatment no Zinc element was found. “For ease, the chemical elements with their percentage of all samples by EDX analysis with and without surface treatment are present in Table 3.14 for comparison purposes.”

Treatment process- In the treatment process, rubber particles are saturated for 2 hours in a 15% sulphuric acid solution and cleaned with water, and then air-dried for one day in an open area. In this rubber treatment process, the H_2SO_4 solution reacts with zinc element and converts into zinc sulfate that can be washed by running tap water because it is soluble in water [14, 99]. The sequence of surface treatment of the rubber crumb process is shown in Fig. 3.10. The drying method of rubber crumbs in the air for 24 hours is shown in Fig. 3.11.

Fig. 3.10 Sequence of surface treatment of the rubber crumbs

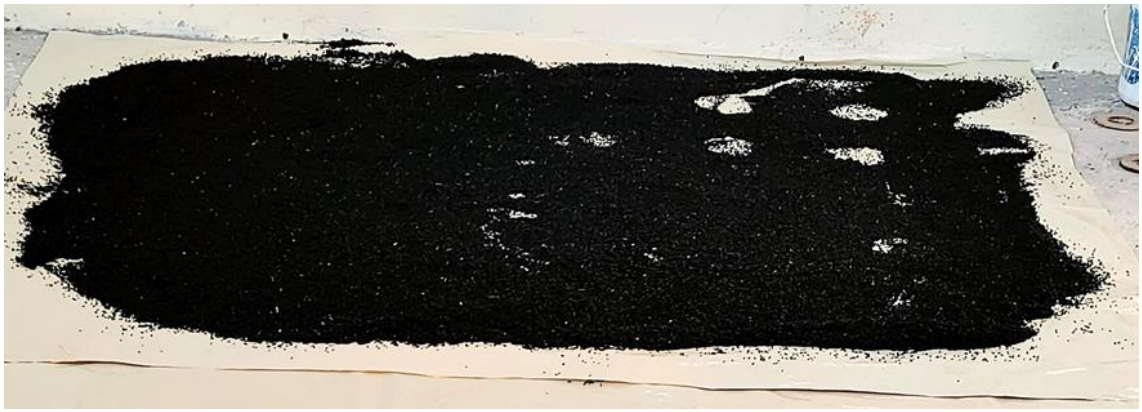

Fig. 3.11 Drying process of rubber crumbs in the air for 24 hours

3.1.6.2 EDX and XRD analysis of rubber

For the efficient use of waste tire rubber, microstructure analysis has been followed up in this study. The rubber crumbs samples are evaluated quantitatively and qualitatively using Energy Dispersive X-Ray Analysis (EDX) analysis. A technique of chemical elemental analysis based on electron microscopy, called EDX microanalysis, exhibits the existence of chemical elements in the specimens. EDX has been done to determine the chemical composition of rubber. The chemical elements and their percentage weight of any material can be found due to this technique. EDX analysis of the material is done with SEM. EDX technique cannot be used without SEM analysis. This technique has an important role in the material's microstructure analysis in the field of civil engineering to check the compatibility of the material. After the EDX analysis, it is found that zinc is present in a rubber tire, which is responsible for weak bonding with the cement matrix. Without surface treatment, rubber particles show nonstick properties due to zinc stearate [13, 14, 99], and it has to be removed to make good bonding between rubber and cement matrix. After EDX analysis of rubber without surface treatment, Zn is found to be 0.88% by weight, presented in Table 3.11. EDX data of untreated rubber in Fig. 3.12 show all chemical elements present in the rubber.

In materials science, XRD is a method for identifying a material's crystalline structure. A material is exposed to incoming X-rays in the process of XRD, and the intensities and scattering angles of the X-rays leaving the material are then measured. Identification of minerals based on their diffraction pattern is one of the main applications of XRD examination. In addition to providing information on unit cell measurements, XRD is a quick analytical method used mainly for the phase determination of a material. XRD

gives informative data belonging to XRD peaks, like miller indices, d-spacing, chemical formula, and crystal system. The analysed material needs to be homogenised and crushed to a fine powder. In civil engineering applications, this technique is used to find the chemical compound present in the materials before using them in construction materials. Due to this technique, harmful chemical compounds can be identified. The XRD analysis is done on rubber powder passing through 150 µm and retained on the 45 µm size sieve, according to ASTM [100]. The results of XRD are analyzed by the software X'Pert HighScore Plus, and the selected chemical elements in the software are C, O, Al, Si, S, Ca, Zn, N, Mg, Mn, and Fe. XRD analysis indicates rubber's mineralogical properties and the peaks show silica and calcium carbonate in Fig. 3.15. The nature of rubber crumbs is found crystalline before the surface treatment by sulphuric acid solution.

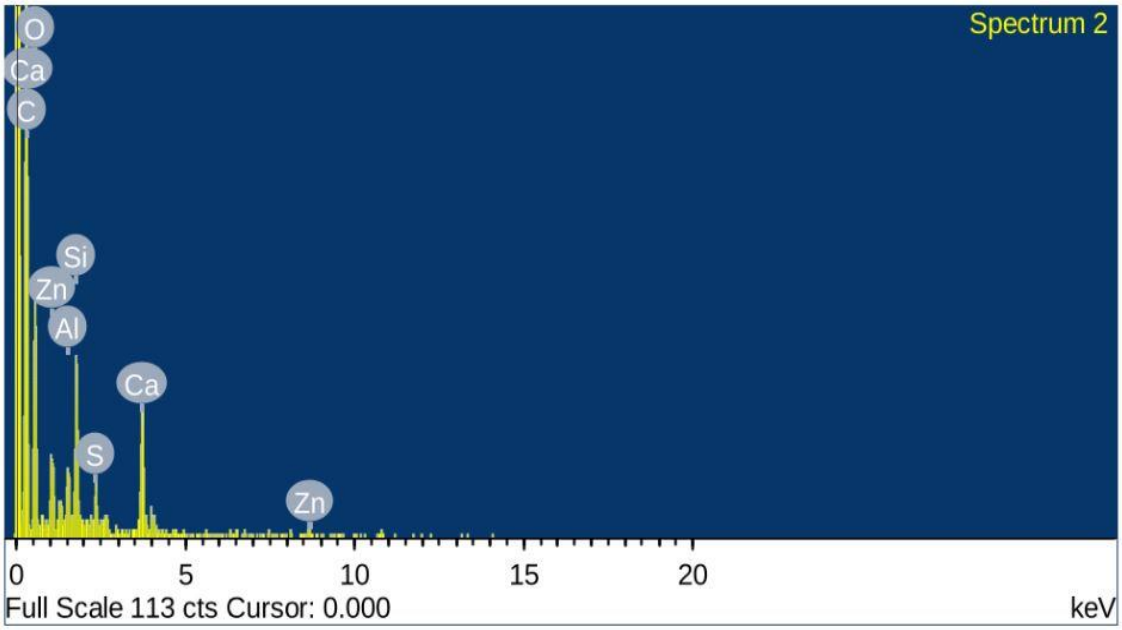

Fig. 3.12 EDX data of rubber without surface treatment

Table 3.11 Percentage weight of chemical elements without surface treatment

Element	Weight %	Atomic %
C K	62.80	71.52
O K	29.92	25.58
Al K	0.80	0.40
Si K	2.39	1.16
S K	0.64	0.27
Ca K	2.56	0.87
Zn K	0.88	0.18
Total	100	

Then 10 wt% sulphuric acid solution is used for the rubber's surface treatment, and again EDX analysis is done to find the elements. After analysing, zinc is found 0.09% in EDX analysis Fig. 3.13. All the chemical elements are present in Table 3.12 after surface treatment of rubber by 10 wt% of H_2SO_4. In this event, the amount of carbon is increased compared to without treated rubber particles. The zinc element is present in rubber crumbs in this process which should be removed from the rubber surface to enhance the bonding property of rubber and cement.

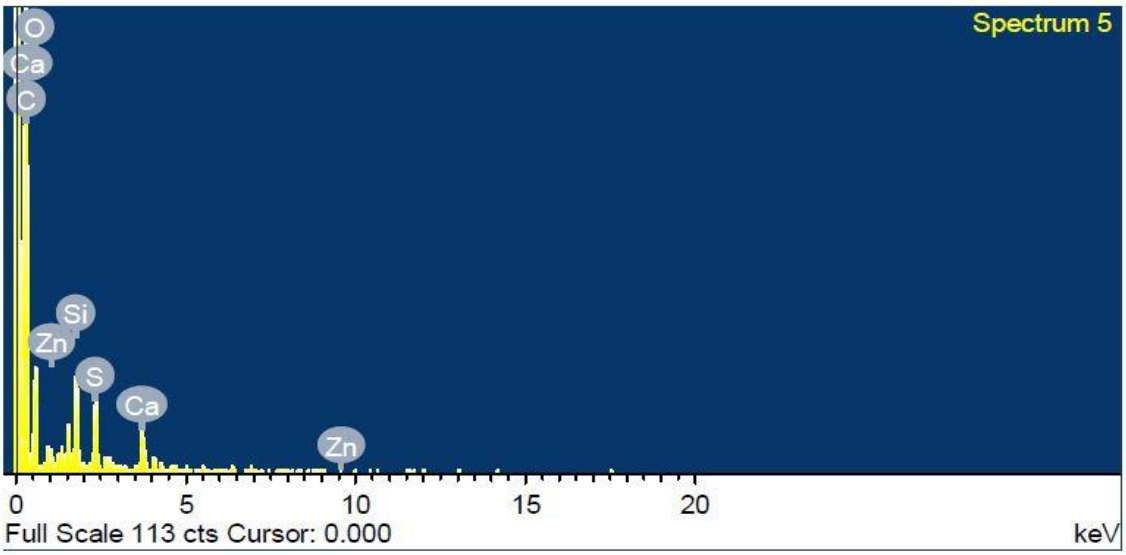

Fig. 3.13 EDX data of rubber with surface treatment by 10% H_2SO_4

Table 3.12 Percentage weight of chemical elements with surface treatment by 10% H_2SO_4

Element	Weight %	Atomic %
C K	73.24	80.13
O K	21.69	17.82
Si K	1.85	0.86
S K	1.67	0.68
Ca K	1.46	0.48
Zn K	0.09	0.02
Total	100	

Due to this issue, rubber is again treated with 15 wt% sulphuric acid solution, and then another time EDX analysis is done. After investigating the results of EDX, it is found that the Zn element is completely removed from the rubber particles and is ready to use for making the RuC. All the outcomes of the EDX analysis are shown in Table 3.13, Fig.

3.14. For ease, the chemical elements with their percentage of all samples by EDX analysis with and without surface treatment are present in Table 3.14 for comparison purposes. XRD analysis of rubber particles treated with 15% H_2SO_4 solution offers mineralogical properties in Fig. 3.15. The significant peaks show silica in the majority, and at this stage, calcium carbonate did not form. All the informative data belonging to XRD peaks, like miller indices, d-spacing, chemical formula, and crystal system, are present in Table 3.15. The nature of rubber crumb is found crystalline after the surface treatment by sulphuric acid solution, and no harmful compound is found before mixing it in the concrete.

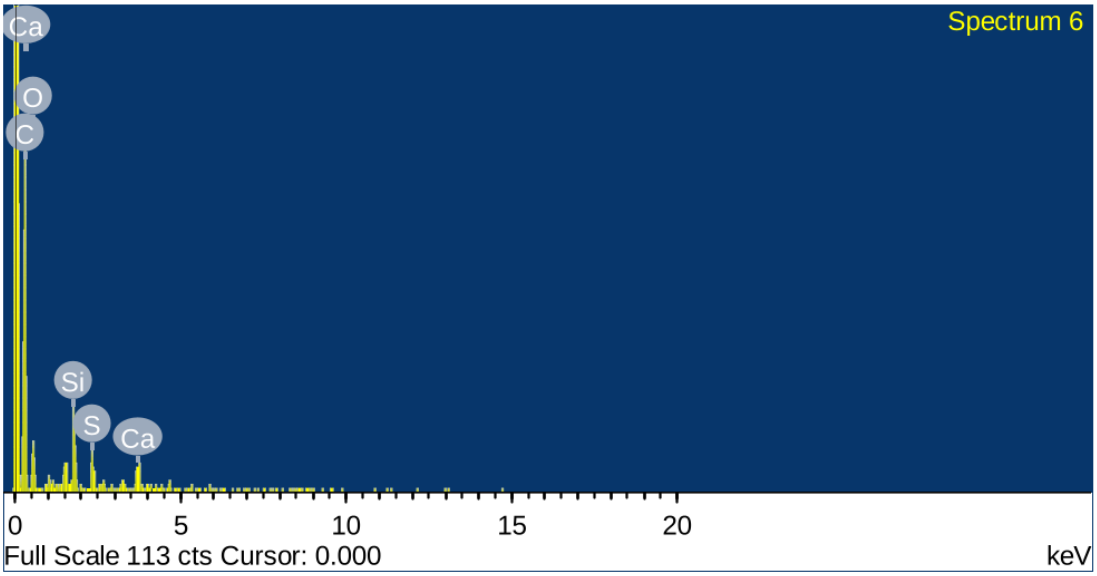

Fig. 3.14 EDX data of rubber with surface treatment by 15% H_2SO_4

Table 3.13 Percentage weight of chemical elements with surface treatment by 15% H_2SO_4

Element	Weight %	Atomic %
C K	70.25	78.10
O K	22.71	18.95
Si K	3.20	1.52
S K	1.74	0.72
Ca K	2.10	0.70
Total	100	

Table 3.14 Comparison of all samples of chemical elements with and without surface treatment

Element	Without surface treatment		With surface treatment 10% H_2SO_4		With surface treatment 15% H_2SO_4	
	Weight %	Atomic %	Weight %	Atomic %	Weight %	Atomic %
C K	62.80	71.52	73.24	80.13	70.25	78.10
O K	29.92	25.58	21.69	17.82	22.71	18.95
Si K	2.39	1.16	1.85	0.86	3.20	1.52
S K	0.64	0.27	1.67	0.68	1.74	0.72
Ca K	2.56	0.87	1.46	0.48	2.10	0.70
Zn K	0.88	0.18	0.09	0.02	-	-
Al K	0.80	0.40	-	-	-	-
Total	100		100		100	

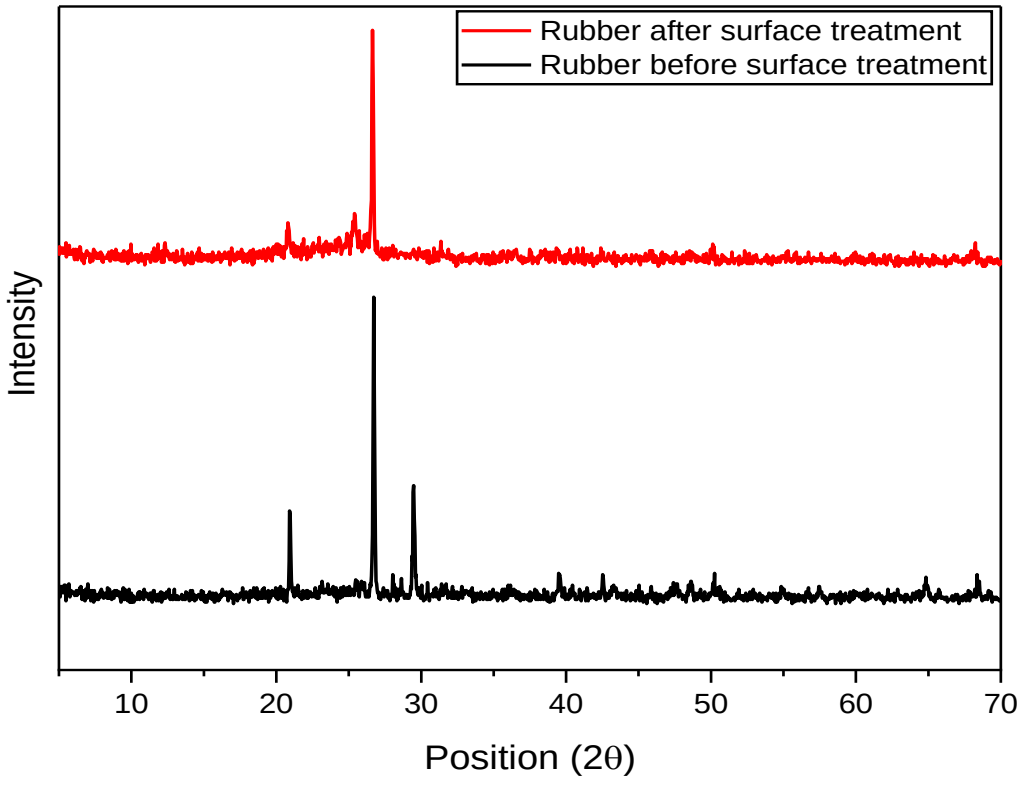

Fig. 3.15 XRD data of rubber before surface treatment and after surface treatment by 15% H_2SO_4

Table 3.15 XRD data of rubber without surface treatment and after surface treatment

S. no.	Material	Peaks No.	Peaks Angle	h k l	d Spacing	Chemical Formula	Chemical Name	Crystal System
1	Rubber without surface treatment	1	20.9467	1 0 0	4.24108	SiO_2	Silicon Oxide	Hexagonal
		2	26.7382	1 0 1	3.33417	SiO_2	Silicon Oxide	Hexagonal
		3	29.4805	1 0 4	3.02997	$CaCO_3$	Calcium Carbonate	Rhombohedral
		4	42.5557	2 0 0	2.12443	SiO_2	Silicon Oxide	Hexagonal
		5	50.3433	1 1 2	1.81255	SiO_2	Silicon Oxide	Hexagonal
		6	64.854	3 0 0	1.43652	$CaCO_3$	Calcium Carbonate	Rhombohedral
2	Rubber after surface treatment	1	20.8198	1 0 0	4.26665	SiO_2	Silicon Oxide	Hexagonal
		2	25.4372	1 1 1	3.50166	SO_2	Sulfur Oxide	Orthorhombic
		3	26.6557	0 1 1	3.34429	SiO_2	Silicon Oxide	Hexagonal
		4	50.1246	0 0 3	1.81995	SiO_2	Silicon Oxide	Hexagonal
		5	68.1166	2 0 3	1.37544	SiO_2	Silicon Oxide	Hexagonal

So 15 wt% H_2SO_4 solution is used to treat rubber tire particles in this study to remove zinc from the rubber crumbs and enhance the mechanical property of RuC instead of rubber crumbs without treatment and treated with 10 wt% H_2SO_4 solution. The H_2SO_4 solution reacts with the zinc element in this treatment process, forming zinc sulfate, which can be washed away with tap water because it is soluble in water. This process reduces the hydrophobic nature and enhances the hydrophilic nature of rubber crumbs so the rubber can make a better bond with the cement matrix and enhance the mechanical properties of RuC.

3.1.6.3 TGA and DTG of Rubber

Thermal gravimetric analysis (TGA) has been done on two rubber samples to analyze the weight-temperature relationship of the material. TGA is primarily used to characterize materials by measuring their change in mass as a function of temperature. Through this process and the measurements that can be very accurately derived from it. TGA can be used to determine a substance's: changes in mass due to decomposition, oxidation, evaporation, or combustion and volatilization rate of materials. Moreover, TGA provides

information about physical phenomena, such as phase transitions, absorption, adsorption and desorption; as well as thermal decomposition, and solid-gas reactions (e.g., oxidation or reduction). TGA is especially useful for studying polymer-based products that need to react to high heat or rapid temperature changes. The most common application of TGA in the industry is to test the thermal resistance of products for quality assurance and safety purposes. For example, industries including polymer manufacturing, plastic manufacturing and general manufacturing may use TGA. By testing a material's resistance to heat and temperature fluctuations, as well as identifying the points at which it decomposes, evaporates, or otherwise breaks, analysts can determine whether a product meets industry-standard quality and stability parameters for safe use. TGA is used for quality control and assurance and thermal stability determination because rubber crumbs are polymer material and it has to be tested for thermal analysis before using in the concrete. It is necessary to check the thermal stability of rubber crumbs because when it will be used in concrete, the structural components of RuC can deteriorate due to high thermal exposure. This technique is very useful in the field of civil engineering because the thermal stability of concrete materials can be analysed. The mass or phase changes due to high temperature in rubber crumbs can be identified by TGA. The experimental procedure and results are given below.

There are two rubber crumbs samples are tested, one is without surface treatment and another is with surface treatment by 15% concentration H_2SO_4 solution. After analysing both the rubber samples by comparing their results, a decision can be made about which sample should be used in RuC. A small amount of rubber particle, approx 10 mg, is taken for TGA in this process. The sample is burned from 0 to 550℃ with a nitrogen atmosphere at the rate of 10℃/min and then cooled down to 350℃. In the second stage, the sample again burns up to 800℃ with the oxygen atmosphere. These specific settings are selected according to ASTM D6370-99 (Reapproved 2019) [101]. The weight of the sample is weighed simultaneously with the burning process. For rubber crumbs without surface treatment in TGA, 73.42% of the weight is lost in the first stage due to evaporation, oils, and an organic substance present in rubber crumbs. In the second stage, 7.29% of the weight is lost due to carbon black present in the rubber crumb, and 19.28% of residue remains. It is challenging to analyze the proper temperature of weight loss from the TGA graph, so its derivative is necessary to examine the exact temperature of

phase changes. The phase changes with proper temperature can be measured from the DTG (Derivative Thermogravimetry) curve. In the DTG graph, the phase of the rubber crumb changes from 300℃ to 500℃ Fig. 3.16(a).

From the second sample of rubber particles after surface treatment by H_2SO_4 solution, 58.33% of the weight is lost in the first stage due to evaporation, oils, and an organic substance present in the rubber crumb. In the second stage, 14.50% of the weight is lost due to carbon black, which is present in rubber crumbs, and 27.33% of residue remains. In the DTG graph, the first phase of the rubber crumbs changes from 300℃ to 500℃, and the second phase is changed from 600℃-750℃ Fig. 3.16(b).

From Fig. 3.16(a) & (b), after the rubber sample's burning process, only 26.58% of the residue is retained in untreated rubber, but the treated rubber remaining residue is 41.67% at the temperature range of 300-500℃, which is confirmed by DTG graph. The surface-treated rubber has more stability against temperature compared to untreated rubber. As a result, RuC after acid treatment of rubber crumbs is more temperature stable than RuC without acid treatment of rubber crumbs.

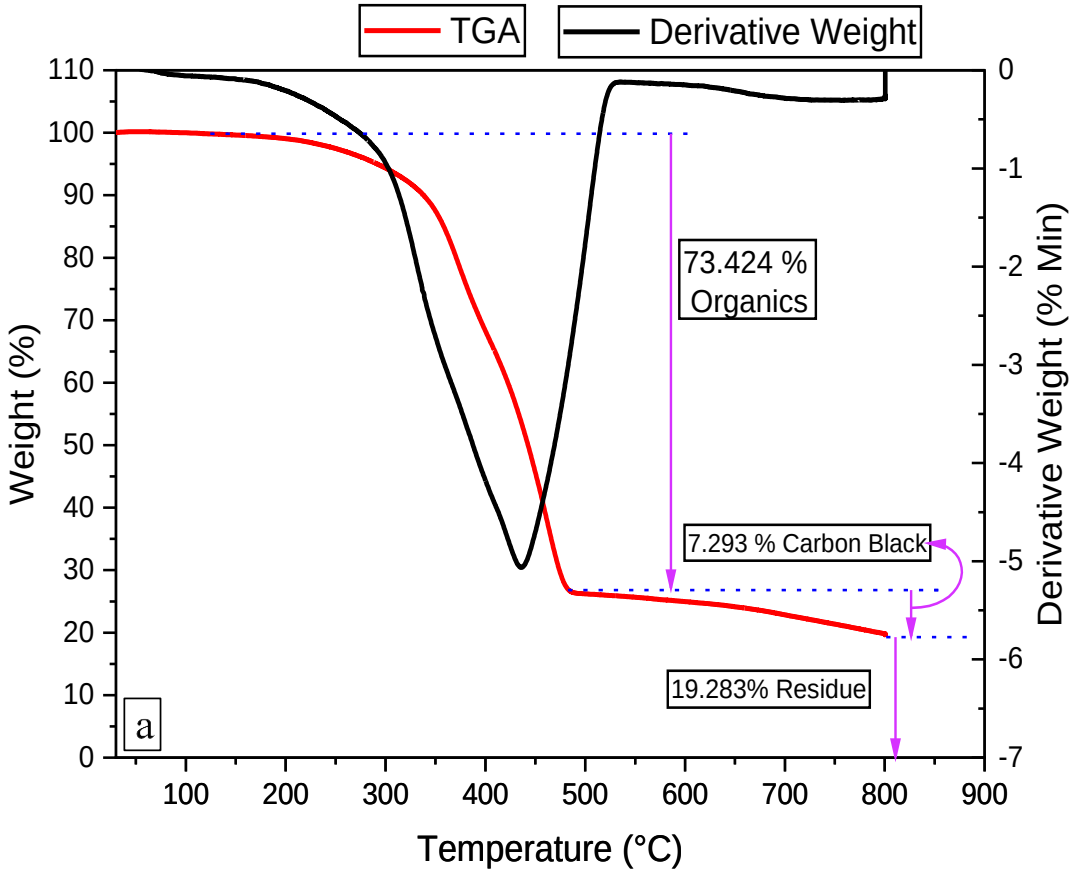

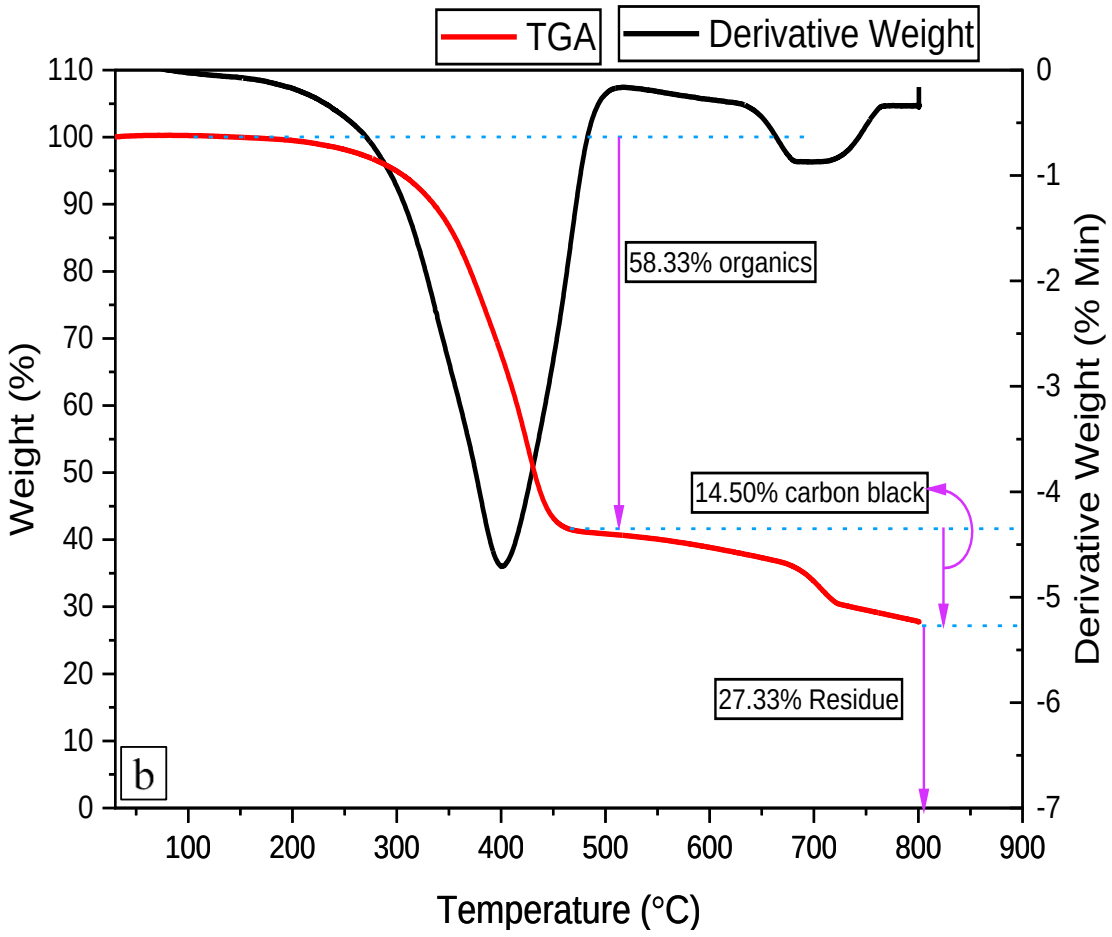

Fig. 3.16 (a) TGA analysis of rubber without surface treatment (b) TGA analysis of rubber with surface treatment by 15% H_2SO_4

3.2 Mix Design (IS 10262:2008)

After the material samples have been tested for concrete control, the mix design calculations are completed. The concrete mixes are prepared with a w/c ratio of 0.38 with a partial replacement of FA by rubber particles with a 0-30% replacement level by weight. Mix design is made for M_{40} grade concrete. The different mix designs utilised in the study for the testing are listed in Table 3.16. According to IS 10262:2008 [102], the concrete mix design was made.

Target strength for mix proportioning

$$F'_{ck} = f_{ck} + 1.65s \quad \text{(i)}$$

where

F'_{ck} = Target average compressive strength at 28 days

f_{ck} = Characteristics compressive strength at 28 days

s = Standard deviation

From Table I of IS 10262:2009, standard deviation, s = 5 N/mm^2.

Therefore, target strength = 40 + 1.65 x 5 = 48.25 N/mm^2.

Selection of water-cement ratio

From Table 5 of IS 456 for very severe exposure maximum water-cement ratio is 0.40

Based on experience water-cement ratio = 0.38

0.38 < 0.40 Hence ok.

Selection of water content

From Table 2 of IS 10262:2009, maximum water content for 20 mm aggregate = 186 litres (for 25 to 50 mm slump range)

Estimated water content for 100 mm slump (based on trials)

$$= 186 + \left(\frac{3}{100}\right) X 186 = 191.58 \text{ litres} \quad \text{(ii)}$$

(Note: If SP is used, the water content can be reduced up to 20% and above.)

Based on trials with SP, water content reduction of 23% has been achieved; hence the arrived water content

$$= 191.58 - [191.58 X \left(\frac{23}{100}\right)] = 148 \text{ litres.} \quad \text{(iii)}$$

Calculation of cement content

Adopted w/c Ratio = 0.38

Cement content = $\frac{148}{0.38} = 390$ kg/m^3

From Table 5 of IS 456, the minimum cement content for ‘Very severe’ exposure conditions is 360kg/m^3

390 kg/m^3 > 360 kg/m^3 hence ok.

The proportion of the volume of CA and FA content

From Table 3 of (IS 10262:2009), the volume of CA corresponds to 20 mm size aggregate and FA (Zone II) for the water-cement ratio of 0.50 =0.62.

In the present case, the water-cement ratio is 0.38. Therefore, the volume of CA is required to be increased to decrease the FA content. As the water-cement ratio is lower by 0.10, the proportion of the volume of CA is increased by 0.02 (at the rate of -/+ 0.01 for every ± 0.05 change in water-cement ratio).

Therefore, the corrected proportion of the volume of CA for the water-cement ratio of 0.38 = 0.644

Volume of FA content = 1 – 0.644= 0.356

Mix calculations

The mix calculations per unit volume of concrete shall be as follows:

a) Volume of concrete = 1 m^3 (iv)

b) Volume of cement = $\frac{[Mass\ of\ cement]}{\{[Specific\ Gravity\ of\ Cement]X\ 1000\}}$ (v)

$$= \frac{[390]}{\{2.92X\ 1000\}} = 0.133\ m^3$$

c) Volume of water = $\frac{[\boldsymbol{Mass\ of\ water}]}{\{[\boldsymbol{Specific\ Gravity\ of\ water}]\boldsymbol{X\ 1000}\}}$ (vi)

$$= \frac{[148]}{\{1X\ 1000\}} = 0.148\ m^3$$

d) Volume of chemical admixture (By marsh cone apparatus used 1.4% by the weight cement) = $\frac{[Mass\ of\ \text{chemical admixture}]}{\{[Specific\ Gravity\ of\ \text{chemical admixture}]X\ 1000\}}$

$$= \frac{[5.46]}{\{[1.09]X\ 1000\}} = 0.00500\ \text{litres/}\ m^3 \quad \text{(vii)}$$

e) Volume of all in aggregate = [(iii) - {(iv) + (v) + (vi)}]

= [1-(0.133+0.148+0.00500)] = 0.7140 m^3 (viii)

f) Mass of CA = e X volume of CA X Sp. Gr. of CA X 1000

= 0.7140 X 0.644 X 2.79 X 1000 = 1283 kg/m^3 (ix)

g) Mass of FA = e X Volume of FA X Sp. Gr. of FA X 1000

= 0.7140 X 0.356 X 2.62 X 1000 = 666 kg/m^3 (x)

Cement	**Fine aggregate**	**Coarse aggregate**
(Kg\m^3)	**(Kg\m^3)**	**(Kg\m^3)**
390	666	1283
1	1.70	3.28

Table 3.16 Mix designs of various mixes

Mix no.	**Cement (kg/m^3)**	**FA (kg/m^3)**	**CA (kg/m^3)**		**RC (wt %)**	**RC (kg/m^3)**	**W/C ratio**	**SP (%)**
			(20 mm)	(10 mm)				
R1	390	666	770	513	0	0	0.38	1.4
R2	390	599	770	513	10	67	0.38	1.4
R3	390	566	770	513	15	100	0.38	1.4
R4	390	533	770	513	20	133	0.38	1.4
R5	390	500	770	513	25	166	0.38	1.4
R6	390	466	770	513	30	200	0.38	1.4

3.3 Mixing, Casting, and Curing

All of the materials are mixed in the pan mixture according to their proportions in the mix designs for making the controlled PPC concrete and RuC. According to the IS code, the mixing process was used [103]. It is necessary to maintain the workability of concrete mixes; the amount of SP is used at 1.4%. Machine mixing is adopted for the homogeneity of the concrete shown in Fig. 3.18. First, dry mixing of material is done for 2-3 minutes,

then water and SP are mixed with materials and cast in the mould of the specimens for 24 hours. A mechanical vibrator is used for the compaction and uniformity of the concrete. One of the issues is that the vibration's additional time pushes up the rubber particles on top of the concrete. Due to this problem, RuC is not homogeneous. Vibration time for mix has been adopted 5-10 seconds to overcome this problem [43], or other hands can be tried for self-compacting RuC. The concrete specimens are cured in the clean water tank free from oils shown in Fig.3.19. For testing, specimens in the shapes of a cube, a cylinder, and a beam are formed from both kinds of concrete.

Fig. 3.17 Weighing of materials

Fig. 3.18 Pan mixture in the laboratory

Fig. 3.19 Curing of concrete specimens in clean water

3.4 Test Setup

3.4.1 Slump

Slump tests are used to evaluate the workability (physical property) of fresh concrete in accordance with the IS code [104]. Concrete workability testing on-site or in a lab is most frequently done by using the slump. The workability of concrete is essential for selecting any waste material for its potential use in concrete. Lack of compaction in concrete will lead to air voids and will impact on strength and durability of concrete. To minimize the effect of air voids and ensure the excellent compaction of concrete, a suitable w/c ratio should be selected. A proper quantity of 1.4% admixture Auramix 400 is added to maintain the workability of RuC. A slump test is used to measure RuC's workability. The slump cone top dia.100 mm, bottom dia. is 200 mm and 300 mm in height shown in Fig. 3.20.

Fig. 3.20 Apparatus for slump test

3.4.2 Density

This test is done to determine the density of RuC to check what impact will occur on the density of RuC after incorporating rubber crumbs in concrete. A denser concrete generally provides higher strength, durability and resistance to permeability. In general, concrete has a stronger overall composition when its density is greater. The density of concrete has a direct impact on the concrete's strength, porosity, permeability, and other properties. Prior to destructive testing, the specimens' weight and volume show the density of the specimens. 28 days after casting, the cubed weight is the main factor in determining the density of the mixtures. The cube specimens' mass-to-volume ratio is used to determine the density. The image of a specimen being weighed on a digital scale is shown in Fig. 3.21.

Fig. 3.21 Digital weight machine for finding density by weight of the cube

3.4.3 Compressive strength

The compression tests are mainly used to determine whether the concrete mixture brought to the work location satisfies the specifications for the specified strength. Mechanical tests determine the highest compressive force that a substance can withstand before breaking. The compressive strength of concrete is the primary mechanical

property of hardened concrete. The compressive strength of concrete mixes is tested on cube samples under the CTM machine at a 140 kg/cm^2/min loading rate statically applied to the specimens [105]. The mould's size for cubes is 150X150X150 mm as per the IS code [106]. The mix samples are tested at 7, 14, 28, and 90 days after casting the specimens. Fig. 3.22 shows the picture of a cube specimen during the compressive strength test on the UTM. The cube's testing surface should be placed so that the cube mold's free surface should not be placed between the hydraulic machine's surface, as shown in Fig. 3.22.

Fig. 3.22 Testing setup for compressive strength in the CTM

3.4.4 Splitting Tensile Strength

Tensile strength is one of the crucial characteristics of concrete because structural stresses make it susceptible to tensile cracking. Splitting tensile strength is the indirect tensile strength test for concrete because the direct tensile test is difficult for concrete. Being brittle, concrete is weak under tension and susceptible to cracking. So it is important to perform the split tensile strength test of concrete. The Split tensile strength of concrete is tested on cylinder specimens with 150 mm diameter and 300 mm height as per the Indian Standard code [106]. The load shall be applied within the range of rate 1.2 N/(mm^2/min) to 2.4 N/(mm^2/min) without shock and maintain the loading rate until failure. The cylinder specimen shall be placed along the top and bottom of the plane of loading of the specimen. Two iron plates shall be positioned for testing, one is above, and the other is below the cylinder specimen. Fig. 3.23 shows the picture of the cylinder specimen for the splitting tensile test.

Fig. 3.23 Testing setup for splitting tensile strength of concrete

3.4.5 Flexural Strength

Flexural strength is also called a rupture of the concrete used to find the bending capability of the concrete specimens. It is a measurement of a concrete slab's or beam's ability to withstand failure in bending. If the maximum aggregate size is less than equal

to 20 mm, then the standard size 100X100X500 mm beam is used for the cast specimens to analyze the flexural strength [106]. A two-point load (third-point loading) is applied along the transverse direction of the specimens for the test on the flexural testing machine. The load shall be applied to the specimen's uppermost surface along two lines having spaced 13.3 mm. The specimen shall be placed on two rollers 400 mm apart, as shown in Fig.3.24. Fig. 3.25 shows the picture of a prism or beam specimen during the flexural strength test. The load shall be applied at the 180 kg/min rate without shock and maintain the loading rate until failure.

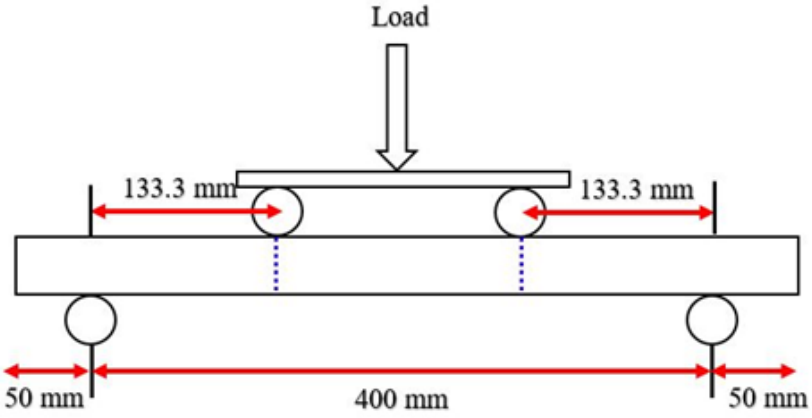

Fig. 3.24 Marking and position of specimen for testing flexural strength of concrete

Fig. 3.25 Testing setup for flexural strength of concrete

3.4.6 Elastic Modulus and Poisson Ratio

This test is used to measure the stiffness or rigidity of concrete under static loading conditions. This test evaluates its ability to resist deformation when subjected to an external force or load. The Poisson's ratio is determined by the ratio of transverse strain to axial strain when concrete is subjected to compressive load. This test is used to determine its capability to resist lateral deformation when the compressive force is applied to the concrete column specimen. The concrete mix's elastic modulus and Poisson ratio are determined by testing cylindrical specimens. The Poisson ratio is calculated from the displacements through the ratio of horizontal strain to vertical strain. The elastic modulus finds through the load applied to the cylindrical specimens, about one-third of their strength and release and going continuously for the same procedure many times; then, draw the stress-strain graph and find the elastic modulus as per the IS code [105]. Poisson's ratio, MOE, is also tested on the universal testing machine with the help of LVDTs (Linear Variable Differential Transformer) on a specimen size of 300 mm X 150 mm [106]. LVDTs are also used to find the lateral and longitudinal deformation of standard and RuC. The loading rate is applied gradually to the sample at 140 kg/cm^2/min for the concrete test's modulus of elasticity [105]. For specimen preparation, neat cement capping is done after 2-3 hours of casting. The uniformity of capping is checked by a perpendicular tool in Fig. 3.26(a). The specimen's marking should be such that the extensometer's upper and lower ring makes an equal distance from the specimen's upper surface and lower surface. The middle ring of the extensometer for Poisson's ratio is placed at the exact mid-height of the cylinder specimen in Fig. 3.26(b). Two LVDTs are placed to find the modulus of elasticity and Poisson's ratio; one LVDT is placed in the axial direction of load, and the second LVDT is placed in the lateral position of the axial load. The arrangements of LVDTs and extensometer of cylinder specimen are shown in Fig. 3.26(c). For measuring and controlling LVDTs, AI 8000+ Data Acquisition and Control System with "Prosof" software is used for MOE, and Poisson's ratio Fig. 3.26(d) according to IS code [105]. Fig. 3.26(e) shows the testing setup for static MOE and Poisson's ratio.

Fig. 3.26 (a) Capping of the cylinder specimen, (b) Marking of the cylinder specimen, (c) Arrangements of extensometer and LVDTs, (d) Data accusation system for LVDTs, (e) Testing setup of the cylinder for modulus of elasticity and poison's ratio

3.4.7 Rebound Hammer

A rebound hammer identifies the strength through the surface indentation of the concrete samples. Before the destructive test on the samples, the rebound strength of all mix specimens is measured at 7, 14, and 28 days after casting. Proceq Schmidt Digital Concrete Test Hammer is used to analyse the compressive strength of concrete according to IS code [107]. The surface hardness of the specimens influences the rebound strength of the concrete. The rebound test should be performed when the cube specimen is fixed between both faces of the hydraulic machine, as shown in Fig. 3.27. This technique gives

accurate compressive strength results, but when the specimen is on the floor, the testing is done in a downward direction; it does not provide accuracy.

Fig. 3.27 Rebound hammer testing of the cube for the compressive strength test

3.4.8 UPVT (Ultrasonic pulse velocity test)

The ultrasonic pulse velocity (UPV) test is a non-destructive test for concrete strength, analyzed through the speed of passing ultrasonic pulse waves through the concrete. UPVT also analyses the dynamic Poisson ratio and dynamic MOE of the concrete by testing beam specimens of that mix [108]. A non-destructive test by 'MATEST' UPV tester is performed on prism samples to examine wave propagation's velocity in the material and the dynamic MOE of the different concrete mixes, as shown in Fig. 3.28 according to IS code [109]. A UPV measuring instrument and two transducers with a frequency of 54 kHz are used to measure the wave's propagation time through the specimen. An adequate amount of gel is applied between the concrete prism's surface and the transducer to confirm the proper connection. The measured ultrasonic pulse velocity is used for calculating the dynamic MOE. The UPV test measures the passage of time from the specimens to determine the performance of the hard material. When the time transit of the UPV wave through the specimen is large, it indicates that the concrete is weaker and vice versa.

Fig. 3.28 Ultrasonic pulse velocity testing setup of standard concrete and RuC

3.4.9 Impact resistance by flexural loading test

This test is used for determining the impact resistance by flexural loading test. Impact resistance is the capacity of concrete to absorb energy and resist repeated impacts without suffering detrimental effects like cracking and spalling. When concrete is subjected to frequent shock loads or impact loads, impact resistance is a key factor in how well it performs. This test is performed on three prism specimens of every mix (R1-R6), and prism specimens are 100X100X500 mm in size and are measured on a 400 mm centre-to-centre simply supported span. From a height of 200 mm, a 2 kg hammer is released to test the impact resistance. Testing setup for measuring impact energy by the flexural loading of standard and RuC is shown in Fig. 3.29. The procedure is performed continuously until the prism fails, and the number of drops until collapse is counted and represented by N*f* [23]. E_{fl} is the accumulated energy that the dropping hammer provides to the specimens (where subscript *fl* indicates flexural loading) and is estimated as follows:

$$\mathbf{E}_{fl} = \sum_{\mathbf{i=1}}^{\mathbf{Nf}} \mathbf{m_i gh} \tag{3.1}$$

where m_i = mass of drop hammer (2.0 kg), and h = drop height (200 mm).

Fig. 3.29 Testing setup for impact energy by the flexural loading of standard and RuC

3.4.10 Impact Resistance by Rebound Test

This test is used for determining the impact resistance by rebound test. The examination for rebound impact loading is performed on 150 mm cube specimens. Three specimens are cast for each mix to test the impact resistance of concrete. Testing setup for finding impact resistance by rebound test of standard and RuC is shown in Fig. 3.30. A steel ball weighing 300 gm is used to transmit impact energy from a height of 1.0 m to the specimens in the testing. A sensitive camera is used to monitor the height of the ball's rebound after contact. The energy imparted to the cube specimen is considered to be the difference between the original and final potential energy. "The initial and final potential energies are denoted by $E_{p,ri,}$ and $E_{p,rf}$ respectively (the subscripts *p*, *ri*, and *rf* indicate potential energy at initial and final rebound stages, respectively), and can be calculated as follows" [49]:

$$\mathbf{E}_{p,ri} = \mathbf{mgh}_i \tag{3.2}$$

$$\mathbf{E}_{p,rf} = \mathbf{mgh}_f \tag{3.3}$$

where m = mass of steel ball (0.3 kg)

h_i = preliminary height of steel ball (1.0 m)

h_f = height noted after a rebound.

The discrepancy between the final and initial potential energy is used to assess the energy absorption capacity of the concrete specimen $E_{p,r}$.

$$\mathbf{E}_{p,r} = \mathbf{E}_{p,ri} - \mathbf{E}_{p,rf} \tag{3.4}$$

Fig. 3.30 Testing setup for impact resistance by rebound test of standard and RuC

3.4.11 Pull Off test

The direct tensile strength of a material or the bond strength of an interface is measured using concrete pull-off tests. Following ASTM D7234-19, the Standard test method for the tensile strength of concrete surfaces and the bond strength by direct tension is the procedure used in this testing. The test establishes the maximum perpendicular tension force that a surface can withstand before a material plug detaches. The weakest plane within the concrete will experience failure. In RuC, rubber crumbs are used and the bonding of rubber crumbs and the concrete matrix is weak, so we have to test the direct tensile or bond strength of RuC. The Pull-Off test is performed on concrete specimens according to the recommendations of ASTM [110]. Concrete slabs of 50X35X6 cm are moulded in the laboratory with various concrete mixes to investigate the pull-off test. Three specimens are cast for every mix to test the pull-off strength of the concrete. An aluminium disc with a diameter of 50 mm is used in the experiment. The investigation is carried out using a 10 mm deep scouring using the core cutter shown in Fig. 3.31(a) according to the metallic disc's size. The scouring of the concrete specimen is done to evade the influence of the concrete's adjacent surface. Fig. 3.31(b) shows the scouring pattern of the specimen. The surfaces are primed with a grinder before beginning the bonding of metallic discs on the concrete surface to ensure strong adhesion. An epoxy resin is used as an adhesive, and the specimen is left for 24 hours to make a good bonding between the disk and the specimen shown in Fig. 3.31(c). The bonding area is carefully chosen to confirm that the adhesive should be present along the whole contact surface between the disc and the concrete, allowing the tensile force to be exerted evenly throughout the bonding region. A thin adhesive layer is added between the disc and the concrete surface for strong bonding. A compact device, the "DYNA Z6 Proceq," applies a tensile force to the disc by applying the epoxy resin used for sticking the disc to the concrete shown in Fig. 3.31(d). With the help of a digital meter placed on the instrument, the incremental rise in pull-off strength can be observed, and the ultimate pull-off strength is reported as soon as the concrete fails.

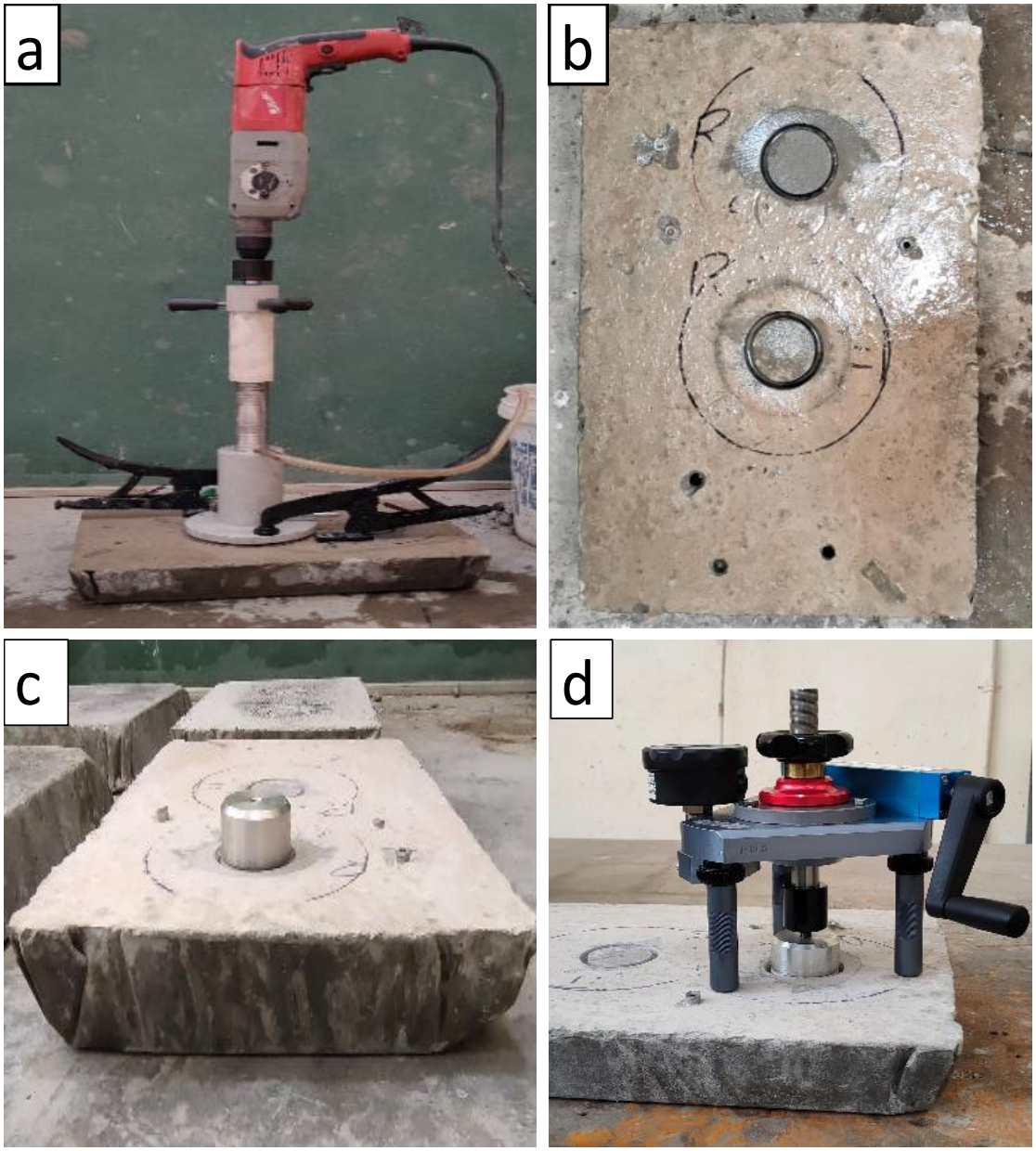

Fig. 3.31 Testing setup of the pull-off test (a) scouring of the specimen by core cutter (b) scouring pattern and surface preparation (c) adhesion of disk and the specimen (d) pull-off testing of concrete

Fig. 3.32 Side view of the pull-off tester on slab specimen

Fig. 3.33 Top view of the pull-off tester with a digital recorder on slab specimen

3.4.12 Four-probe resistivity test

This test is used for assessing the quality or durability of RuC. This is the one common method which is quite easy to use on-site is the Wenner Four-probe resistivity test. The resistivity that concrete is going to be conducting through its interconnected porosity. Moreover, resistivity gives a direct measurement of the permeability or interconnectivity of the pores in the system. The testing setup for the experiment is present in Fig. 3.34. This test is used to measure the durability of concrete according to IS 15736:2007 [111]. If the concrete has a very less amount of pores' interconnectivity, the resistivity is expected to be high, which means the durable concrete will have a higher resistivity. A portable Proceq resistivity meter with four probes mounted foam in base equidistance to each other is used to test the resistivity of the standard and RuC. Two outer probes apply the current, while the two inner probes measure the potential. One major drawback of this test is the concrete should be fully saturated. If the concrete is unsaturated the resistivity will be very high because of the lack of moisture in the porosity. The porosity has to be filled with water for conductivity or else this test will not give exact results.

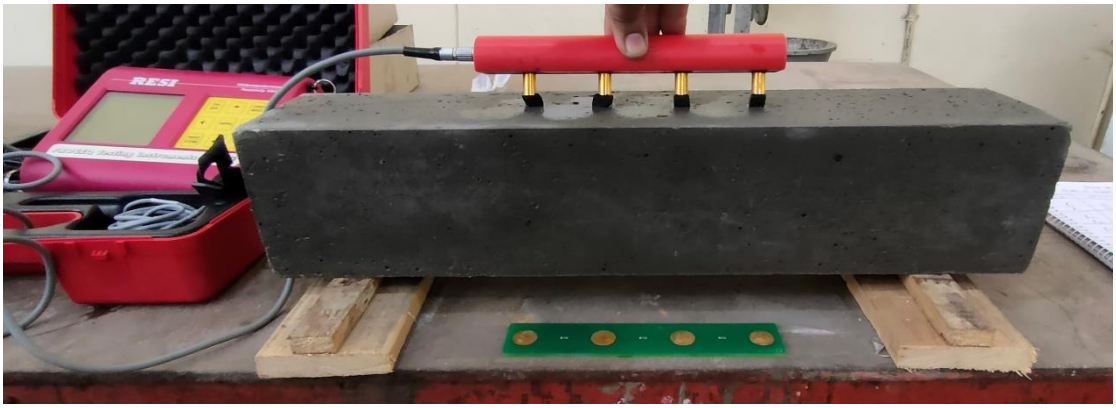

Fig. 3.34 Testing setup for resistivity of the concrete

3.4.13 Water absorption

The water absorption test is used for determining the durability of concrete. The test is used to measure the increase in concrete sample mass caused by water absorption when the specimen is exposed to water. The water absorption rate (sorptivity) is assessed using the water absorption test. The process of determining water absorption in different ways is explained below according to ASTM C462 [112].

Oven-dry weight - The cube specimen is placed in an oven at 110°C for 24 hours after 28 days of curing. The specimen is then allowed to cool in the air at room temperature

after removing it from the oven to measure the weight of the specimens. The specimens' weight is tested after the first 24 hours of oven-drying and again after another 24 hours of drying. If the weight difference between the first and second weights is greater than 0.5 percent, put it in the oven for a third time for 24 hours to dry. If the weight of the cubes after the third drying period is near to the weight after the second, it is called a dry specimen; otherwise, place the specimens in the oven for an additional 24 hours and continue until the discrepancy between any two consecutive values is less than 0.5 percent.

Saturated mass after immersion - After final drying and cooling, the specimens are immersed in water for at least 48 hours at about 21°C. The weight of the specimens is noted after being surface-dried by extracting surface moisture with a towel. The specimens are immersed in water for 24 hours until the surface-dried sample's consecutive weight values indicate a mass rise of less than 0.5 percent. It is called the surface-dry weight after final immersion.

Saturated mass after boiling - The specimens are boiled for 5 hours after placing them in an appropriate boiling tank and are covered with tap water. The specimens should be allowed to cool to a final temperature of 20 to 25°C by natural heat loss for at least 14 hours. The weight of the specimens is noted after removing the surface moisture with a towel. It is called the saturated weight after boiling and surface drying.

3.4.14 Acid attack

The acid attack test is used to determine the durability of RuC. this test gives information on how the RuC reacts/resists due to exposure to acid. The tests includes under acid attacks such as visual inspection, mass loss and compressive strength loss. Visual examination can provide an extensive amount of information that could help positively identify the source of any suffering (cracks, spalling) that is being experienced. The compressive strength and weight difference test gives information about how much strength and weight is loose after exposure to acids. For the study, the test specimens are in collections of three specimens. Before the immersion in acid, the specimens are water-cured for 28 days. After curing, two measures are taken for each specimen, one at mid-height and the other perpendicular to the load axis. The specimens are weighed on a digital weighing machine after the curing period, and the results are recorded. A short

overview of the colour and surface texture of the specimens is recorded before immersing them in acid. The weighted specimens are submerged in acid solutions on their sides in an appropriate tank, taking care not to allow the cube's faces to come into contact with one another. The specimens are cleaned by rinsing them under cool running water and wiping them off quickly with a clean cloth after removing them from the acid solution. The test specimens are allowed to rest in the air for 30 minutes to dry their surfaces after the final wipe-out before weighing. All specimens are weighed to the nearest 0.001 gm. After 30 days of immersion in acid solution, an automatic hydraulic machine is used to determine the specimens' compressive strength. The weight loss or gain of the specimens is calculated after the immersion period. In cases where initial weight differences are significant, visual examination of the specimens for surface cracks, lack of gloss, etching, pitting, softening, and other issues are essential.

3.4.15 Freeze-Thaw

The Freeze-thaw test is also used to determine the durability of RuC. This test gives information on how the RuC reacts/resists due to exposure to very low temperatures. The tests include under Freeze-thaw cycles such as visual inspection, mass loss and compressive strength loss. Visual examination can provide an extensive amount of information that could help positively identify the source of any suffering (cracks, spalling) that is being experienced. The compressive strength and weight difference test gives information about how much strength and weight is lost after exposure to freeze-thaw cycles. The resistance of RuC to freeze-thaw is tested according to ASTM C666/C666M [113]. The Freeze-Thaw process of concrete specimens is performed by Haier deep freezer with model number HDF-245SD/285SD with an external thermometer. Before performing the testing procedure, unplug the freezer before cleaning. Plug the freezer into an electrical outlet with 220 volts and 15 amps after it's in its proper horizontal or non-inclined position. The freezer is equipped with a fast freeze switch, which will allow reducing the temperature quickly. After the freezer is in operation, don't touch the cold surface in the freezer compartment, mainly when hands are wet. The skin may adhere to these extremely cold surfaces. Fig. 3.35 shows the testing setup for freeze-thaw cycles of RuC specimens, and the thermometer shows the lowest temperature of the deep freezer. Before testing, molded specimens are cured for 28 days. Between the moment the specimens are removed from the curing tank and the freeze-

thaw processes are initiated and protected from moisture loss. The specimens are submerged in the thawing water to start the thawing cycle process to continue the freezing-and-thawing experiments. The thawed specimens are removed from the thawing water, keeping the specimens against moisture loss when taken out from the thawing water. The specimens are placed in the deep freezer and kept there for 5 hours at -28°C. The specimens' temperature is alternately dropped from 4 to -28°C for a maximum of 5 hours for the freezing cycle and then raised from -28 to 4°C for the next 2 hours for the thawing cycle. The specimens are adequately supported by a flat spiral of 3 mm wire placed in the bottom of the deep freezer. After every 15 cycles, the concrete specimen's mass, cross-section measurements, and UPV are tested after the thawing cycle or before the freezing cycle. Again, the specimens are placed in the deep freezer. All tests are repeated for each specimen at 15-cycle intervals until exposed to the 90 cycles. Make a record of the visual appearance and any deficiencies when the specimen is checked for mass change, UPV, and dimension change. If the freezing and thawing processes must be broken, keep the specimens frozen.

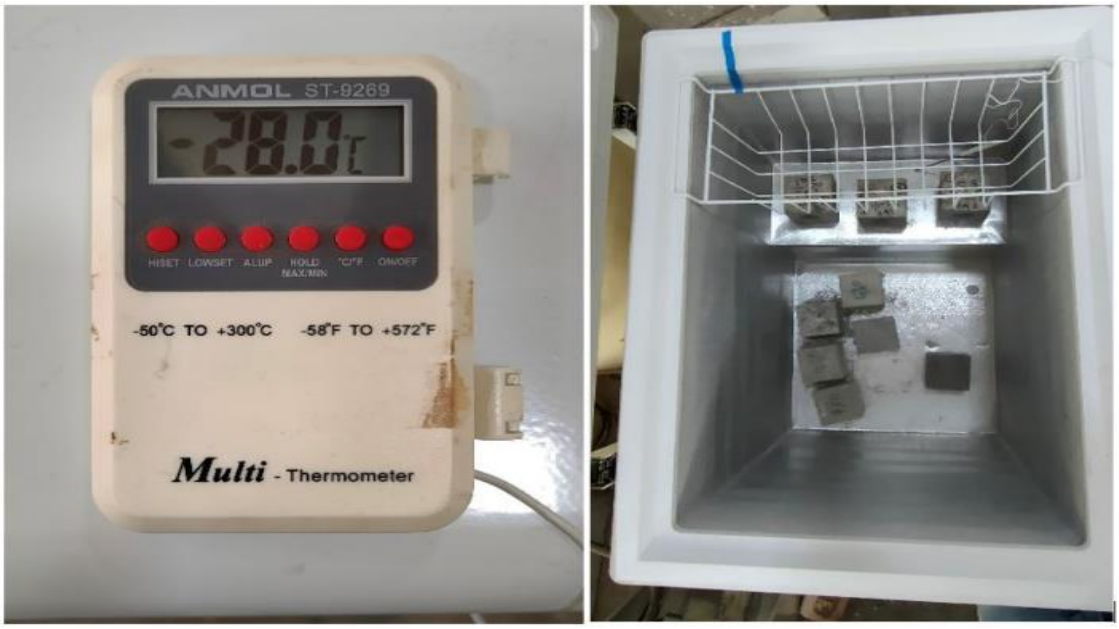

Fig. 3.35 Testing setup for freeze-thaw cycles of RuC specimens

CHAPTER 4 RESULTS AND DISCUSSION

This chapter describes all the experimental results from the mixed design specimens and shows them in the graphs. All the result data obtained from the tests of the specimens are shown in the tables. The experimental investigation tests the specimens for the results of workability, density, compressive strength, splitting tensile, flexural strength, Poisson ratio, elastic modulus, impact resistance by flexural loading and rebound test, pull-off test, and non-destructive tests such as rebound strength, Four-probe resistivity test, and UPVT. The various parameters used to analyze the behaviour of the mix design of the RuC are as follows:

- The effect of the surface treatment of RC by H_2SO_4 solution
- The effect of acid attack
- The effect of freeze-thaw conditions

4.1 The effect of the surface treatment of RC by H_2SO_4 solution

4.1.1 Workability

At the time of batch mixing, 1.4% SP by the weight of cement is used to maintain the workability of concrete. The slump cone results for all mixes are shown in Fig 4.1 and Table 4.1. The results show that RuC's workability decreases with increasing the quantity of RC. For medium workable concrete, the slump value should be 50-100 mm so that all mixes are in the medium range of workability. This range of slump is used for the making of beams, walls, and columns. So this RuC has medium workability so it can be used in beams, walls, and columns. The RuC, replacement level of up to 30%, can be used with reinforced concrete members, and no need to add extra SP to make the concrete workable. A similar decreasing pattern of the slump after increasing RC in concrete is found in past studies [5, 15]. The rubber particles have a rough surface and lead to large undulations in concrete. The greater the rubber content in the mixture, the reduction in the value of the compaction factor would be the more. The inter-particle resistance between the cement matrix and the rubber particles around them is strong, decreasing the mixture's consistency. The RuC mix density decreases in the fresh state, which is the cause of reducing the degree of compaction of the mix [26]. According to Gupta et al. [5][114] the slump value is 73 mm at 15% level of RC without any chemical treatment but in this study, the slump value is 94 mm after chemical treatment of RC which is a better result than from the previous literature.

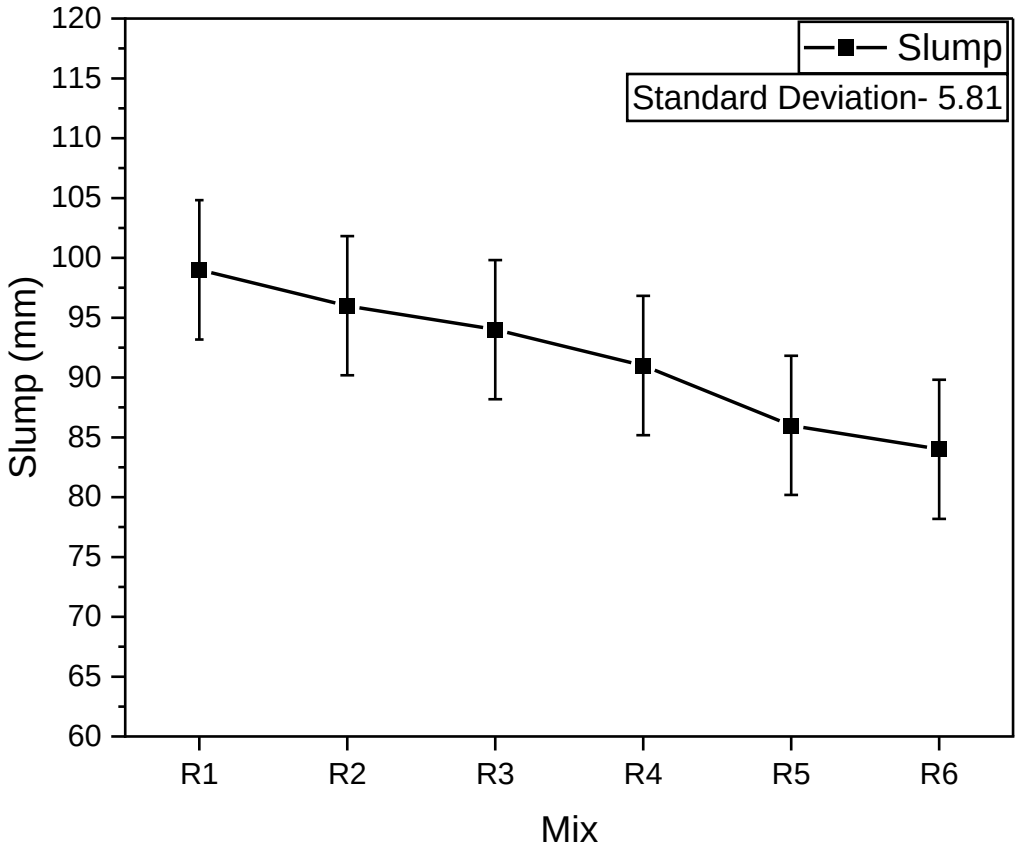

Fig. 4.1 Results of slump for all mixes

Table 4.1 Results of slump for all mixes

Mix	Slump (mm)
R1	99
R2	96
R3	94
R4	91
R5	86
R6	84

4.1.2 Density

The mix's density results are shown in Fig. 4.2 and Table 4.2. The results show that the density of concrete mixtures decreases with increasing the quantity of RC in concrete. The mechanical properties of concrete are highly influenced by its density. A denser concrete generally provides higher strength, durability and resistance to permeability. In general, concrete has a stronger overall composition when its density is greater. The density of concrete has a direct impact on the concrete's strength, porosity, permeability,

and other properties. In this study, the density of the RuC at the 15% replacement level of RC is 2373.33 Kg\m^3 which means this concrete has good concrete and can have good strength and durability. This RuC has low porosity and can resist permeability. So this RuC can be used for construction purposes. The RC has low Sp. Gr. than the FA, which is the reason for the decrement pattern in the density of RuC. A similar decreasing pattern of the density after increasing RC in concrete is found in past studies [5, 15]. "Owing to a low specific gravity value of rubber particles which replaces dense M-sand, the decrease in density ought to have been observed [115]". The sp. Gr. of natural FA is much higher than the waste tire RC, so the density of RuC will decrease. The appearance of entrapped air on rubber particles' rough surfaces could be another explanation for the decrement in the density of RuC [23, 116]. According to Gupta et al., [5, 15] the density value is 2300 Kg\m^3 at 15% level of RC without any chemical treatment but in this study, the density value is 2373.33 Kg\m^3 after chemical treatment of RC which is a better result than from the previous literature.

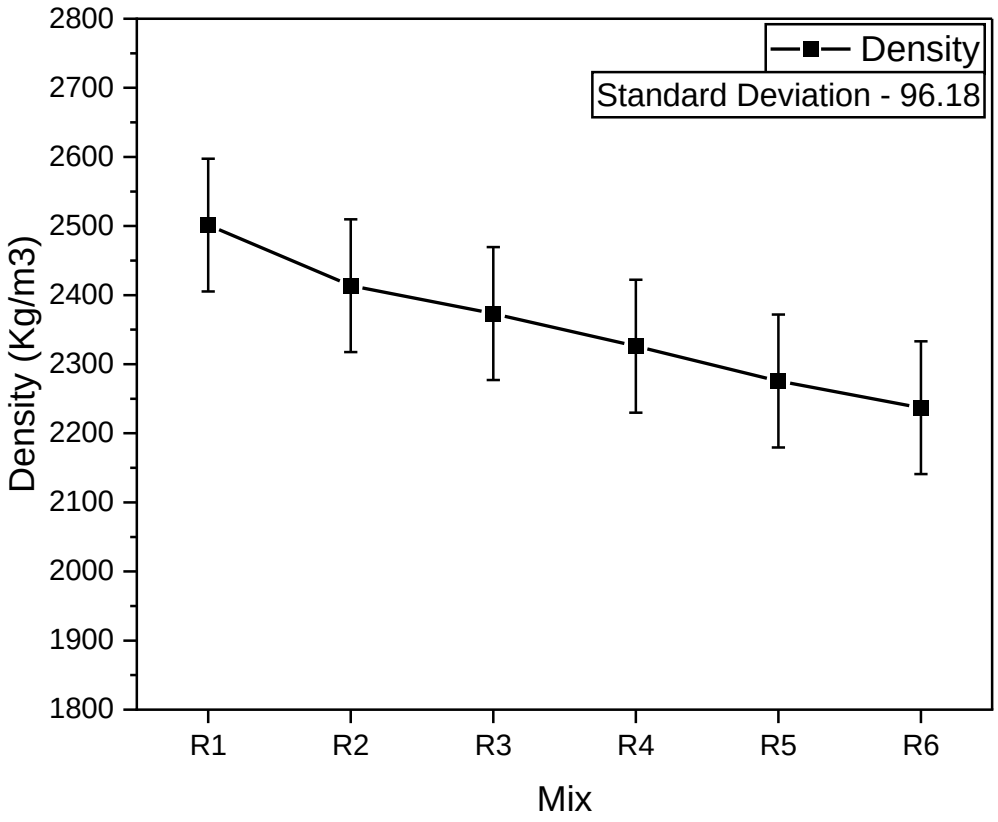

Fig. 4.2 Results of density of all mixes

Table 4.2 Results of density of all mixes

Mix	Density (Kg\m^3)
R1	2501.33
R2	2413.62
R3	2373.33
R4	2325.92
R5	2275.55
R6	2237.03

4.1.3 Compressive Strength

The results of compression tests are mainly used to determine whether the concrete mixture brought to the work location satisfies the specifications for the specified strength. Mechanical tests determine the highest compressive force that a substance can withstand before breaking. The stated strength is used by design engineers to build structural components. In order to reduce the chance of not meeting the strength standard, the concrete mixture should be created that produces an average strength greater than that required. So the compressive strength of concrete should be as much as we require in a specific structural member. The results of the compressive strength of mixes at 7 days, 14 days, 28 days, and 90 days are shown in Fig. 4.3 with replacement levels of RC 0, 10, 15, 20, 25, and 30%. After investigating the results of RuC and comparing it with standard concrete, it is found that there is a decrement in the compressive strength of RuC with an increment of RC in the concrete; however, the 90 days results are more significant than the 28 days results. At 90 days, the compressive strength is enhanced by approximately 9% up to 15% replacement only, compared to 28 days of strength results. After 15% replacement, the curing days don't affect compressive strength, and it is approximately the same as the results of 28 days of curing. The loss in the compressive strength of RuC compared to standard concrete is 18-67% at 7 days, 17-65% at 14 days, 16-64% at 28 days, and 18-66% at 90 days, with the replacement level of RC by 10-30% respectively. The decrement in the compressive strength at the 15% replacement level of RC is just 20.36% after 28 days of curing, and the compressive strength of the RuC is

40.12 MPa, which is suitable for the M40 classification. At 90 days, the compressive strength is 43.38 MPa after surface treatment of rubber by H_2SO_4 and this RuC can be used for the column or other structural members in civil engineering applications. The compressive strength of RuC is not much affected at 15% replacement level of RC after surface treatment of rubber by H_2SO_4.

The concrete's mechanical strength reduction is due to weak bonding between the concrete and the rubber, resulting in slight or no adhesion at the concrete-rubber interface. The hydrophobic characteristic of crumb rubber, which repels water and leads to air entrapment in the RuC microstructure, causes the strength decrease of RuC [14]. The weak interfacial bonding between RC and cement paste is the most likely source of this crack propagation in RuC. A crack can quickly form around the rubber particles because of the poor bonding between rubber particles and the cement paste's surface. After the compression test, the RuC's failure surface inspection revealed that fractures are propagating around the RC particles. On behalf of Uygunoğlu, Topçu, the compressive strength is decreased by 40-64% and 48-58% at 7 and 28 days, respectively, using rubber aggregate without chemical treatment in the concrete mix [58], but in this study, after the treatment process, the decrement is 18-22% at 7-days and 16-21% at 28 days up to 15% replacement of rubber which may be considered as positive results. According to Gupta et al. [5, 15], the replacement level of RC can be used up to 10% only without treatment of RC, but in this study, after surface treatment of RC, the replacement of FA by RC can be up to 15% without significant compressive strength loss. Moreover, according to Qingwen Ma, the reduction in compressive strength at 20% replacement level of RC after rubber treatment by NaOH is 48.95%. Still, in this study, the reduction is 20.36% at 28 days after surface treatment by H_2SO_4 [56]. According to past studies, the compressive strength of concrete decreases by increasing the replacement level of rubber particles in concrete, and they show the same pattern as found in the present study [4, 5, 118, 119, 12, 14, 16, 28, 42, 43, 60, 117]. The surface treatment of RC sulfuric acid reduces the loss in the compressive strength of RuC.

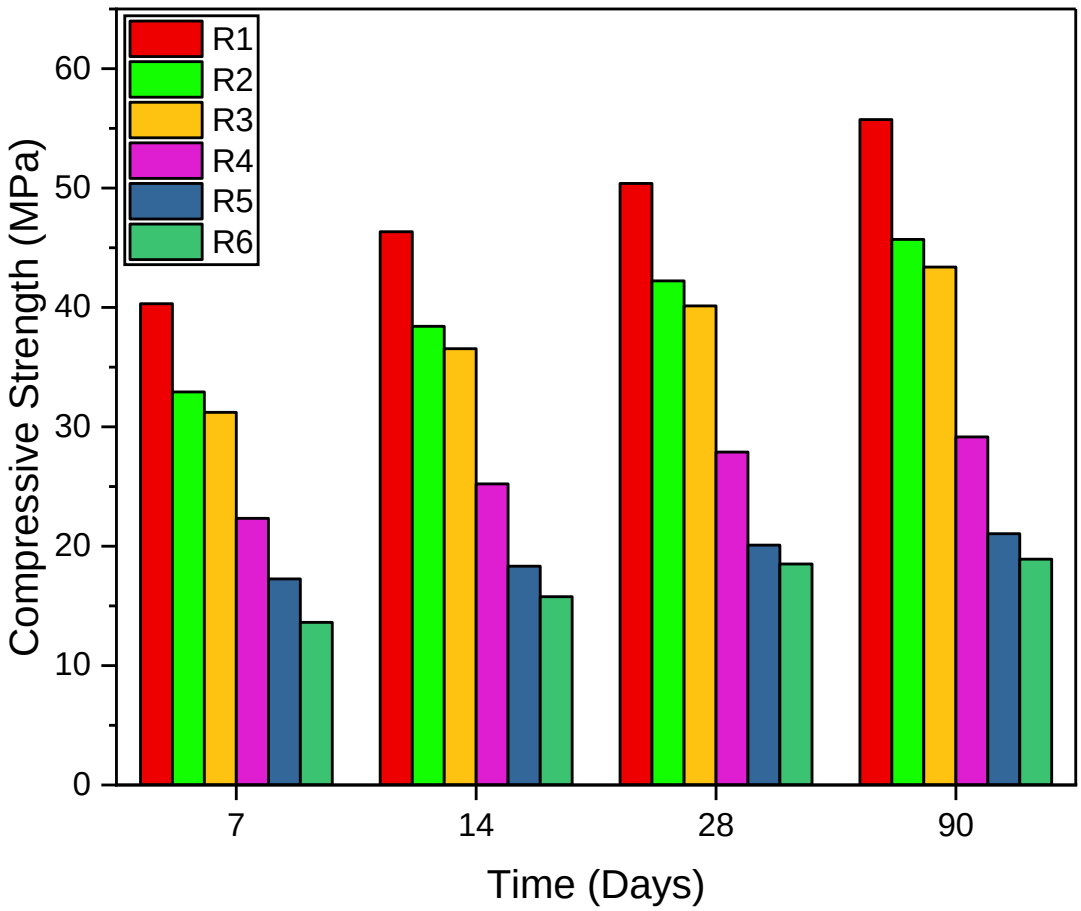

Fig. 4.3 Compressive strength of standard concrete and RuC

Table 4.3 Results of compressive strength of standard concrete and RuC

Mix	f_c (MPa)			
	7 days	**14 days**	**28 days**	**90 days**
R1	40.30	46.342	50.38	55.74
R2	32.93	38.42	42.22	45.70
R3	31.21	36.54	40.12	43.38
R4	22.34	25.22	27.89	29.15
R5	17.26	18.32	20.08	21.04
R6	13.63	15.77	18.51	18.92

4.1.4 Splitting Tensile Strength

Tensile strength is one of the crucial characteristics of concrete because structural stresses make it susceptible to tensile cracking. This test defines the split tensile strength of concrete using a cylinder specimen which splits across the vertical diameter. This test

aims to determine the tensile strength of concrete by indirect method because the direct tensile test is difficult for concrete. Being brittle, concrete is weak under tension and susceptible to cracking. So it is important to perform the split tensile strength test of concrete. According to estimates, the tensile strength of concrete is equivalent to approximately 10% of its compressive strength.

The results of the Split tensile strength of mixes at 7 days, 14 days, 28 days, and 90 days are shown in Fig. 4.4 with replacement levels of RC 0, 10, 15, 20, 25, and 30%. After examining the split tensile strength of RuC and comparing it with standard concrete, it decreases with the increment of RC in concrete. In this study, at a 15% replacement level of RC, split tensile strength is found to be 3.24 MPa. The outcomes are consistent with the work stated by H.A. Toutanji [120]. The split tensile strength is achieved at approximately 8-11 % of the concrete's compressive strength at 28 days of curing.

At 90 days of curing, the outcomes are improved by 4-5% compared to 28 days of curing results, like the compressive strength of RuC, but enhancement in strength is only up to 15% replacement of the RC. Because PPC is utilized in this study, the RuC's later strength is enhanced due to pozzolanic reaction, and the age of curing improves the mechanical characteristics of RuC. The loss in split tensile strength of RuC is 17-60% at 7 days, 16-58% at 14 days, 16-60% at 28 days, and 18-59% at 90 days with the replacement level of RC by 10%, 15%, 20%, 25%, and 30% respectively. Because of the weak bonding between RC and cement, the RuC doesn't bear much tensile load than standard concrete, and the gaps between RC and cement become larger quickly. The RuC doesn't make a strong bond between the RC and cement as the standard concrete makes the bond between FA and cement. Literature also observed a similar decrement in the splitting tensile strength of RuC as the RC quantity increased in the concrete due to low sp gr and the gap between the cement matrix and the RC [41, 42, 119, 121, 122]. There is a less substantial loss in split tensile strength of RuC after the surface treatment of the RC. Gurunandan et al. [42] found a 37.43% reduction in split tensile strength, but the reduction is only 22.48% at the 15% replacement level of RC after the surface treatment in this study.

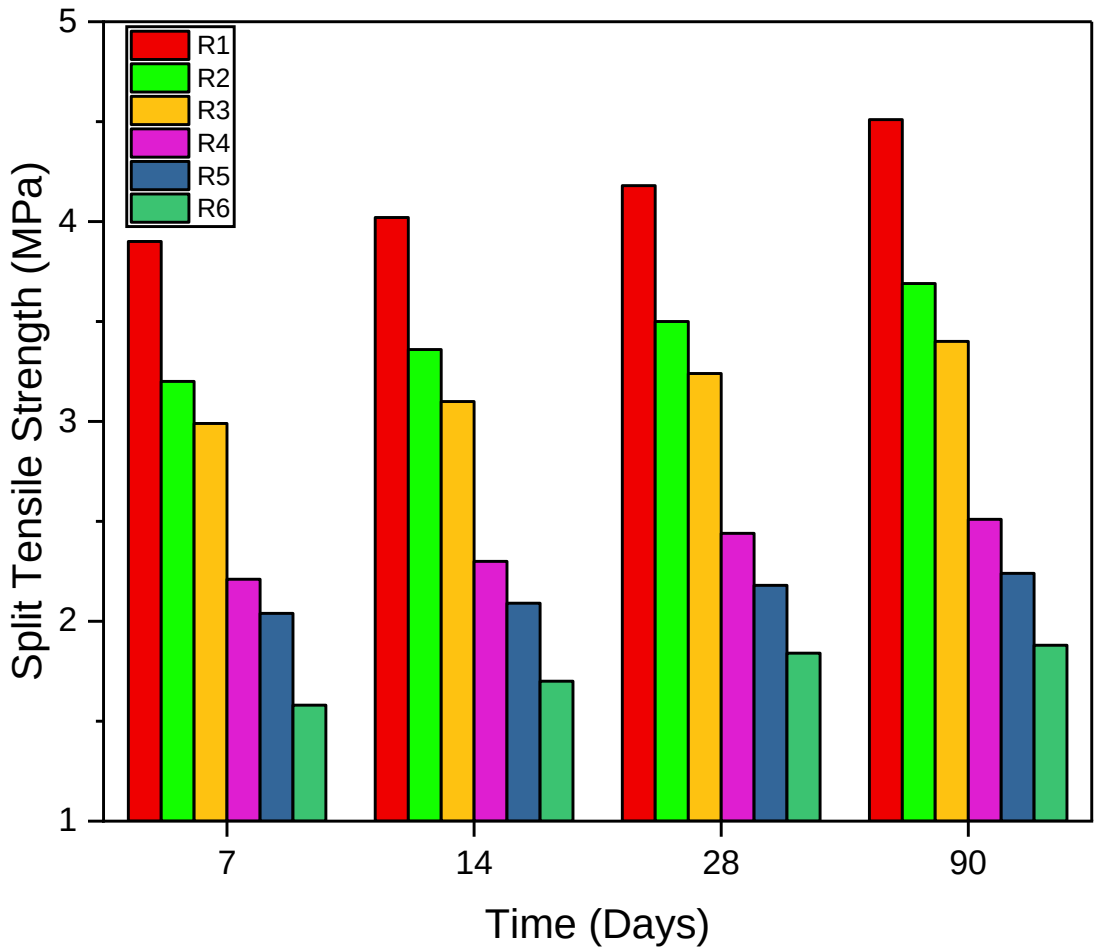

Fig. 4.4 Split tensile strength of standard concrete and RuC

Table 4.4 Results of split tensile strength of standard concrete and RuC

Mix	f_{st} (MPa)			
	7 days	14 days	28 days	90 days
R1	3.90	4.02	4.18	4.51
R2	3.20	3.36	3.50	3.69
R3	2.99	3.10	3.24	3.40
R4	2.21	2.30	2.44	2.51
R5	2.04	2.09	2.18	2.24
R6	1.58	1.70	1.84	1.88

4.1.5 Flexural Strength

Flexural strength is also called a rupture of the concrete used to find the bending capability of the concrete specimens. It is a measurement of a concrete slab's or beam's

ability to withstand failure in bending. Concrete is tested using the flexural test for the application of pavement and slab construction.

The Flexural strength results of all mixes at 7 days, 14 days, 28 days, and 90 days are shown in Fig. 4.5 with replacement levels of RC 0, 10, 15, 20, 25, and 30%. After evaluating the results of RuC and comparing it with standard concrete, it is found that with an increment of inclusion of RC in the concrete, the flexural strength of RuC decreases. In this study, at 15% replacement level of RC, the reduction is 28% at 28 days of curing, and the flexural strength is found to be 4.00 MPa. At 90 days of curing, the flexural strength of RuC is found to be 4.40 MPa, so it can be used for the beam member for M_{40} grade concrete. There is no significant loss in flexural strength of RuC after the surface treatment of the RC. The flexural strength is achieved at approximately 9-14 % of the concrete's compressive strength at 28 days of curing.

The loss in flexural strength of RuC is 18-59% at 7 days, 16-56% at 14 days, 17-53% at 28 days, and 16-57% at 90 days, with the replacement level of RC 10-30%, respectively. The curing days have little effect on flexural strength after 15% substitution of RC, and the findings at 90 days are similar to those obtained after 28 days of curing. At 90 days, the flexural strength of RuC is enhanced by approximately 10% at a 15% replacement level of RC compared to 28 days strength results.

Since micro-crack forms when the post-peak region is reached and propagates after exceeding this stage in flexural strength testing, cracking may begin before the maximum load is applied. A similar decreasing pattern of flexural strength after increasing RC in concrete is found in past studies [15, 49]. According to Najim, flexural strength decrement was 11% for a 5% rubber replacement level, but at 15% rubber replacement level without chemical treatment, the decrement was 39% [26]. Still, in this study, the reduction is only 28%, and it can be considered a positive result after the surface treatment of RC by sulphuric acid. According to the literature, the primary concern of adding rubber of several sizes or quantities into concrete decreases the flexural strength of RuC [15]. Literature also observed a reduction in flexural strength as the RC quantity increased, which is to be expected given that the compressive strength of RuC reduces as the rubber quantity rises [123].

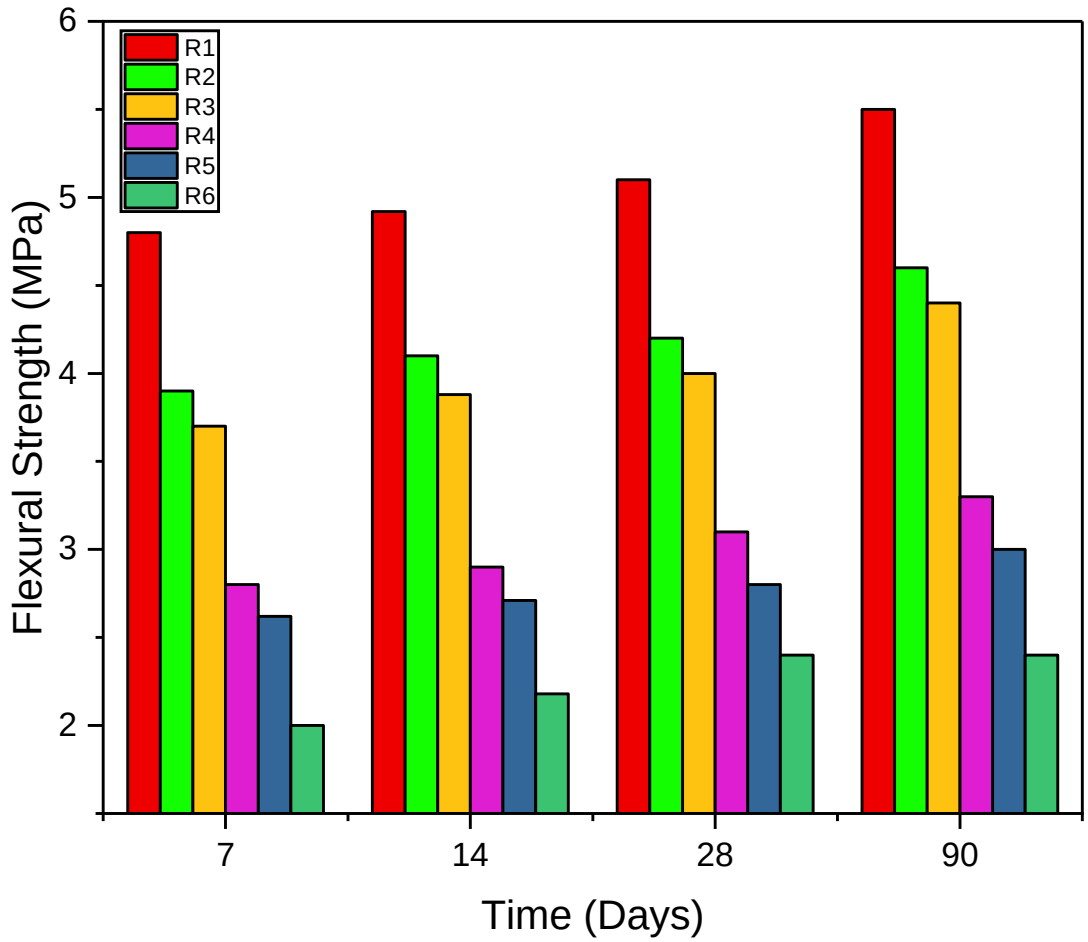

Fig. 4.5 Flexural strength of standard concrete and RuC

Table 4.5 Results of flexural strength of standard concrete and RuC

Mix	f_{fs} (MPa)			
	7 days	**14 days**	**28 days**	**90 days**
R1	4.80	4.92	5.10	5.50
R2	3.90	4.10	4.20	4.60
R3	3.70	3.88	4.00	4.40
R4	2.80	2.90	3.10	3.30
R5	2.62	2.71	2.80	3.00
R6	2.00	2.18	2.40	2.40

4.1.6 Compressive Strength using Rebound Hammer test

Before the destructive test on the samples, the compressive strength using a rebound hammer of all mix specimens is measured at 7, 14, and 28 days after casting. Proceq Schmidt Digital Concrete Test Hammer is used to analyze the compressive strength of concrete according to IS code [107]. The compressive strength results for all mixes are

shown in Fig 4.6 and Table 4.6. After analyzing the results, the compressive strength of concrete mixes by rebound hammer is slightly greater than the hydraulic compression testing machine results. The surface hardness of the specimens influences the rebound strength of the concrete. The rebound test should be performed when the cube specimen is fixed between the upper and lower faces of the hydraulic machine. This technique gives accurate compressive strength results, but when the specimen is on the floor, the testing is done in a downward direction; it does not provide accuracy.

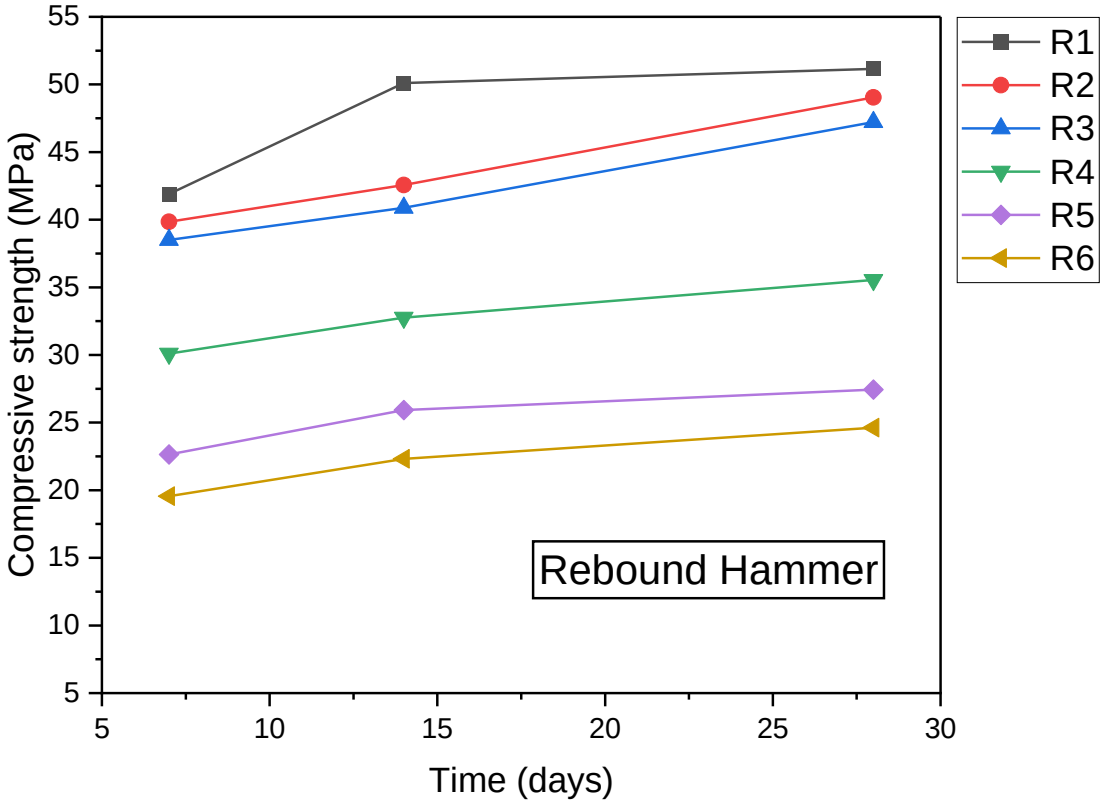

Fig. 4.6 Compressive strength of standard and RuC by rebound hammer test

Table 4.6 Results of compressive strength by rebound hammer

Mix	f_c (MPa)		
	7 days	**14 days**	**28 days**
R1	41.9	50.1	51.15
R2	39.85	42.56	49.05
R3	38.5	40.88	47.22
R4	30.1	32.76	35.54
R5	22.64	25.92	27.44
R6	19.56	22.32	24.62

4.1.7 UPVT (Ultrasonic pulse velocity test)

According to IS code, a non-destructive test by the 'MATEST' UPV tester is performed on prism samples to examine wave propagation's velocity in the material and the dynamic MOE of the different concrete mixes [109]. The UPV test measures the passage of time from the specimens to determine the performance of the hard material. When the time transit of the UPV wave through the specimen is large, it indicates that the concrete is weaker and vice versa. This test shows the quality of the concrete. The UPV results for prism specimens for concrete mixes with replacement levels of RC by 0%, 10%, 15%, 20%, 25%, and 30% at 28 and 90 days are shown in Fig. 4.7 and Table 4.7. The curing time of 90 days doesn't affect the results of UPV, and the results are approximately the same as 28 days of curing.

The UPV is also reduced by replacing the FA with RC because rubber makes a void-like structure in concrete which increases the time of UPV. The rubber particles serve as voids in concrete and are responsible for the decrement in UPV by absorbing the velocity. According to K.B. Najim and M.R. Hall, [124] UPV was found 3.8 Km/s and according to Khaloo et al., [66] UPV was found 3.5 Km/s at 15% rubber replacement level without chemical treatment. In this study at 15% replacement level of RC, the UPV is found 4.25 Km/Sec, which shows the good quality of the concrete according to IS code it can be considered a positive result after the surface treatment of RC by sulphuric acid. A similar pattern of the UPV results after increasing RC in concrete is found in past studies [5, 15, 26, 125]. The decrease in UPV observed may be due to low-density rubber or an increase in a porous structure that promotes ultrasonic wave absorption [126, 127].

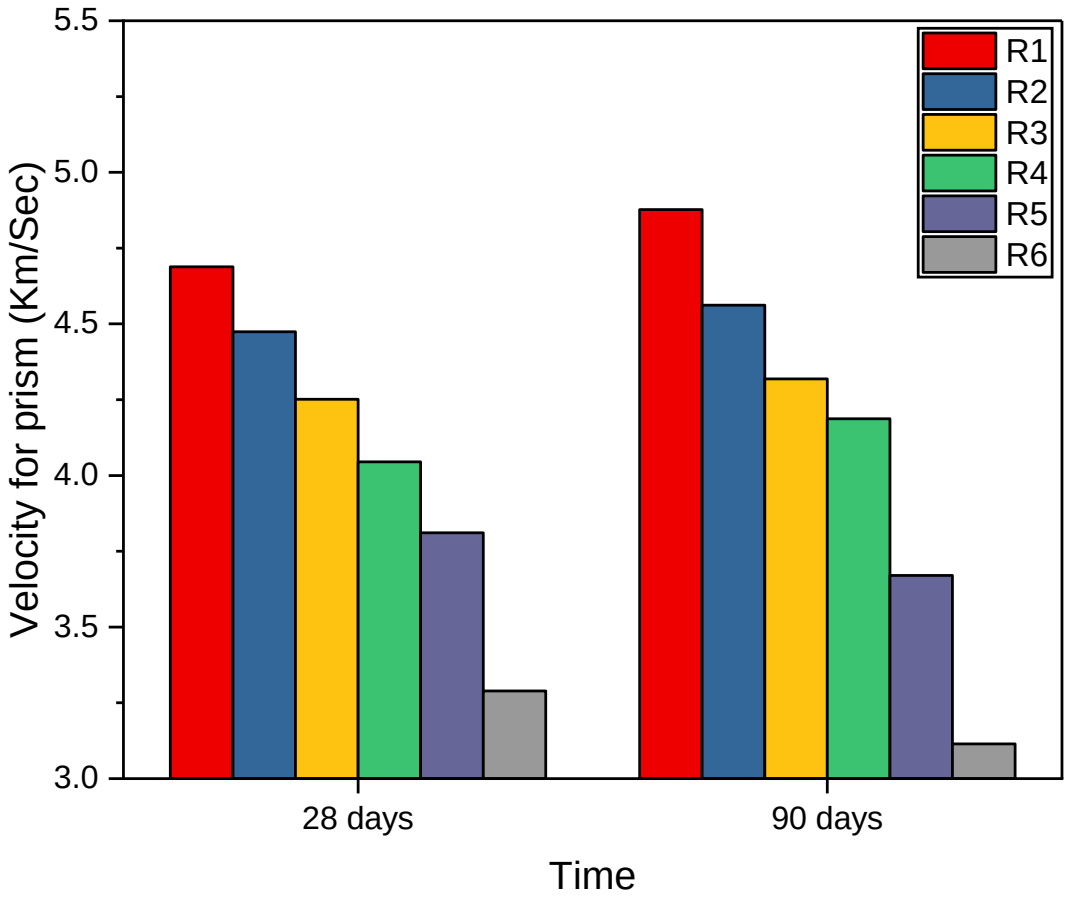

Fig. 4.7 UPV of all mixes at 28 and 90 days

Table 4.7 Results of UPV of all mixes at 28 and 90 days

Mix	UPV (Km/Sec)	
	28 days	90 days
R1	4.688	4.877
R2	4.474	4.562
R3	4.251	4.318
R4	4.045	4.186
R5	3.810	3.670
R6	3.288	3.114

4.1.8 Static modulus of elasticity and Poisson's ratio

This test aims to measure the stiffness or rigidity of concrete under static loading conditions. This test evaluates its ability to resist deformation when subjected to an

external force or load. This information is important in the design and construction of structures that require a certain level of rigidity, stiffness or flexibility. The static MOE is also used to calculate the deflection of structural members. The test involves subjecting a concrete sample to an increasing compressive load and measuring the resulting strain or deformation.

The static MOE and Poisson's ratio are evaluated to observe standard concrete and RuC's stiffness and deformation capacity. Static MOE results at 28 days after casting are shown in Fig. 4.10 and Table 4.8. Fig. 4.8 expresses the axial stress vs axial strain pattern. The static MOE decreases with increasing the RC in the concrete. When 0, 10, 15, 20, and 25 % FA is replaced with RC, the MOE of RuC decreases by 24.11%, 30.35%, 34.29 %, and 56.98 %, respectively, compared to standard concrete. This decrement in elastic modulus offers higher flexibility, which can be considered a positive advantage in RuC mixtures. In the initial loading phases, the curves indicate a parabolic form, but as it passes failure loads, it smooths out and becomes a straight line. Standard concrete's static MOE is found to be as high as 29.48 GPa, indicating that it is a very stiff concrete compared to RuC. Since rubber has an elastically deformable capacity, it improves the ductility of RuC when mixed with concrete. This increased ductility and ability to withstand large deformations before failure is due to its low MOE of RuC. In certain applications, such as in earthquake-resistant construction, flexibility is an important property of concrete. By allowing the concrete to deform and absorb energy under stress, rather than cracking or failing, flexibility can help to improve the overall durability of the structure. So this RuC can be used where high flexibility is required to reduce the effect of external load. MOE of standard and RuC is calculated from the initial slope of the axial stress-strain curves. According to Gupta et al., [5] static MOE was found approx 21 MPa and according to K.S. Son et al., [57] static MOE was found 21.71 MPa at 15% rubber replacement level without chemical treatment. In this study at 15% replacement level of RC, the static MOE is found 20.53 MPa, after the surface treatment of RC by sulphuric acid. No changes were found in the static MOE of RuC with surface treatment or without surface treatment of RC. A similar decreasing pattern of MOE after increasing the quantity of RC in concrete has been found in past studies [5, 15, 35, 60, 128].

The Poisson's ratio is determined by the ratio of transverse strain to axial strain when concrete is subjected to compressive load. The aim of this test is to determine its

capability to resist lateral deformation when the compressive force is applied to the concrete column specimen. The design and study of concrete structures that need a certain amount of deformation benefit greatly from this test. Engineers can construct buildings that are safer and more effective by understanding concrete's Poisson's ratio and better predicting how it will respond under various loading circumstances. The Poisson's ratio results at 28 days after casting are shown in Fig. 4.11 and Table 4.8. Fig. 4.9 offers the pattern of axial stress vs lateral strain. The Poisso's ratio is found 0.3 at 15% RC replacement level, approximately double the value of standard concrete. Poisson's ratio increases by increasing RC in the concrete. Due to the higher value of Poisson's ratio, the RuC has a higher deformable capacity. The RuC can deform under stress and can reduce the chance of cracking before failure. By incorporating RC in concrete the RuC can deform transversely and enhance the deformation capacity of RuC. But this increase in deformation capacity reduces the compressive strength of RuC. So we should add that much amount of RC to the concrete so that the compressive strength of the RuC should not be below the required strength. In this study 15% RC replacement level is sufficient and the compressive strength is in the required range. So this RuC can be used where high deformation capacity is required such as tunnels in squeezing grounds, or swelling soils as soft supports. It's essential to notice that RuC's behaviour isn't completely elastic, so Poisson's ratio isn't stable in the loading phase. Similar findings of Poisson's ratio are observed in past studies [41, 66, 129] and no effect is found of the chemical treatment of RC on Poisson's ratio after comparison of RuC without chemical treatment in the previous literature.

IS 456-2000 gives empirical equation (4.1) for expecting Ec (Static MOE) using concrete's compressive strength. The following empirical Equation is

$$\mathbf{Ec = 5000\sqrt{f_{ck}}\ (MPa)} \qquad \mathbf{(4.1)}$$

The actual results of Ec by experiment and predicted by this empirical equation are presented in Table 4.8. From the experimental and empirical results, it is analyzed that the value of Ec by the empirical formula is larger than the experimental value of Ec.

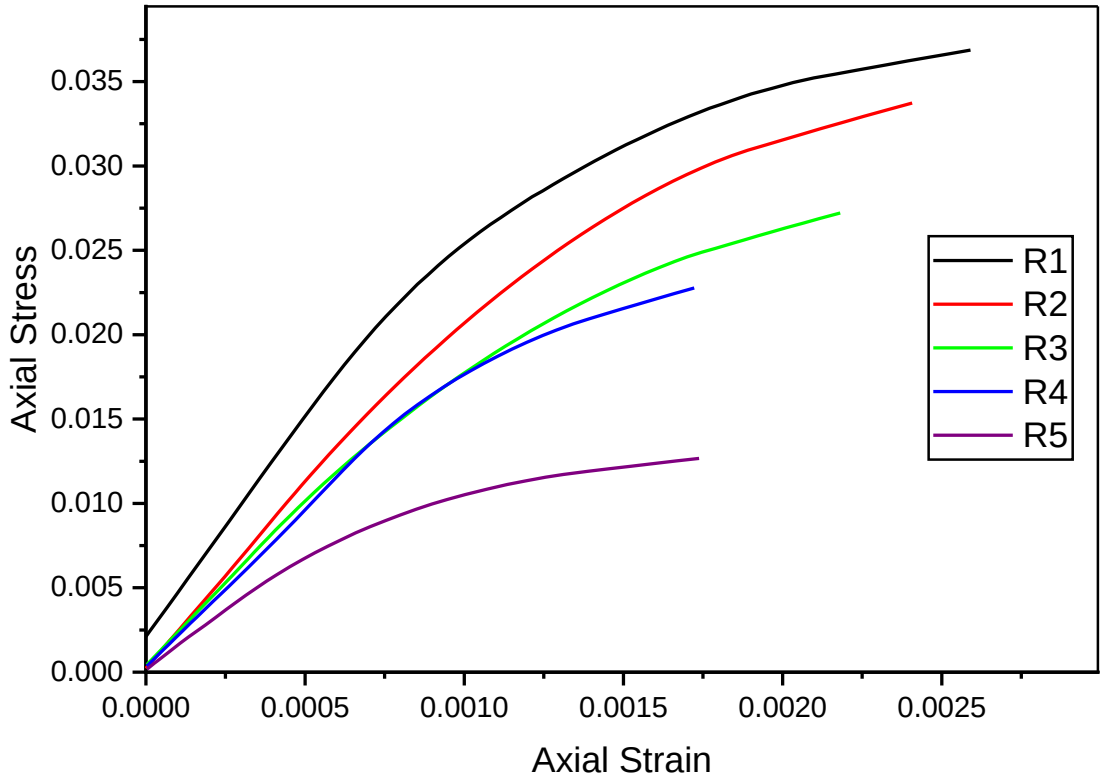

Fig. 4.8 Axial stress vs. axial strain diagram of mixes at 28 days

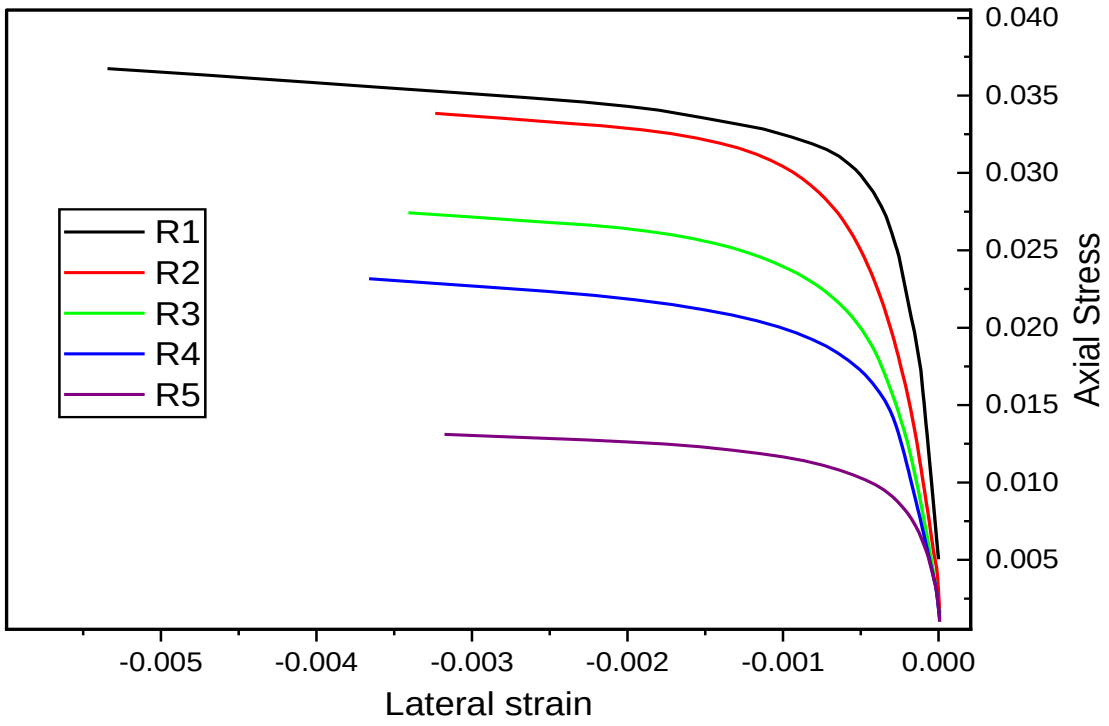

Fig. 4.9 Axial stress vs. lateral strain diagram of mixes at 28 days

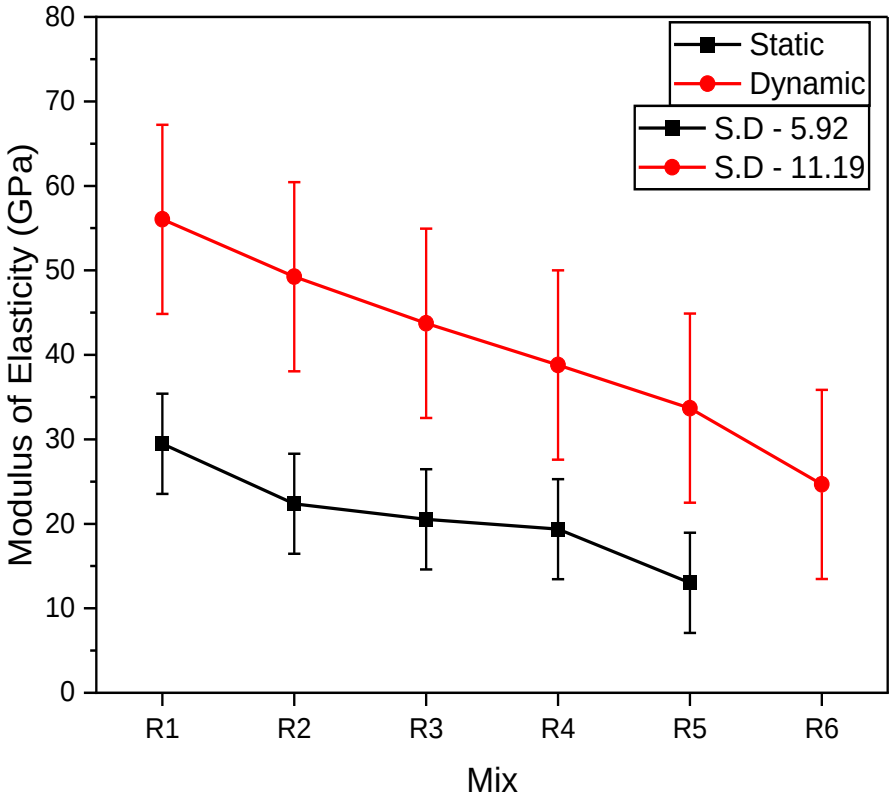

Fig. 4.10 Static and Dynamic modulus of elasticity of mixes at 28 days

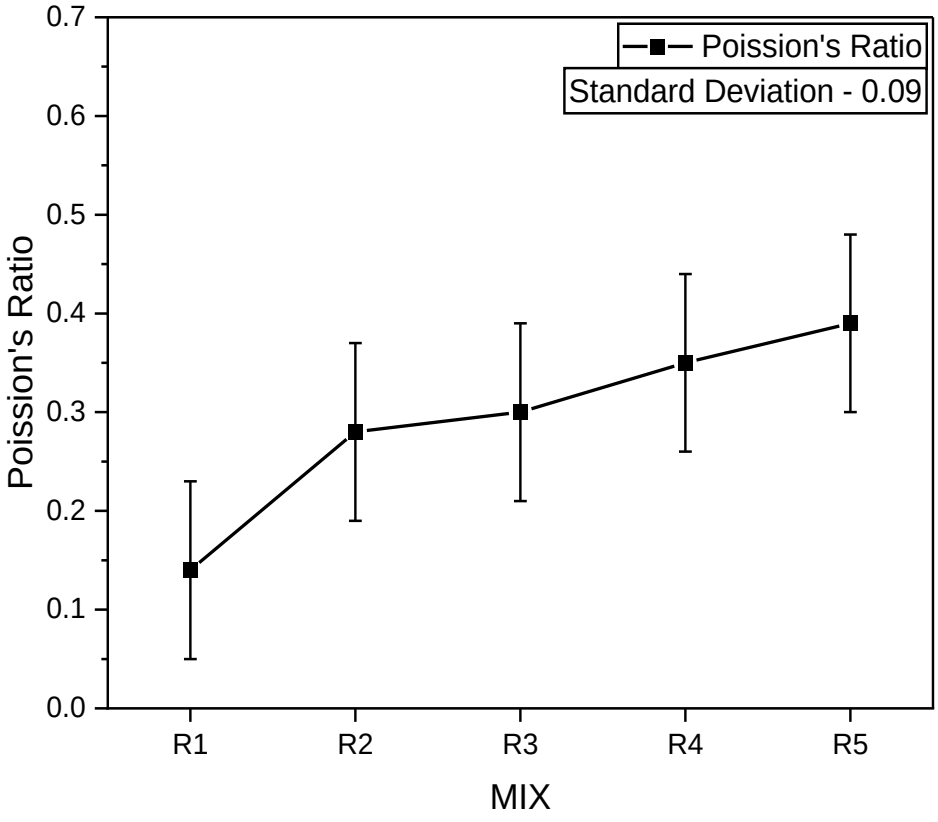

Fig. 4.11 Poisson's ratio of all mixes at 28 days

Table 4.8 Results of Static MOE, Poisson's ratio, and dynamic MOE.

Mix	Compressive Strength (MPa)	Static MOE (GPa) (Experimental)	Static MOE (GPa) IS Code [130]	Poisson's ratio (Experimental)	Dynamic MOE (GPa)
R1	50.38	29.48	35.48	0.14	56.04
R2	42.22	22.37	32.48	0.28	49.25
R3	40.12	20.53	31.67	0.3	43.73
R4	27.89	19.37	26.40	0.35	38.79
R5	20.08	12.68	22.40	0.39	33.68
R6	18.51	#	21.51	#	24.66

Specimen failure

4.1.9 Dynamic Modulus of Elasticity

It is the concrete's elasticity under dynamic stresses like axial and transverse tremors. A material's dynamic modulus of elasticity is a parameter that reveals how a body will respond to strain and stress. As a result, the dynamic modulus of elasticity shows evidence of the material's expansion when subjected to dynamic stress and strain.

The results of the dynamic MOE for different mixes are shown in Fig. 4.10. The dynamic MOE decreases with increasing the RC as a partial replacement in the concrete mix in a similar way observed in concrete's compressive strength because of the porous structure. The dynamic MOE results in a replacement level of 0, 10, 15, 20, 25, and 30% by RC, shown in Table 4.8. The dynamic MOE is found to be slightly larger than the static MOE, as described by IS code [109]. The decrease in dynamic MOE is due to FA replacement with RC, which shows the absorption of ultrasonic waves. This decrement in elastic modulus offers higher flexibility, which can be considered a positive advantage in RuC mixtures. According to Gupta et al., [15] dynamic MOE was found approximately 30 GPa and according to A.R. Khaloo et al., [66] dynamic MOE was found approximately 15 GPa at 15% rubber replacement level without chemical treatment. But in this study, the dynamic MOE is 43.73 GPa, and it can be considered a positive result after the surface treatment of RC by sulphuric acid. A similar decreasing pattern of the dynamic MOE results after increasing RC in concrete is found in past studies [5, 15, 26, 55].

4.1.10 Impact Resistance by Flexural Loading

Impact resistance is the capacity of concrete to absorb energy and resist repeated impacts without suffering detrimental effects like cracking and spalling. When concrete is subjected to frequent shock loads or impact loads, impact resistance is a key factor in how well it performs. As a result of this type of load, concrete may break, fracture, or damage. Concrete is subjected to impact testing, which analyzes the energy absorbed during fracture to assess the materials' impact resistance or toughness.

The impact resistance results from flexural loading of mixes at 28 days are shown in Fig. 4.12, with replacement levels of RC 0, 10, 15, 20, 25, and 30%. The results establish that increasing the RC replacement level develops the impact energy absorption ability of the concrete considerably. The impact energy on the concrete specimens by hammer increases from 47.08 to 78.48 Joule with an entire 30% replacement of FA by RC in the concrete mix. It is found that with a 15% addition of RC as FA, the resistance of impact energy of concrete specimen increased 33.33% by flexural loading. This is a promising step for RuC, and it will be helpful in the absorption of seismic impact energy. In accordance with [23, 24], the rubber particles have less stiffness, RuC has higher flexibility and can absorb a significant amount of impact energy. Because of the low stiffness of the rubber particles, RuC is more flexible and absorbs a significant amount of impact energy compared to standard concrete. According to Taha et al. [23], the incorporation of tire rubber particles into standard concrete resulted in various toughening methods, including the ability to stretch, compress, and twist. The RuC consumes more energy than standard concrete since the tire rubber particles absorb more energy.

According to Gupta et al., [24] impact resistance of RuC under flexural loading was found 55 joules and according to A. Abdelmonem et al., [131] impact resistance was found approximately 40 J at 15% rubber replacement level without chemical treatment. But in this study, the Impact resistance is 62.78 J, and it can be considered a positive result after the surface treatment of RC by sulphuric acid.

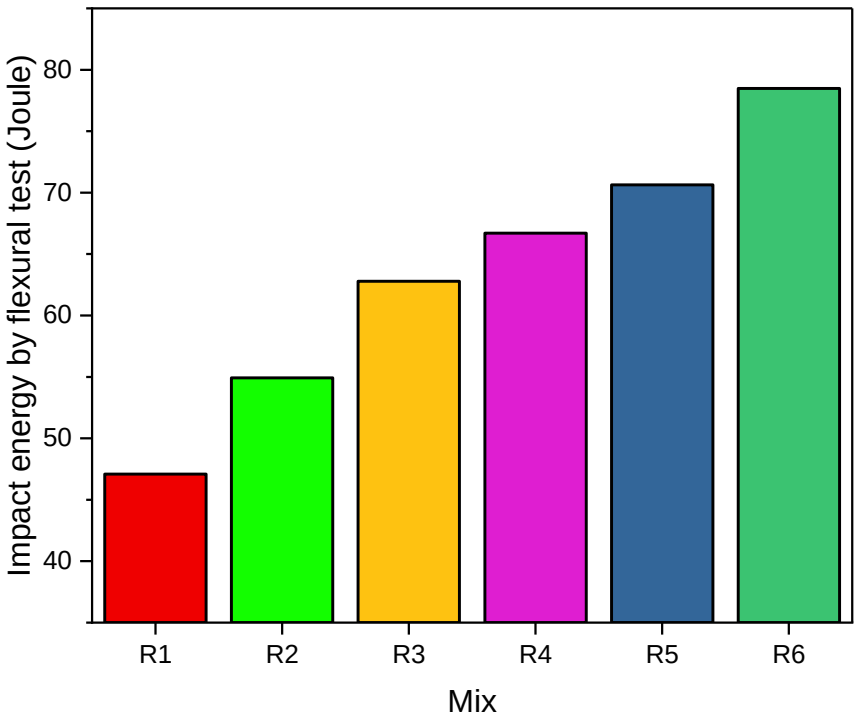

Fig. 4.12 Impact energy by the flexural loading of standard and RuC mixes

Table 4.9 Results of impact energy by the flexural loading of standard and RuC mixes

Mix	Accumulated impact energy by flexural test (Joule)
R1	47.08
R2	54.93
R3	62.78
R4	66.70
R5	70.63
R6	78.48

4.1.11 Impact resistance by rebound Test

Fig. 4.13 illustrates the impact energy absorbed by standard and RuC in the rebound test. Based on the findings, it is discovered that increasing the amount of rubber in concrete increases resistance to the impact of RuC after being compared with standard concrete. The absorbed impact energy by RuC increases from 2.75 to 2.90 J with an entire 30% replacement of FA by RC in the concrete mix. The absorption of impact energy by the rebound test of the concrete increases from 2.56 to 2.82 J (0 - 10.15%) by a 15% replacement level of RC in the concrete mix. This is a good development for RuC and is

useful for the absorption of impact energy due to seismic loading. so this RuC can be used as a structural member in the field of civil engineering because it can absorption of impact energy due to external loads such as blasts or earthquakes. Similar explanations are given by [24, 25] for RuC and rubber fibre concrete. According to Gupta et al., [24, 49] impact resistance of RuC in the rebound test was increased by approximately 5.08% (1.77 J to 1.86 J) and according to A. Abdelmonem et al., [131] impact resistance was increased by approximately 5.55% at 15% rubber replacement level without chemical treatment. But in this study, the Impact resistance in the rebound test is 10.15%, and it can be considered a positive result after the surface treatment of RC by sulphuric acid.

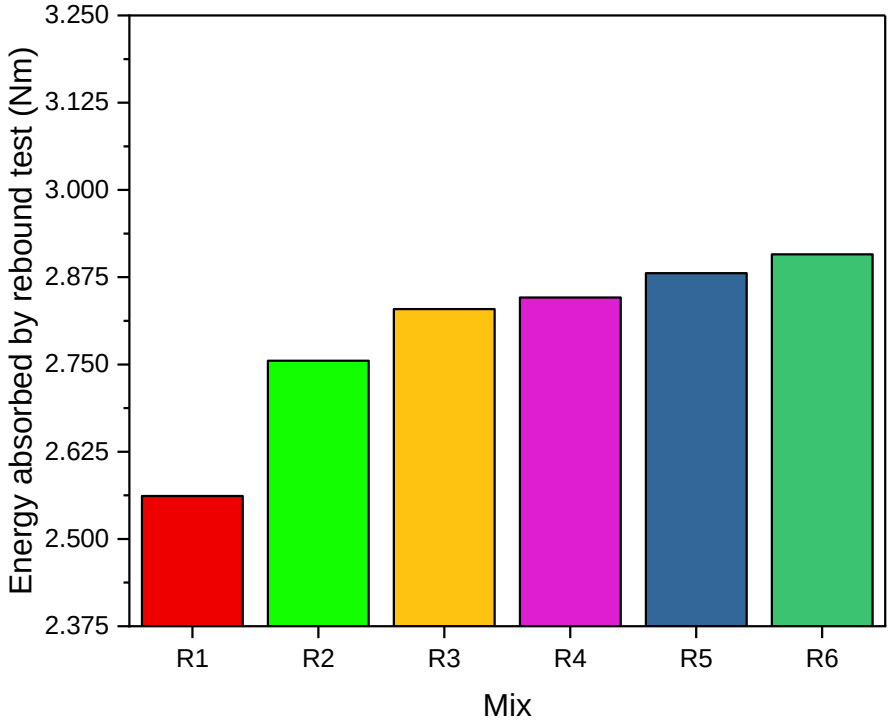

Fig. 4.13 Impact energy absorbed by the rebound test of standard and RuC mixes

Table 4.10 Results of impact energy absorbed by the rebound test of standard and RuC mixes

Mix	Impact energy absorbed by rebound test (Nm)
R1	2.561
R2	2.755
R3	2.829
R4	2.845
R5	2.880
R6	2.907

4.1.12 Pull-off Test

The direct tensile strength of a material or the bond strength of an interface is measured using concrete pull-off tests. Following ASTM D7234-19, the Standard test method for the tensile strength of concrete surfaces and the bond strength by direct tension is the procedure used in this testing. The test establishes the maximum perpendicular tension force that a surface can withstand before a material plug detaches. The weakest plane within the concrete will experience failure. In RuC, rubber crumbs are used and the bonding of rubber crumbs and the concrete matrix is weak, so we have to test the direct tensile or bond strength of RuC. this test can be used on other types of concrete to check the bond strength of concrete.

The Pull-off test results after 28 days of curing of the specimen are 4.427, 3.457, 2.555, 1.722, 0.897, and 0.756 MPa with replacement levels of RC by 0%, 10%, 15%, 20%, 25%, and 30% respectively. The bond strength results of all concrete mixes are shown in Fig. 4.15 and Table 4.11. From the test results, it is analyzed that the bonding strength of RuC decreases with the increment of RC in the concrete. After surface treatment of RC by sulfuric acid, the bonding strength does not bother up to 15% replacement level of RC. The pull-off strength of RuC decreases 21.91%, 42.28%, 61.10%, 79.73%, and 82.92% with replacement levels of RC by 10%, 15%, 20%, 25%, and 30% respectively compared to standard concrete. The loss in pull-off strength of RuC is due to the weak bonding between the RC and cement matrix. The failure pattern of standard and RuC in the pull-off test is shown in Fig. 4.14. RuC with chemically treated rubber enhances the bonding between rubber particles and concrete, but it does not eliminate the bonding problem entirely. An advanced technique is needed for the surface treatment of rubber particles to enhance rubber and cement bonding characteristics. Any researcher in any article did not perform this test earlier, so comparing and supporting these results is not possible.

Fig. 4.14 Failure pattern of standard and RuC in pull-off test

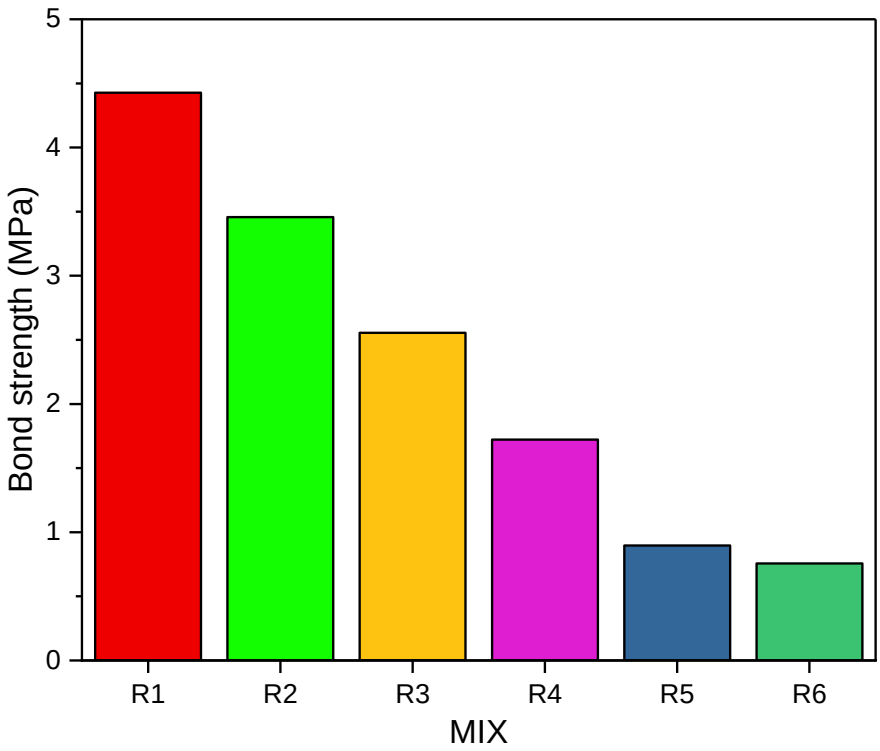

Fig. 4.15 Bond strength results of all concrete mix

Table 4.11 Results of bond strength results of all concrete mix

Mix	Bond strength (MPa)
R1	4.427
R2	3.457
R3	2.555
R4	1.722
R5	0.897
R6	0.756

4.1.13 Four-probe resistivity test

This test is used for assessing the quality or durability of RuC. This is the one common method which is quite easy to use on-site is the Wenner Four-probe resistivity test. The resistivity that concrete is going to be conducting through its interconnected porosity. When there is interconnectivity then conduction will happen. So resistivity is the opposite of resistivity. So if the concrete has a very less amount of interconnectivity of pores the resistivity will be high. So that the durable concrete should have higher resistivity. Moreover, resistivity gives a direct measurement of the permeability or interconnectivity of the pores in the system.

The results of the resistivity test of standard and RuC are shown in Fig. 4.16 and Table 4.12. According to the results, the mix R1- R4 is in the range of resistivity of 50 - 100 KΩcm, which means that up to 20% replacement level of RC the RuC is in normal quality. So up to 15% replacement level of RC, the RuC is durable and can be used for construction purposes. After mixture R4, the concrete's resistivity of mix R5 and R6 decreases, and it falls into a zone of poor quality. For the durability aspect, rubber's replacement level can not be more than 20% in the concrete; otherwise, the concrete's quality will compromise. Any researcher in any article did not perform this test earlier on RuC, so comparing and supporting these results is not possible.

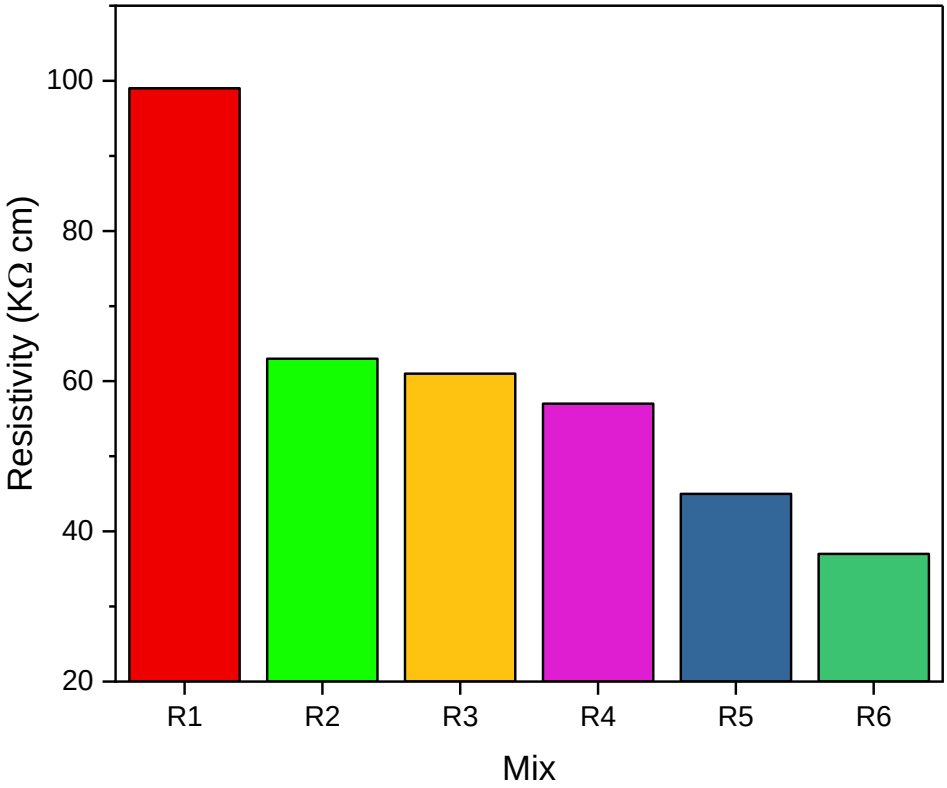

Fig. 4.16 Result of resistivity of standard and RuC

Table 4.12 Results of resistivity of standard and RuC

Mix	Resistivity (KΩcm)
R1	99
R2	63
R3	61
R4	57
R5	45
R6	37

4.1.14 Microstructure analysis (XRD and SEM)

XRD - For crystal structure identification and phase composition analysis, all materials are characterized using a RIGAKU ULTIMA IV X-ray diffractometer with $CuK_{\alpha 1}$ radiation (λ=1.54Å). With a step size of 0.02º, the XRD data are obtained throughout an angular range of 10-70º. According to ASTM, the XRD analysis is done on all concrete mix after 28 days of curing after making the fine powder [100]. XRD analysis indicates the mineralogical properties of all mixes in Fig. 4.17. All the mixes are crystalline in

nature because they have definite and regular geometry. All the informative data belonging to XRD peaks like position, miller indices, d-spacing, chemical formula, chemical name, and crystal system are present in Table 4.13.

All the mixes of standard and RuC have the hexagonal shape of crystalline silicon oxide in the majority. Crystalline quartz is significantly less reactive, and it will not react at normal conditions, only react at a very high temperature which is beneficial for RuC. Since quartz is an anhydrite of an acid, it would not be attacked by acids in general. Gypsum and ettringite are the two chemical compounds that can harm the RuC by creating internal stress and expanding the inner materials of the concrete. These compounds are generated by a reaction between sulfuric acid and calcium hydroxide. For this reason, rubber is washed with tap water several times in the treatment process to remove the effect of sulfuric acid. In Table 4.13, in all mixes of RuC, no traces are found of any harmful chemical compounds in XRD analysis that can deteriorate the RuC. Furthermore, the treatment process of RC will not harm the properties of RuC.

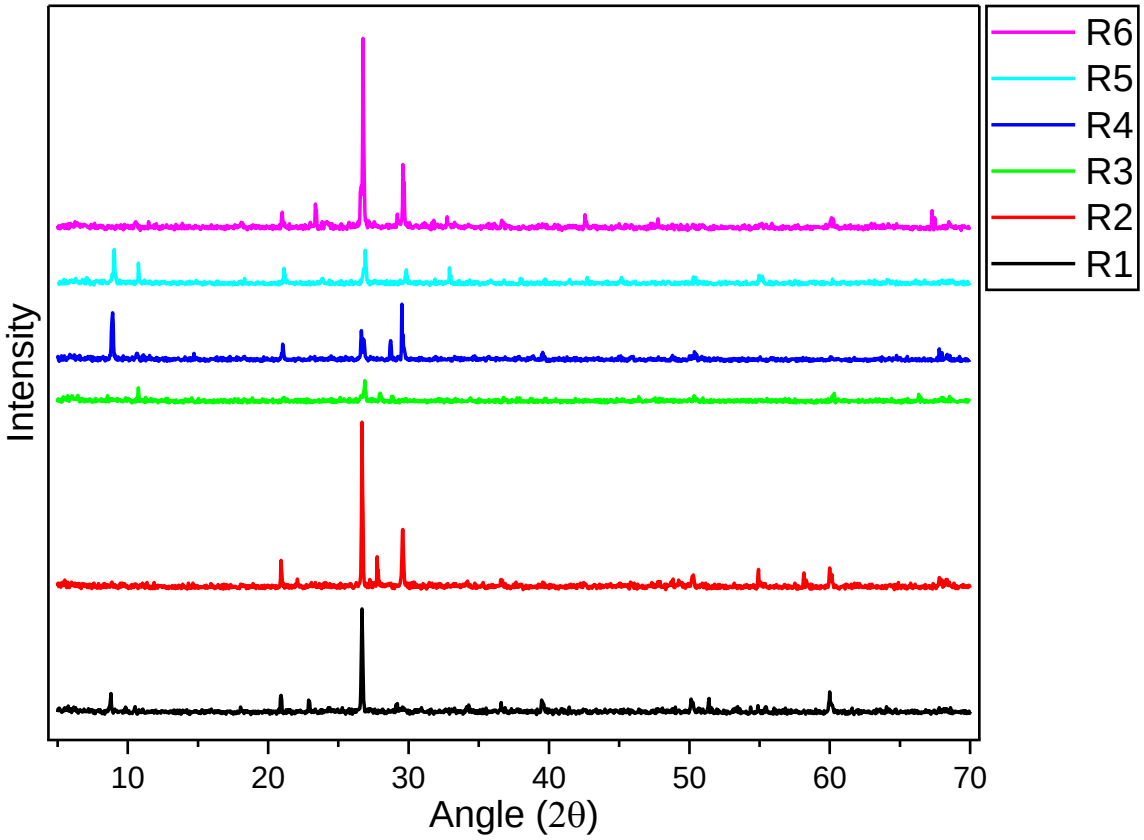

Fig. 4.17 XRD results of all mixes after 28 days

Table 4.13 XRD data of standard and RuC mixes.

S. no.	Mix	Peaks No.	Peaks Angle	h k l	d Spacing	Chemical Formula	Chemical Name	Crystal System
1	R1 MIX	1	20.91	1 0 0	4.24431	SiO_2	Silicon Oxide	Hexagonal
		2	22.89	1 0 1	3.88184	S_6	Sulfur	Hexagonal
		3	26.67	1 0 1	3.33954	SiO_2	Silicon Oxide	Hexagonal
		4	29.08	1 1 2	3.06824	CS_2	Carbon Sulfide	Orthorhombic
		5	39.51	1 0 2	2.27858	SiO_2	Silicon Oxide	Hexagonal
		6	50.15	1 1 2	1.81736	SiO_2	Silicon Oxide	Hexagonal
		7	59.99	1 2 1	1.54061	SiO_2	Silicon Oxide	Hexagonal
2	R2 MIX	1	20.96	1 0 0	4.23391	SiO_2	Silicon Oxide	Hexagonal
		2	26.68	1 0 1	3.33821	SiO_2	Silicon Oxide	Hexagonal
		3	27.78	1 1 1	3.20783	Ca	Calcium	Cubic
		4	29.56	1 1 0	3.01877	Na	Sodium	Cubic
		5	50.22	1 1 2	1.81514	SiO_2	Silicon Oxide	Hexagonal
		6	54.91	3 1 1	1.67068	Ca	Calcium	Cubic
3	R3 MIX	1	10.73	1 1 1	8.24048	C_{60}	Carbon	Cubic
		2	26.90	1 0 0	3.31386	SiO_2	Silicon Oxide	Hexagonal
		3	27.97	3 3 1	3.18903	C_{60}	Carbon	Cubic
		4	50.31	1 1 2	1.8134	SiO_2	Silicon Oxide	Hexagonal
		5	60.32	1 2 1	1.53442	SiO_2	Silicon Oxide	Hexagonal
		6	66.36	3 0 0	1.40752	SiO_2	Silicon Oxide	Hexagonal
4	R4 MIX	1	8.90	-2 0 1	9.92662	SiO_2	Silicon Oxide	Monoclinic
		2	21.04	1 0 0	4.22223	SiO_2	Silicon Oxide	Hexagonal
		3	26.72	1 0 1	3.33543	SiO_2	Silicon Oxide	Hexagonal
		4	28.74	0 1 1	3.10612	SiO_2	Silicon Oxide	Hexagonal
		5	29.55	1 1 0	3.02268	Na	Sodium	Cubic
		6	39.59	0 1 2	2.27633	SiO_2	Silicon Oxide	Hexagonal
		7	50.26	1 1 2	1.81506	SiO_2	Silicon Oxide	Hexagonal
5	R5 MIX	1	9.04	1 0 0	9.77795	Mn_6O_{12}	Manganese Oxide	Monoclinic
		2	10.75	1 1 1	8.22558	C_{60}	Carbon	Cubic
		3	21.13	1 0 0	4.20434	SiO_2	Silicon Oxide	Hexagonal
		4	26.93	1 0 1	3.31004	SiO_2	Silicon Oxide	Hexagonal
		5	32.92	2 2 2	2.72025	Mn_2O_3	Manganese Oxide	Cubic
		6	55.10	4 4 0	1.66539	Mn_2O_3	Manganese Oxide	Cubic
6	R6 MIX	1	20.99	1 0 0	4.2315	SiO_2	Silicon Oxide	Hexagonal
		2	26.77	0 1 1	3.32919	SiO_2	Silicon Oxide	Hexagonal
		3	29.63	1 1 0	3.01449	Na	Sodium	Cubic
		4	42.59	2 0 0	2.12263	SiO_2	Silicon Oxide	Hexagonal
		5	60.12	1 2 1	1.539	SiO_2	Silicon Oxide	Hexagonal
		6	68.49	2 0 3	1.36883	SiO_2	Silicon Oxide	Hexagonal

SEM - The SEM analysis is done on RuC before and after the surface treatment of rubber particles with H_2SO_4 after 28 days of curing. SEM image of RuC before and after treating rubber particles with H_2SO_4 is shown in Fig. 4.18. According to the SEM study, the rubber particles with no surface treatment show a wide gap between the rubber particle and the concrete compared to the rubber particles with surface treatment by H_2SO_4. The Interfacial transition zone between the untreated RC and concrete is large, making the weak concrete. According to L. P. Rivas-Va'zquez et al., the mechanical properties of RuC are not improved by treating the rubber surface with 10% acetone. With surface treatment by NaOH solution, the SEM picture reveals a poor adhesion between the phases of concrete and rubber [35]. Previous studies [22, 23] found similar results for the gaps between RC and cement in tire rubber waste concrete. Because of the rubber particles' hydrophobic nature, the gaps are caused by inadequate compaction of the cement paste around them. Gupta et al. [5, 15] presented a similar argument about the interfacial zone cement and rubber particles.

In this study, after surface treatment of RC by sulfuric acid solution, the gaps between rubber and cement are less compared to untreated rubber particles. This process enhances the bonding properties of RuC. The etching of the tire crumb surface and the elimination of hydrophobic admixtures from the tire crumbs are two factors that contribute to the treatment process. By producing improved hydrophilic characteristics, this process can help to improve the bonding between RC and cement paste. Before making the RuC, the RC should be treated with 15% sulfuric acid solution. The RuC with treated rubber by sulfuric acid reduces the space between the rubber particle and the concrete but can not eliminate the gaps entirely. So, surface treatment of rubber particles necessitates a more modern process.

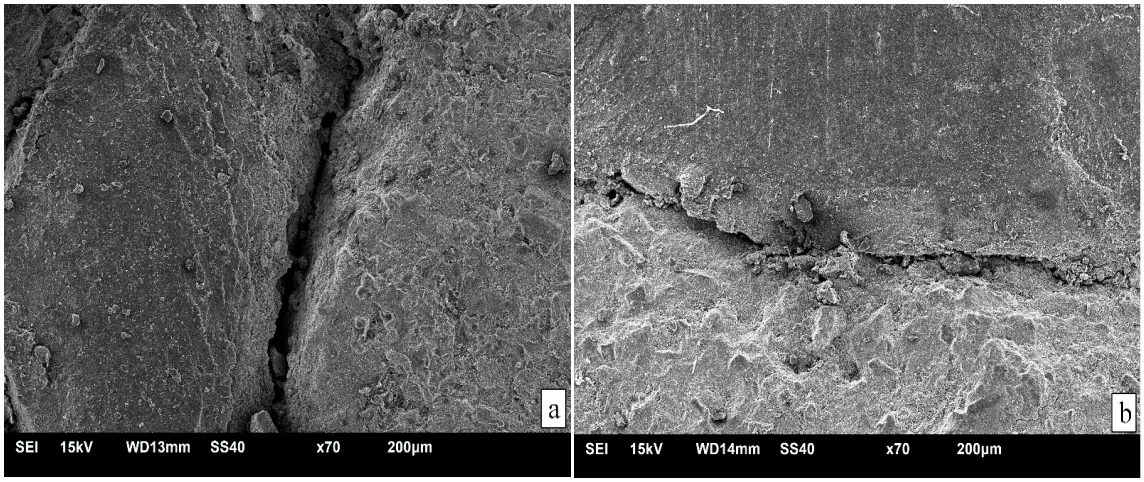

Fig. 4.18 (a) SEM image of RuC without treatment of rubber particles (b) SEM image of RuC after treatment of rubber particles with sulfuric acid

4.2 Effect of acid attack

The acid attack means making an acidic water solution with a 5% concentration of acid as per the ASTM code in the laboratory. Exposure to two distinct kinds of acids, sulfuric and hydrochloric acid, is used to test the acid attack resistance of RuC. The 100 mm cube specimens of the R1 and R3 mix are immersed in 5% acid concentration solutions for 30 days before being tested [132]. For a 30-day exposure time, visual appearance, differences in weight, and compressive strength of conventional and RuC are recorded.

4.2.1 Visual appearance

Visual examination can provide an extensive amount of information that could help positively identify the source of any suffering that is being experienced. The efficiency of visual examination is influenced by the investigator's expertise and knowledge. One of the first phases in the assessment of a concrete structure, visual inspection is one of the most adaptable and effective NDT techniques. In order to understand the information from a visual examination, an engineer needs to have a thorough understanding of structural engineering, concrete materials, and construction techniques. The apparent drawback of visual examination is that it can only check surfaces that are visible. The information about the internal imperfection of concrete can not be identified by visual inspection. Because of such purposes, additional non-destructive testing techniques, including the concrete test hammer and UPVT, are typically used together with a visual inspection.

The visual appearance of the R3 mix immersed in 5% H_2SO_4 is shown in Fig. 4.19(a) and immersed in 5% HCl is shown in Fig. 4.19(b) after 30 days. In Fig. 4.19 (a), it is found that the R3 mix exposed to H_2SO_4 presented a moderate degree of spalling of cement paste, RC, and aggregates, but in Fig. 4.19(b), when the R3 mix is exposed to HCl, it showed a mild degree of spalling of cement paste, RC, and aggregates. When the R3 specimen is exposed to H_2SO_4, the mortar, RC, and aggregates spalled significantly, resulting in an uneven shape, porous surface structure, and a smaller specimen than before immersion. This is related to the increased depth of H_2SO_4 infiltration in RuC. It is found that with an equal duration of immersion and equal concentration of H_2SO_4 and HCl, the RuC is less degraded on its surface by HCl. The specimens are measured, and it is discovered that when the specimens are immersed in H_2SO_4 solution, their dimensions are shorter than when they are immersed in HCl solution.

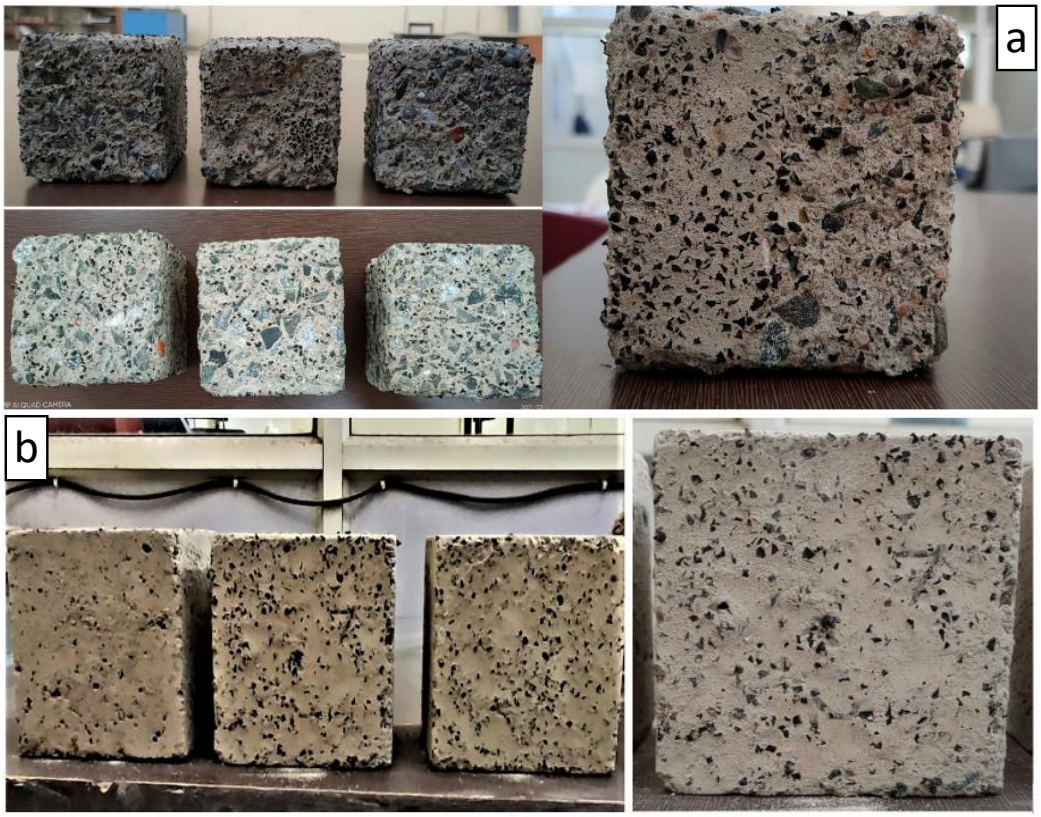

Fig. 4.19 (a) Visual appearance of RuC after immersion in 5% H_2SO_4 solution for 30 days (b) Visual appearance of RuC after immersion in 5% HCl solution for 30 days

4.2.2 Weight difference

The weight differences between the R1 mix and the R3 mix exposed to 5% H_2SO_4 and 5% HCl acids solution for 30 days are shown in Fig. 4.20. It is found that the R1 and R3

mix loses their weight when immersed in H_2SO_4 and HCl acid. When the R1 and R3 mix is immersed in H_2SO_4, the weight loss is 8.47% and 6.33%, but when immersed in HCl, the weight loss is 4.27% and 2.10%, respectively. RuC reduces the loss in weight by 2.14% and 2.17% when exposed to H_2SO_4 and HCl compared to conventional concrete. A similar trend of results in weight loss of RuC is found in past studies [28, 133]. In the chemical analysis, calcium sulfate is generated as a result of H_2SO_4 action. In cement, calcium sulfate interacts with calcium aluminate and creates a compound calcium sulphoaluminate known as ettringite. When ettringite crystallizes, it causes concrete to expand and crack. The loss in weight can be attributed to the H_2SO_4 attack on $Ca(OH)_2$ phases present in PPC [134, 135].

$$\mathbf{H_2SO_4 + Ca(OH)_2 \rightarrow CaSO_4 \cdot 2H_2O} \quad \mathbf{(4.2)}$$

$$\mathbf{3CaO \cdot Al_2O_3 \cdot 6H_2O + 3CaSO_4 + 25H_2O \rightarrow 3CaO \cdot Al_2O_3 \cdot 3CaSO_4 \cdot 31H_2O} \quad \mathbf{(4.3)}$$

The ettringite formed, as shown in equation (4.3), is very expansive. It produces high internal stresses in hydrated cement materials resulting in spalling, cracking, and general concrete weight loss.

The neutralization of the alkaline property of the cement matrix via the disintegration of hydration products can be described as the process of HCl acid attack. After reacting with HCl, the $Ca(OH)_2$ and C-S-H (calcium silicate hydrate) make soluble calcium chloride and water, as described in equations (4.4) and (4.5) [136, 137].

$$\mathbf{2HCl + Ca(OH)_2 \rightarrow CaCl_2 + 2H_2O} \quad \mathbf{(4.4)}$$

$$\mathbf{C - S - H + HCl \rightarrow CaCl_2 + Si(OH)_4 + H_2O} \quad \mathbf{(4.5)}$$

The weight loss in concrete made by pozzolanic cement is less compared to OPC concrete because pozzolana reacts with $Ca(OH)_2$ in the presence of water, makes C-S-H gel, and reduces the capillary pores, which are good for PPC concrete [136]. The existence of pozzolana contributed to the less harmful result of $Ca(OH)_2$. That's why in this study, PPC is used to make RuC resistant to acid attacks.

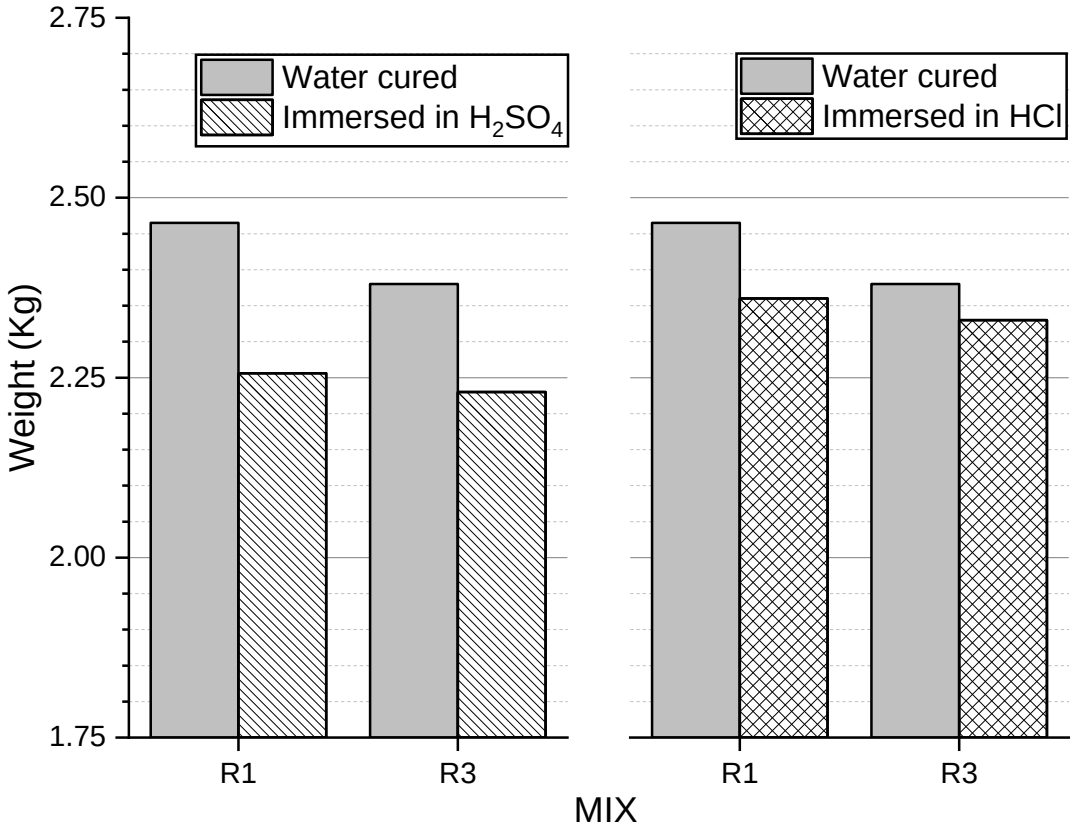

Fig. 4.20 Weight of conventional and RuC before and after immersion in acids

Table 4.14 Results of the weight of conventional and RuC before and after immersion in acids

Mix	Weight (Kg) Water cured	Weight (Kg) Immersed in H_2SO_4	Weight (Kg) Immersed in HCl
R1	2.46	2.25	2.36
R3	2.38	2.23	2.33

4.2.3 Compressive strength after exposure to acids

The compressive strength of the R1 and R3 mix before and after exposure to 5% H_2SO_4 and 5% HCl acids for 30 days are shown in Fig. 4.21 and Table 4.15. It is found that the R3 mix loses more compressive strength when immersed in H_2SO_4 than immersed in HCl acid. When the R1 and R3 mix is immersed in H_2SO_4, the compressive strength loss is 74.56% and 60.01%, but when immersed in HCl, the compressive strength loss is 30.34% and 24.22%, respectively. RuC reduces the loss in compressive strength by 14.55% and

6.12% when exposed to H_2SO_4 and HCl compared to conventional concrete. The RC slow acid penetration in concrete because tires rubber does not decompose by 5% acid solution and delays concrete samples' failure. In addition, RC, which is acid-resistant, provides a more durable type of aggregate than natural FA, resulting in better performance than conventional concrete [133].

Furthermore, the inclusion of PPC increases the amount of hydration products, which slows the disintegration of cement paste, resulting in superior concrete mix performance. Many researchers found similar outcomes by utilizing different kinds of supplementary pozzolanic materials in the concrete mixtures exposed to acid attack [33, 133, 136, 138, 139]. The spacing between RC and binder in RuC, as well as the porosity caused by RC particles, allowed H_2SO_4 and HCl ions to permeate the concrete, increasing $Ca(OH)_2$ and C-S-H dissolution. The pozzolanic reaction results in a denser and less porous cement matrix, which inhibits acid ions from penetrating the interior portion of RuC, resulting in lesser compressive strength loss of RuC integrating PPC.

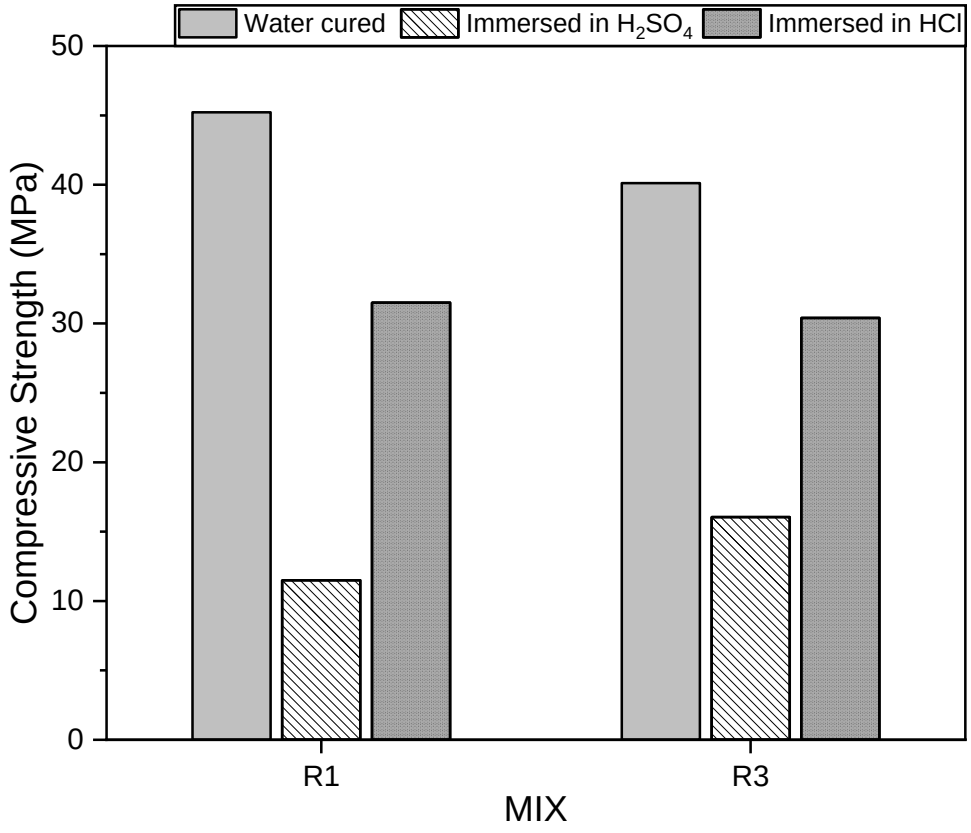

Fig. 4.21 Compressive strength of conventional and RuC before and after immersion in acids

Table 4.15 Results of compressive strength of conventional and RuC before and after immersion in acids

Mix	Compressive Strength (MPa) Water cured	Compressive Strength (MPa) Immersed in H_2SO_4	Compressive Strength (MPa) Immersed in HCl
R1	45.22	11.5	31.5
R3	40.12	16.048	30.4

4.2.4 XRD

The XRD analysis is carried out to determine the crystalline phases of RuC after immersion in HCl and H_2SO_4 solutions, and the results are compared to water-cured RuC. After being removed from the surface layer of RuC that exhibited the highest performance to chemical attacks, the specimens are crushed into powder. According to ASTM C1365-18 [81], the XRD analysis is done on concrete powder passing through 150µm and retained on the 45µm size sieve. The results of XRD are analyzed by the software X'Pert HighScore Plus.

XRD results include peaks angle, miller indices, d spacing, chemical formula, chemical name, crystal system, and JCPDS No. of R3 mix before and after submerging in H_2SO_4 and HCl solution are present in Table 4.16. Fig. 4.22 shows the pattern of the peaks of the R3 mix of RuC before and after immersion in acids for 30 days. When water cured R3 sample is analyzed, Quartz, C-S-H, and calcite peaks are found. C-S-H is the main product of the hydration of cement and is primarily responsible for strength, and its crystal structure is monoclinic. The majority of quartz peaks can be seen in the water-cured R3 sample, which has hexagonal crystal structures. It's important to note that the quartz peaks might be responsible for the existence of SiO_2 in sand particles rather than any of the hydration products [140].

The XRD result of RuC specimens after being immersed in an H_2SO_4 solution indicates Quartz, Calcite, and Gypsum peaks of varying intensities. The calcite and gypsum peaks found in RuC samples with a monoclinic crystal structure suggest a significant risk of degradation of RuC. The gypsum interacts with calcium aluminate and creates a compound calcium sulphoaluminate known as ettringite, which is responsible for the expansion, crack and loss of strength of RuC. Calcite reacts with H_2SO_4 and makes the chemical compound gypsum which transforms into ettringite and reduces the

performance of RuC. These are the reasons for reducing the compressive strength of RuC after exposure to acids. The majority of the quartz in this sample is also observed, and the crystal structure stays unchanged.

The XRD findings revealed Quartz, Calcite, Gypsum, and Calcium Chloride peaks in specimens after being submerged in HCl acid solution. The crystal structure of Calcium chloride is found to be cubic. Calcium chloride has a low-intensity peak due to its high-water solubility. Calcium chloride is responsible for the deterioration of RuC due to aggregate swelling. The calcium chloride in RuC stimulates the alkali-aggregate reaction and expend the inner materials of the RuC. The amount of calcium chloride in excess is responsible for the lower strengths of the concrete. The majority of the quartz in this sample is also observed, and the crystal structure stays unchanged.

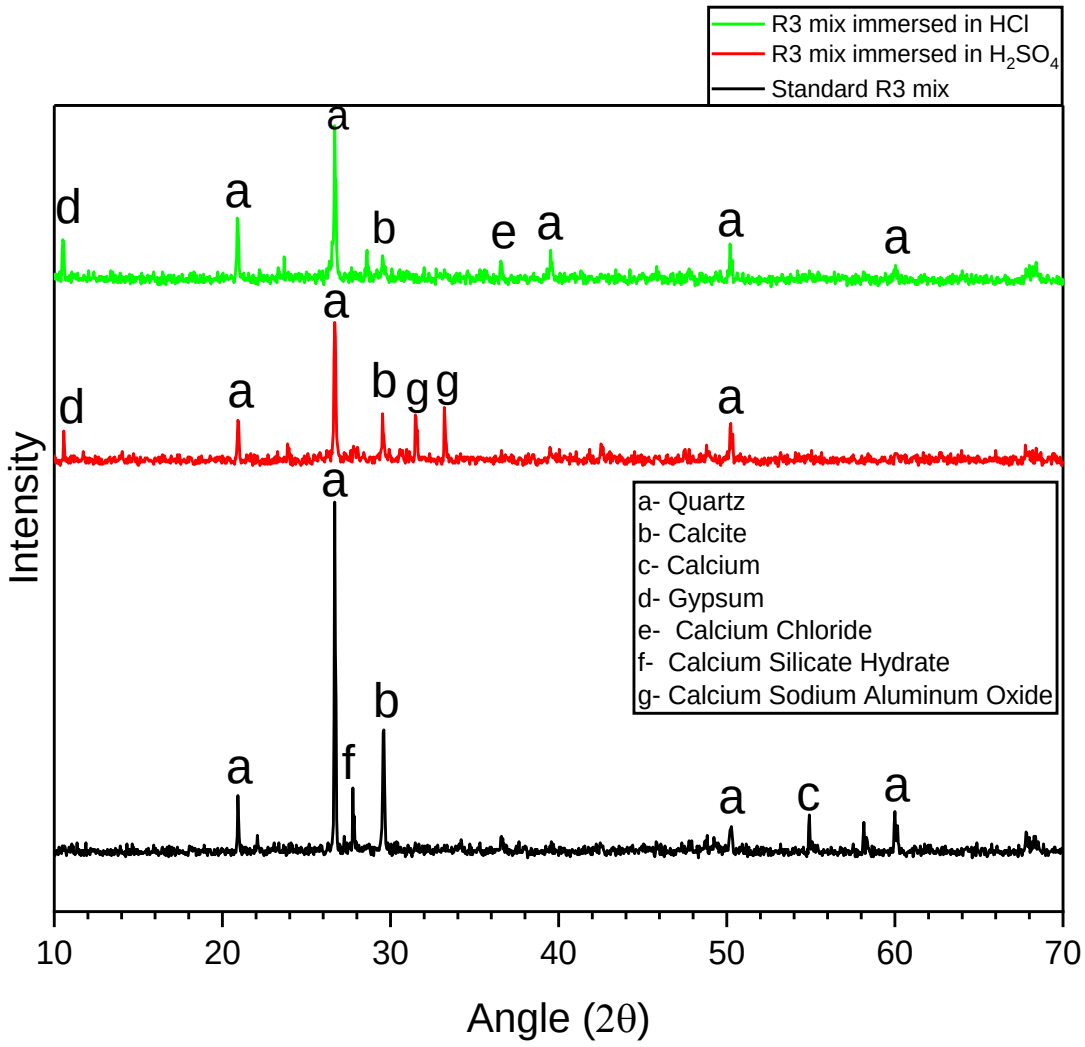

Fig. 4.22 XRD of R3 mix before and after immersion in acids

Table 4.16 XRD analysis of R3 mix before and after submerging in H2SO4 and HCl solution

S. no.	Mix	Peak No.	Peak Angle	h k l	d Spacing	Chemical Formula	Chemical Name	Crystal System	JCPDS No.
1	R3 MIX	1	20.965	1 0 0	4.2339	SiO_2	Quartz	Hexagonal	01-083-2466
		2	26.682	1 0 1	3.3382	SiO_2	Quartz	Hexagonal	01-083-2466
		3	27.507	2 0 2	3.2400	C-S-H	Calcium silicate hydrate	Monoclinic	00-023-0125
		4	29.567	2 0 0	3.0131	$CaCO_3$	Calcite	Monoclinic	01-070-0095
		5	50.222	1 1 2	1.8151	SiO_2	Quartz	Hexagonal	01-083-2466
		6	59.949	2 1 1	1.5418	SiO_2	Quartz	Hexagonal	01-083-2466
		7	59.949	2 1 1	1.5418	SiO_2	Quartz	Hexagonal	01-083-2466
2	R3 MIX after submerge in H_2SO_4 solution	1	10.560	0 2 0	7.5750	$Ca(SO_4)(H_2O)2$	Gypsum	Monoclinic	01-072-0596
		2	20.865	1 0 0	4.2539	SiO_2	Quartz	Hexagonal	01-078-1253
		3	26.651	0 1 1	3.3420	SiO_2	Quartz	Hexagonal	01-078-1253
		4	29.567	2 0 0	3.0131	$CaCO_3$	Calcite	Monoclinic	01-070-0095
		5	31.572	0 2 5	2.8314	$Ca_{8.68}Na_{0.62}(Al_6O_{18})$	Calcium sodium aluminum oxide	Cubic	01-083-1358
		6	33.210	4 0 0	2.6954	$Ca_{8.68}Na_{0.62}(Al_6O_{18})$	Calcium sodium aluminum oxide	Cubic	01-083-1358
		7	50.164	1 1 2	1.8171	SiO_2	Quartz	Hexagonal	01-078-1253
3	R3 MIX after submerge in HCL solution	1	10.560	0 2 0	7.5750	$Ca(SO_4)(H_2O)2$	Gypsum	Monoclinic	01-072-0596
		2	20.965	1 0 0	4.2339	SiO_2	Quartz	Hexagonal	00-033-1161
		3	26.682	1 0 1	3.3382	SiO_2	Quartz	Hexagonal	00-033-1161
		4	29.567	2 0 0	3.0131	$CaCO_3$	Calcite	Monoclinic	01-070-0095
		5	36.600	2 1 1	2.4510	$CaCl_2$	Calcium chloride	Cubic	00-049-1092
		6	39.592	0 1 2	2.2763	SiO_2	Quartz	Hexagonal	00-033-1161
		7	50.222	1 1 2	1.8151	SiO_2	Quartz	Hexagonal	00-033-1161
		8	59.949	2 1 1	1.5418	SiO_2	Quartz	Hexagonal	00-033-1161

4.3 Effects of freeze-thaw

4.3.1 Visual appearance

The visual appearance of the R3 mix concrete samples before and after freeze-thaw cycles is shown in Fig. 4.23. The visual appearance of the R3 mix concrete samples is checked after every 15 freeze-thaw cycles. It is found that the R3 mix exposed freeze-thaw cycles don't present visible microcracks on the surfaces of samples and any spalling of cement paste, RC, and aggregates. In addition, specimens don't show an uneven shape and porous surface structure. After freeze-thaw cycles, the R3 specimens of RuC do not show any reduced measures. The colour of the specimens is also the same as it was before.

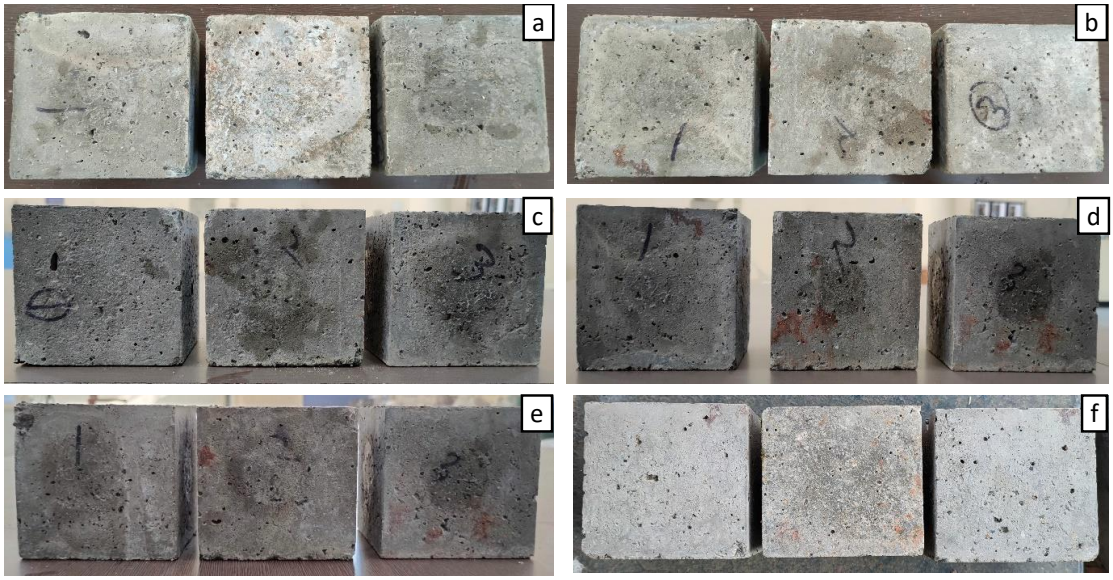

Fig. 4.23 (a) Visual appearance of the R3 mix concrete samples before freeze-thaw cycles (b) Visual appearance of the R3 mix concrete samples after 30 freeze-thaw cycles (c) after 45 freeze-thaw cycles (d) after 60 freeze-thaw cycles (e) after 75 freeze-thaw cycle

4.3.2 Weight difference

Weight differences between the conventional and RuC concerning the number of freeze-thaw cycles are shown in Fig. 4.24. During the freeze-thaw cycles, all R3 specimens of RuC don't experience much weight loss up to 90 cycles. The percentage weight loss is relatively small; however, the weight losses in R3 mix are 0.12%, 0.16%, 0.54%, 0.74%, 0.91% and 1.03% up to 90 cycles at intervals of 15 freeze-thaw cycles. However, the weight losses in conventional concrete are 0.16%, 0.24%, 0.64%, 0.85%, 1.05% and 1.33% up to 90 cycles at intervals of 15 freeze-thaw cycles. Compared to conventional concrete, the optimum mix of RuC reduces the weight loss by 0.3% at 90 freeze-thaw cycles. A similar pattern of results in the weight difference of RuC after freeze-thaw cycles has been found in past studies [20, 61]. During the freeze-thaw process, the R3 mix of RuC lost just a small amount of weight. "Water expands by roughly 9% as it freezes [61]." Pressure is created in the concrete pores when water in wet concrete freezes. The voids will expand and develop cracks if the stress produced exceeds the concrete's tensile strength due to freeze. The cumulative effect of multiple freeze-thaw processes and the disturbance of aggregates and cement paste can cause concrete to expand, crack, and disintegrate. Water is absorbed through pores and microcracks when the weight of RuC increases [141, 142]. This is the reason for the loss in the weight of

RuC. Weight loss is not a reliable indicator of concrete deterioration, according to previous research [143].

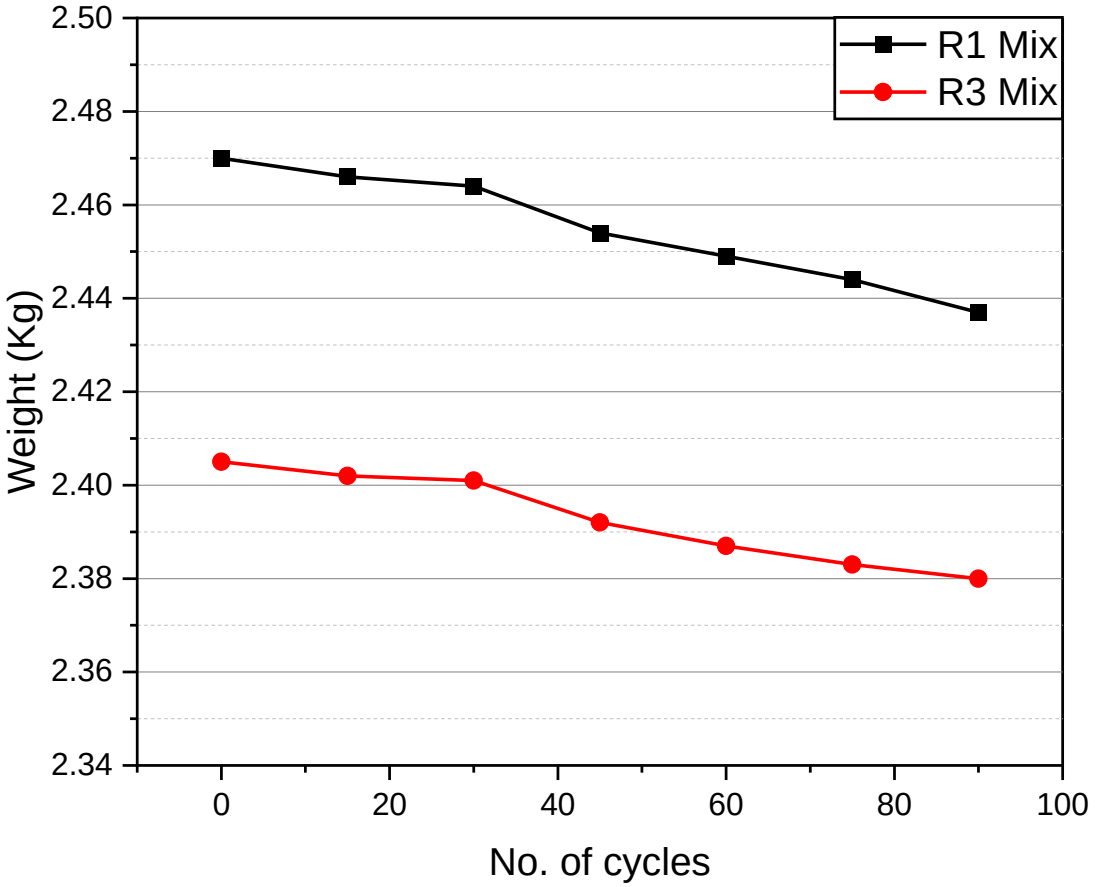

Fig. 4.24 Weight of conventional and RuC with respect to freeze-thaw cycles

Table 4.17 Results of the weight of conventional and RuC with respect to freeze-thaw cycles

Mix	Weight of specimen with respect to freeze-thaw cycles (Kg)						
	0 cycles	15 cycles	30 cycles	45 cycles	60 cycles	75 cycles	90 cycles
R1	2.47	2.46	2.46	2.45	2.44	2.44	2.43
R3	2.40	2.40	2.40	2.39	2.38	2.38	2.38

4.3.3 Compressive strength after exposure to freeze-thaw

The compressive strength of the conventional and optimum mix of RuC is illustrated in Fig. 4.25 at various stages of the test program. The compressive strength losses in R3 mix are 0.02%, 0.09%, 0.27%, 0.39%, 0.49%, 0.57% from 15 to 90 cycles at an interval

of 15 freeze-thaw cycles. However, the compressive strength losses in R1 mix are 0.08%, 0.15%, 0.33%, 0.46%, 0.66%, 0.88% from 15 to 90 cycles at an interval of 15 freeze-thaw cycles. The losses in compressive strength of conventional concrete are more compared to RuC. Compared to conventional concrete, the optimum mix of RuC reduces the compressive strength loss by 0.31% at 90 freeze-thaw cycles. The percentage loss in the compressive strength of RuC is low (0.57%) up to 90 freeze-thaw cycles. So this RuC can be used in the cold regions (North side of India). A similar pattern is found in the loss of compressive strength of RuC after freeze-thaw cycles in past studies [20, 37, 61]. The design strength is not compromised up to 45 freeze-thaw cycles. The compressive strength of the R3 mix is slightly lower after freeze-thaw cycles than the 28 days of water-cured R3 mix of RuC, which shows the impact of the freeze-thaw cycles. When comparing the performance of the RuC in previous studies [20, 61] with this study, there is a clear difference in the RuC's performance, and the reduction in strength is smaller. The results are clear enough to show the benefits of RC, and the performance of RuC can be described by lower-density concrete and greater freeze-thaw protection.

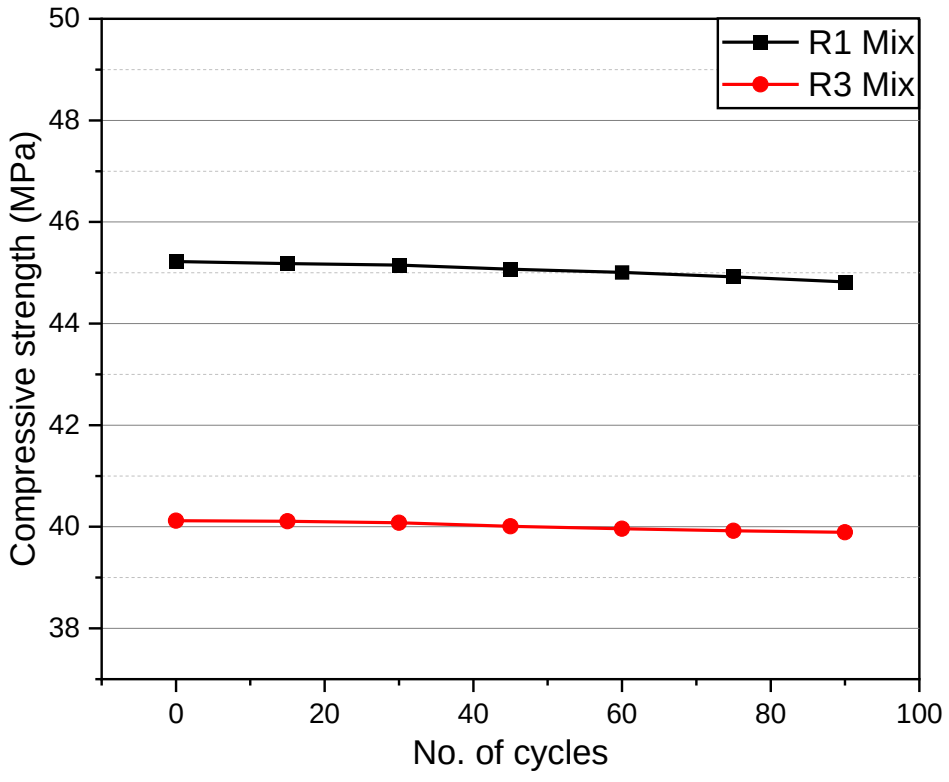

Fig. 4.25 Compressive strength of conventional and RuC with respect to freeze-thaw cycles

Table 4.18 Results of the compressive strength of conventional and RuC with respect to freeze-thaw cycles

Mix	*fc* of specimens with respect to freeze-thaw cycles (MPa)						
	0 cycles	15 cycles	30 cycles	45 cycles	60 cycles	75 cycles	90 cycles
R1	45.22	45.18	45.15	45.07	45.01	44.92	44.82
R3	40.12	40.11	40.08	40.01	39.96	39.92	39.89

4.3.4 UPV

According to IS 13311 Part – 1992 (Reaffirmed 2004) [109], the results of UPV testing are shown in Fig. 4.26, and data is noted at the end of every 15 freeze-thaw cycles shown in Table 4.19. The UPV of the R1 mix and R3 mix of RuC is tested using the 'MATEST' Ultrasonic pulse velocity tester on cube samples with two transducers. The UPV losses in R3 mix are 0.21%, 1.06%, 1.40%, 1.57%, 2.40%, and 2.77% from 15 to 90 cycles at an interval of 15 freeze-thaw cycles. However, the UPV losses in R1 mix are 0.22%, 1.10%, 1.54%, 2.20%, 2.86%, 3.09% from 15 to 90 cycles at an intervals of 15 freeze-thaw cycles. The losses in UPV of conventional concrete are more compared to RuC. Compared to conventional concrete, the optimum mix of RuC reduces the UPV loss by 0.32% at 90 freeze-thaw cycles. It is abundantly clear that the UPV consistently decreased after every 15 cycles. The UPV of RuC is less than conventional concrete due to replacing the FA with RC because rubber makes a void-like structure in concrete and increases the time of UPV. The UPV of RuC is reduced to a smaller amount up to 90 freeze-thaw cycles, and it is still considered to be of good concrete quality as per IS code [109]. So, the quality of RuC is not compromised by the 90 freeze-thaw cycles and remains stable. The UPV results are compared with the work in previous research and found similarities in the pattern [20, 61, 144].

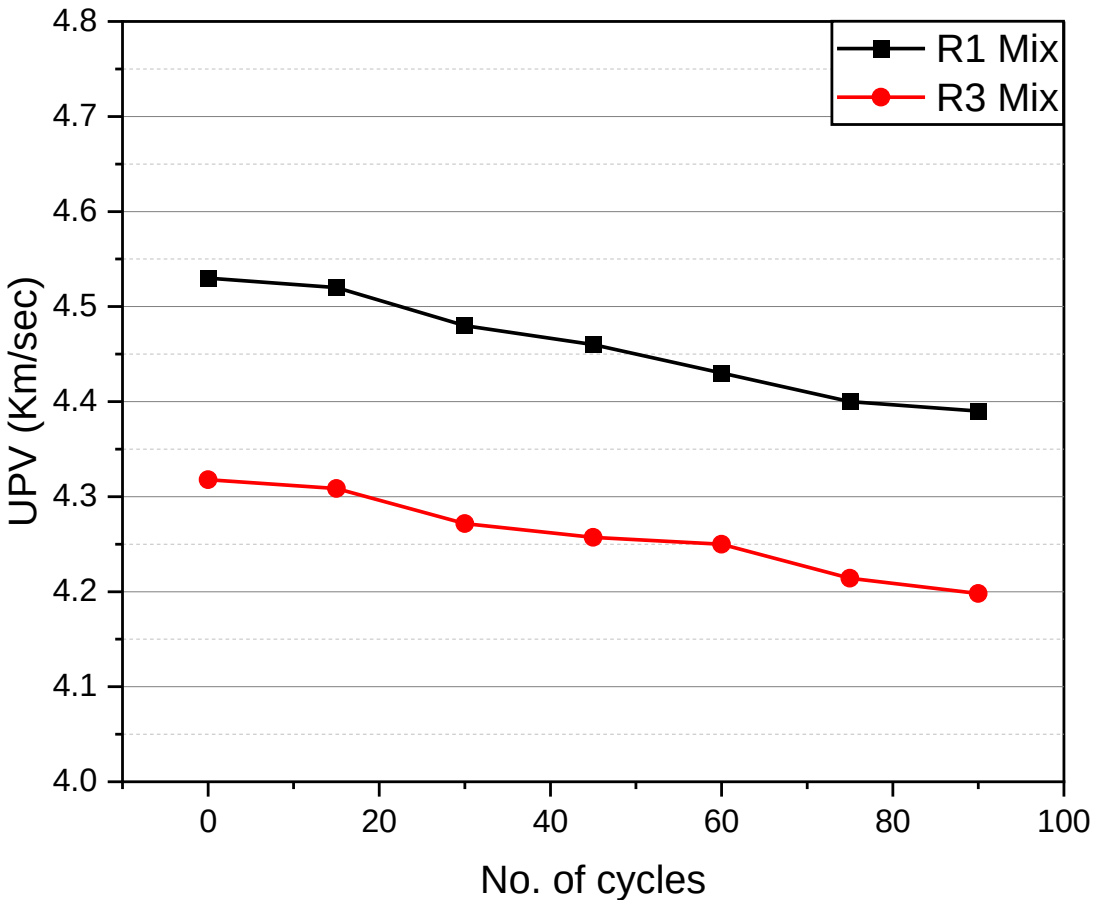

Fig. 4.26 UPV of conventional and RuC with respect to freeze-thaw cycles

Table 4.19 Results of the UPV of conventional and RuC with respect to freeze-thaw cycles

Mix	UPV of the specimen with respect to freeze-thaw cycles (Km/Sec)						
	0 cycles	15 cycles	30 cycles	45 cycles	60 cycles	75 cycles	90 cycles
R1	4.53	4.52	4.48	4.46	4.43	4.4	4.39
R3	4.31	4.30	4.27	4.25	4.24	4.21	4.19

CHAPTER 5 REGRESSION ANALYSIS

5.1 Correlation among the Mechanical Properties

After the experimental investigation, and with the help of regression analysis, four correlation equations have been established. One equation is established between the compressive strength of RuC and the replacement level of RC, and the other three correlation equations are established between the split tensile strength, flexural strength, static MOE, and compressive strength of RuC.

5.1.1 Correlation between replacement level of RC and compressive strength of RuC

After analyzing the results of RuC and comparing it with standard concrete, the compressive strength of RuC can be predicted by the following relationship, which is denoted by equation 1. It should be noted that this proposed equation is derived from the experimental analysis of RuC. The experimental data of the compressive strength of RuC at different replacement levels of RC at 28 days of water curing, shown in Table 5.1, are used to establish this correlation. A linear fitting curve can represent the best-fit curve for the plotted data points for this correlation. The origin software performs this curve fitting. In the correlation analysis, the R^2 is obtained by 0.932, which means this correlation can predict accurate results, approximately near the experimental results. The scattering in the data from the tests on the specimens influences the accuracy of this correlation. There is a linear correlation between the replacement level of the RC and the compressive strength of RuC. The relationship between the replacement level of the RC and the compressive strength of RuC is shown in Fig. 5.1. This relationship is only applicable for RC of size 0.6-2.36 mm and 0.38 w/c ratio. This relationship may be different for larger or smaller-sized particles of RC because, in past studies, the particle size of RC influences the compressive strength of RuC. This correlation should be used to care for different RC contents or different w/c ratios that fall outside this study.

$$f_{cr} = 52.65 - 1.16x \quad (5.1)$$

Where f_{cr} is the compressive strength of RuC and x is the percentage of replacement level of RC

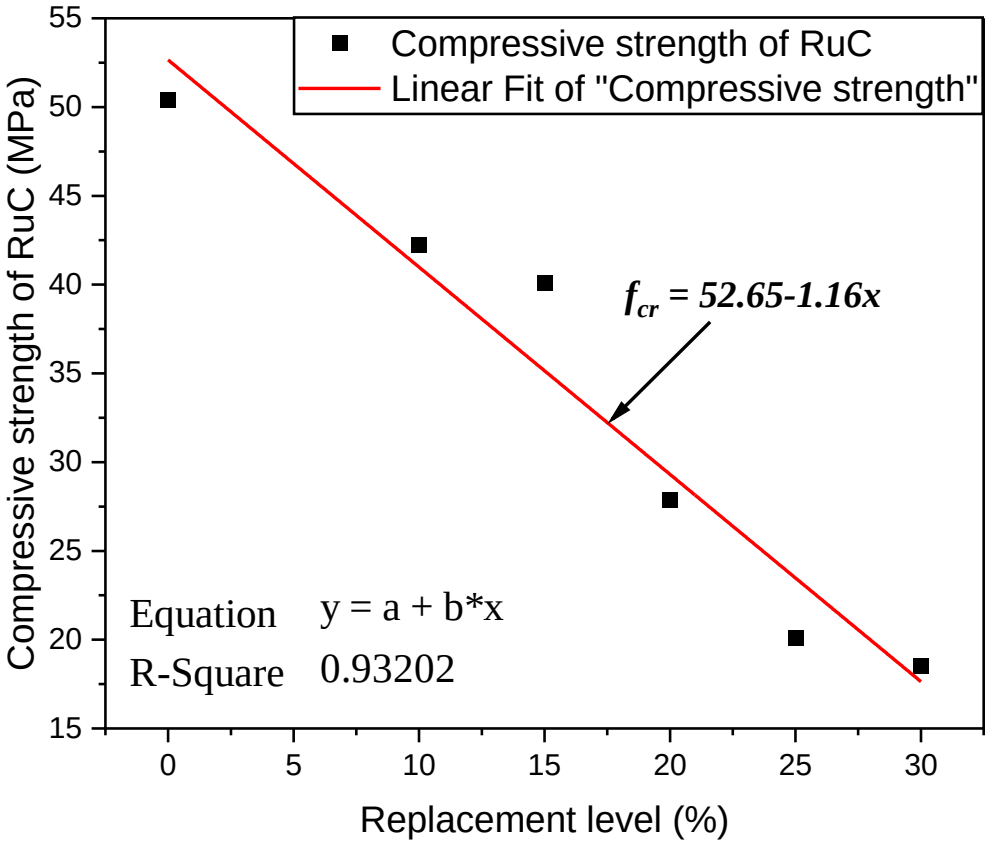

Fig. 5.1 Correlation between replacement level of RC and compressive strength of RuC

Table 5.1 Results of compressive strength and static MOE with respect to the replacement level of RC

Mix	RC (wt %)	Compressive strength (MPa)	Static MOE (GPa)
R1	0	50.38	29.48
R2	10	42.22	22.37
R3	15	40.12	20.53
R4	20	27.89	19.37
R5	25	20.08	12.68
R6	30	18.51	#

Specimen failure

5.1.2 Correlations between split tensile strength and compressive strength

Based on the experimental analysis, a correlation equation (5.2) between the splitting and compressive strength of RuC is proposed and compared with the other correlation equations provided by the code or other researchers. This correlation equation is

established by experimental data of the compressive and split tensile strength of RuC at the optimum replacement level of RC at 7, 14, 28, and 90 days of water curing. Many curves are applied to experimental data of strength; however, the best-fit curve for the plotted data points for this correlation is a non-linear fitting curve. The relationship between the split tensile strength and the compressive strength of RuC is shown in Fig. 5.2. The R^2 in the correlation analysis is 0.947, indicating that this correlation may accurately predict results that are close to those achieved experimentally.

This relationship is only applicable for RCs of size 0.6-2.36 mm and 0.38 w/c ratio. The proposed relationship between the split tensile and compressive strength of RuC is compared with other researchers and codes. The ACI committee gives Eq. (5.3) [145], a committee of euro code international gives Eq. (5.4) in 1990 [146], Eq. (5.5) offered by ACI standard 318-14 [147], Ahmed et al. proposed Eq. (5.6) in 2014 [148], and Ryu et al. presented Eq. (5.7) in 2013 [149]. The proposed equation and results are different because ACI 363R-92 is applicable for high-strength concrete (f_c < 83MPa), CEB-FIP uses standard concrete, ACI 318-14 is applicable for concrete strength f_c < 5000 Psi (34.47 MPa), Ahmed et al. use concrete with and without silica fume and compressive strength range (32.5<f_c < 98MPa) and Ryu et al. uses geopolymer concrete. In this study, RC has been used in concrete with pozzolanic cement so the results are different. No previous researcher has given relation equations on RuC, so it has been impossible to compare with previous literature. All of the correlations are approximately similar, indicating that splitting strength is approximately 12-13% of concrete's compressive strength.

The different equations are seen in Fig. 5.3 and are compared to the suggested equation of Empirical Correlation.

Proposed Equation: $\boldsymbol{f_{st} = 0.776\, f_c^{0.39}}$ **(5.2)**

ACI 363R-92: $\boldsymbol{f_{st} = 0.59 f_c^{0.5}}$ **(5.3)**

CEB-FIP: $\boldsymbol{f_{st} = 0.301 f_c^{0.67}}$ **(5.4)**

ACI 318-14: $\boldsymbol{f_{st} = 0.56\, f_c^{0.5}}$ **(5.5)**

Ahmed et al.: $\boldsymbol{f_{st} = 0.462\, f_c^{0.55}}$ **(5.6)**

Ryu et al.: $\boldsymbol{f_{st} = 0.17\, f_c^{0.75}}$ **(5.7)**

Where f_{st} is the split tensile strength of RuC and f_c is the compressive strength of RuC.

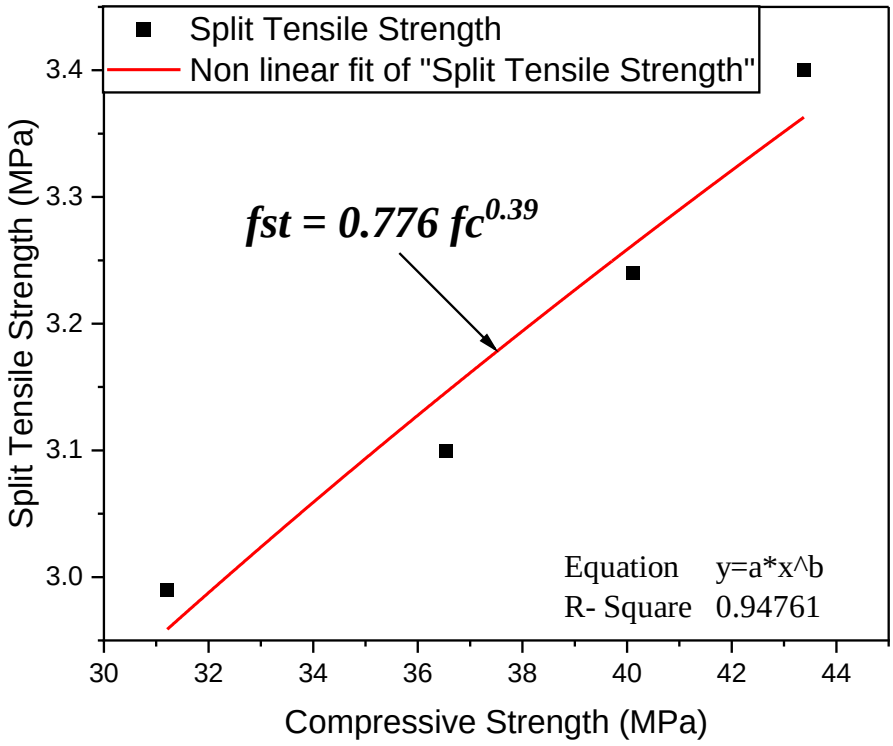

Fig. 5.2 Correlation between compressive strength and split tensile strength of RuC

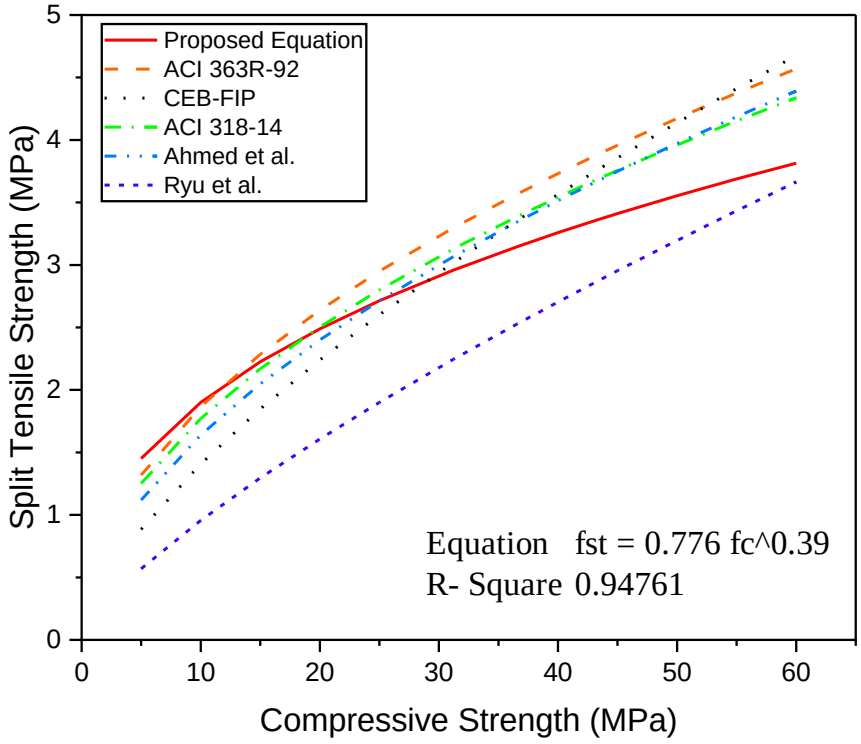

Fig. 5.3 Comparision of the proposed equation split tensile strength with other equations

Table 5.2 Correlation between compressive strength and splitting tensile strength

fc	Proposed Eq.	ACI 363R-92	CEB-FIP	ACI 318-99	Ahmad et al.	Ryu et al.
	fst = 0.776 fc^0.39	**fst =0.59fc^0.5**	**fst= .301(fc)^.67**	**fst= .56(fc)^.5**	**fst= .462(fc)^.55**	**fst = 0.17 fc^0.75**
5	1.45145	1.31928	0.88486	1.2522	1.11963	0.56843
10	1.90053	1.86574	1.40788	1.77088	1.63924	0.95598
15	2.22513	2.28506	1.84734	2.16887	2.04877	1.29574
20	2.48854	2.63856	2.24004	2.5044	2.39998	1.60776
25	2.71414	2.95	2.60128	2.8	2.71337	1.90066
31.21	2.95872	3.29609	3.01817	3.12849	3.06552	2.24476
36.54	3.14582	3.56645	3.35445	3.38511	3.34322	2.52654
40.12	3.26228	3.73708	3.57123	3.54706	3.51958	2.71
43.38	3.36291	3.88595	3.76314	3.68836	3.6741	2.87353
45	3.41121	3.95784	3.85673	3.75659	3.74894	2.95365
50	3.55388	4.17193	4.13882	3.9598	3.97261	3.19651
55	3.68808	4.37556	4.41174	4.15307	4.18641	3.43337
60	3.81502	4.57012	4.67657	4.33774	4.39162	3.6649

5.1.3 Correlations between flexural strength and compressive strength

Based on the experimental observations, the correlation equation (5.8) between the flexural and compressive strength of RuC's is suggested, and it is evaluated to the other correlations proposed by the codes and authors. This correlation equation is based on experimental data of the compressive and flexural strength of RuC at the optimum replacement level of RC at 7, 14, 28, and 90 days of water curing. Many curves are applied to experimental data of strength; however, the best-fit curve for the plotted data points for this correlation is a non-linear fitting curve. The relationship between the flexural strength and the compressive strength of RuC is shown in Fig. 5.4. The R^2 in the correlation analysis is 0.868, indicating that this correlation may accurately predict results that are close to those achieved experimentally. The scattering influences the accuracy of this correlation in the data from the specimen testing. This relationship is only applicable for RC of size 0.6-2.36 mm and 0.38 w/c ratio. Because the particle size of the RC influences the flexural and compressive strength of RuC in previous research, this correlation might be different for larger or smaller RC particles. The proposed relationship between the flexural and compressive strength of RuC is compared with other researchers and codes. ACI committee introduces Eq. (5.9) [145], ACI 318−14 introduce Eq. (5.10) [147], and Australian code AS 3600 for the reinforced concrete design presented the Eq. (5.11) [150] for correlation between the flexural strength and compressive strength of the concrete. The Indian code IS 456 – 2000 also introduced Eq. (5.12) [130], Ahmed et al. proposed Eq. (5.13) [148], and Bellum et al. proposed Eq. (5.14) [151] for correlation between the flexural strength and compressive strength of the concrete. The proposed equation and results are different because code ACI 363R-92 is applicable for high-strength concrete (f_c < 83MPa), code ACI 318-99 is applicable for concrete strength f_c < 5000 Psi (34.47 MPa), code AS 3600 uses compressive strength range 20 to 100 MPa, code IS 456 – 2000 uses plain concrete, M. Ahmed use concrete with and without silica fume and compressive strength range (32.5<f_c < 98MPa) and Bellum et al. uses geopolymer concrete. In this study, RC has been used in concrete with pozzolanic cement so the results are different. No previous researcher has given relation equations of flexural and compressive strength on RuC, so it has been impossible to compare with previous literature. All of the correlations are approximately similar except ACI 363R-92 and M. Ahmed.

The different equations are seen in Fig. 5.5 and are compared to the suggested Equation of Empirical Correlation.

Proposed Equation: $f_{fs} = 0.652\, f_c^{0.5}$ **(5.8)**

ACI 363R-92: $f_{fs} = 0.94 f_c^{0.5}$ **(5.9)**

ACI 318-99: $f_{fs} = 0.62\, f_c^{0.5}$ **(5.10)**

AS 3600: $f_{fs} = 0.6 f_c^{0.5}$ **(5.11)**

IS 456 - 2000: $f_{fs} = 0.7 f_c^{0.5}$ **(5.12)**

M. Ahmed: $f_{fs} = 1.055\, f_c^{0.5}$ **(5.13)**

Bellum et al.: $f_{fs} = 0.57\, f_c^{0.74}$ **(5.14)**

Where f_{fs} is the flexural strength of RuC and f_c is the compressive strength of RuC.

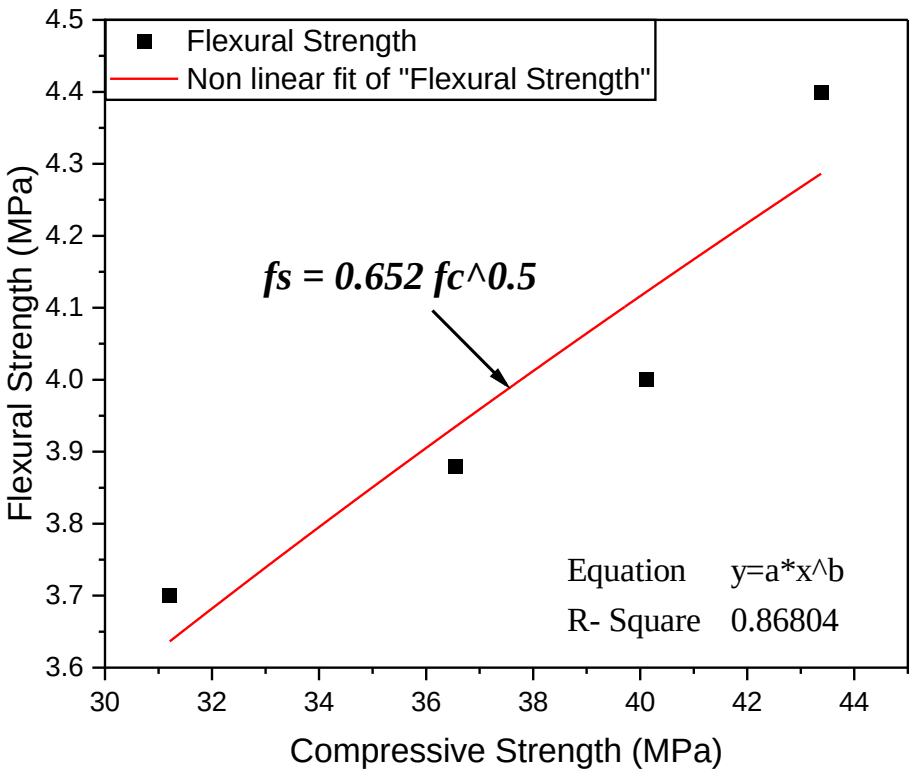

Fig. 5.4 Correlation between compressive strength and flexural strength of RuC

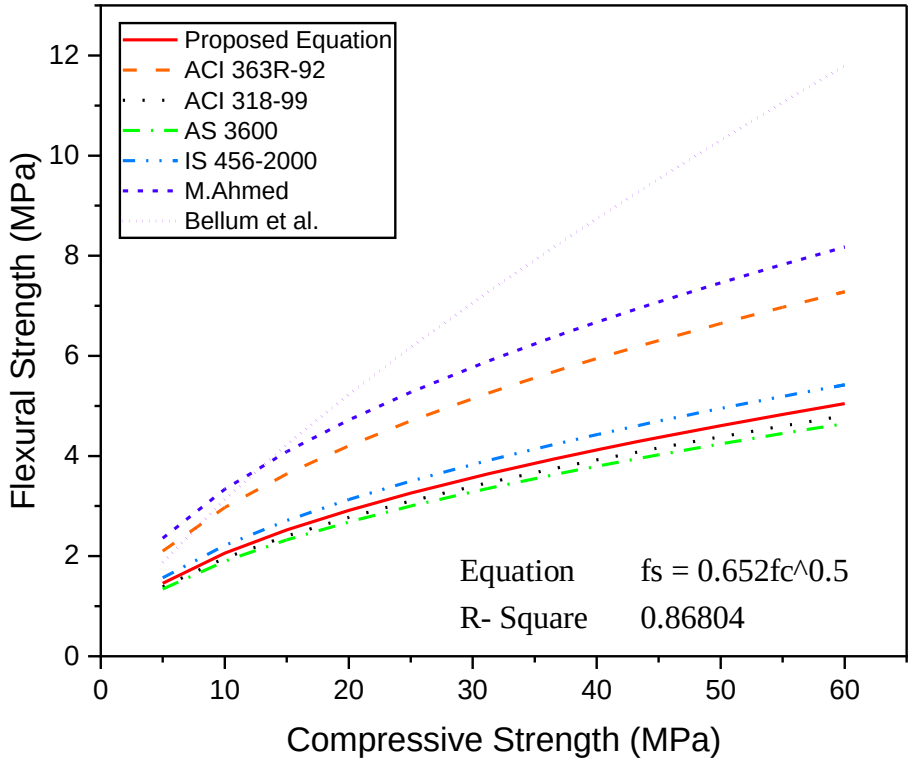

Fig. 5.5 Comparision of the proposed equation of flexural strength with other equations

Table 5.3 Correlation between compressive strength and flexural strength

fc	Proposed Eq.	ACI 363R-92	ACI 318-99	AS 3600	IS 456-2000	M.Ahmed	Bellum et al.
	fs = 0.652 fc^0.5	fs =0.94fc^0.5	fs =0.62 fc^0.5	fs = 0.6fc^0.5	fs = 0.7fc^0.5	fs = 1.055 fc^0.5	fs = 0.57 fc^0.74
5	1.45745	2.1019	1.38636	1.34164	1.56525	2.35905	1.87548
10	2.06086	2.97254	1.96061	1.89737	2.21359	3.3362	3.13238
15	2.52382	3.6406	2.40125	2.32379	2.71109	4.086	4.22846
20	2.91409	4.20381	2.77272	2.68328	3.1305	4.7181	5.23163
25	3.2579	4.7	3.1	3	3.5	5.275	6.17093
31.21	3.63995	5.2514	3.46369	3.35195	3.91061	5.89385	7.27197
36.54	3.9384	5.68214	3.7478	3.6269	4.23138	6.3773	8.17191
40.12	4.12674	5.95399	3.9271	3.80042	4.43382	6.68241	8.75713
43.38	4.29106	6.19117	4.08354	3.95181	4.61044	6.9486	9.27832
45	4.37042	6.30571	4.15909	4.02492	4.69574	7.07716	9.53349
50	4.60673	6.6468	4.38406	4.24264	4.94975	7.45998	10.30653
55	4.83149	6.97123	4.59804	4.44972	5.19134	7.82409	11.0597
60	5.04624	7.28121	4.8025	4.64758	5.42218	8.17199	11.79524

5.1.4 Correlation between compressive strength of RuC and static MOE of RuC

After analyzing the results of RuC, the static MOE of RuC can be predicted by the following proposed relationship, which is denoted by equation 5.15. This proposed equation is based on experimental data. The relationship between the replacement level of the RC and the compressive strength of RuC is shown in Fig. 5.6. The experimental data of the compressive strength and static MOE of RuC of all mixes at 28 days of water curing shown in Table 5.1 is used to establish this correlation. Many curves are applied to this data, but a non-linear fitting curve can represent the best-fit curve for the plotted data points for this correlation. In the correlation analysis, the R^2 is obtained by 0.882, which means this correlation can predict accurate results, approximately near the experimental results. The scattering in the data from the tests on the specimens influences the accuracy of this correlation. This relationship is only applicable for RC of size 0.6-2.36 mm and 0.38 w/c ratio. This relationship may be different for larger or smaller size particles of RC because, in past studies, the particle size of RC influences the compressive strength and static MOE of RuC. The relationship between the compressive strength of RuC and the static MOE of RuC is shown in Fig. 5.7 and compared with other researchers and codes. The results are being compared by some more relationships given by IS 456-2000 [130] in equation 5.16, ACI 318-05 for structural calculation, applicable to normal weight concrete [152] in equation 5.17, Mensur et al. [153] in equation 5.18, Akhtaruzzaman and hasnat [154] in equation 5.19, Rashid et al. [155] in equation 5.20, and Milicević et al. [156] in equation 5.21. The proposed equation and results are different because code IS 456 – 2000 uses plain concrete, code ACI 318-05 gives a relationship for normal weight concrete (density 1500-2500 Kg/m^3), Mensur et al. use concrete with brick aggregate, Akhtaruzzaman and hasnat use crushed brick as aggregate, Rashid et al. also use crushed brick as aggregate and Milicević et al. use crushed brick and roof tiles as aggregate. But in this study, RC is used as a partial replacement of fine aggregates (crushed stones), that's why the relationship is different from other researchers and codes. No previous researcher has given relation equations of static MOE and compressive strength on RuC, so it has been impossible to compare with previous literature. All of the correlations are approximately similar.

These all equations are based on experimental data, which is given below.

Proposed equation $\mathbf{E_c = 1.161 f_c^{0.807}}$ **(GPa)** **(5.15)**

IS 456-2000 $\mathbf{E_c = 5000 f_c^{0.5}}$ **(MPa)** **(5.16)**

ACI 318-05 $\mathbf{E_c = 4.70 f_c^{0.5}}$ **(GPa)** **(5.17)**

Mensur et al. $\mathbf{E_c = 4050 f_c^{0.5}}$ **(MPa)** **(5.18)**

Akhtaruzzaman and hasnat $\mathbf{E_c = 40000 f_c^{0.5}}$ **(Psi)** **(5.19)**

Rashid et al. $\mathbf{E_c = 5324 f_c^{0.5} - 1218}$ **(MPa)** **(5.20)**

Milicević et al. $\mathbf{E_c = 4735.7 f_c^{0.4255}}$ **(MPa)** **(5.21)**

Where $\boldsymbol{f_c}$ is the compressive strength of concrete.

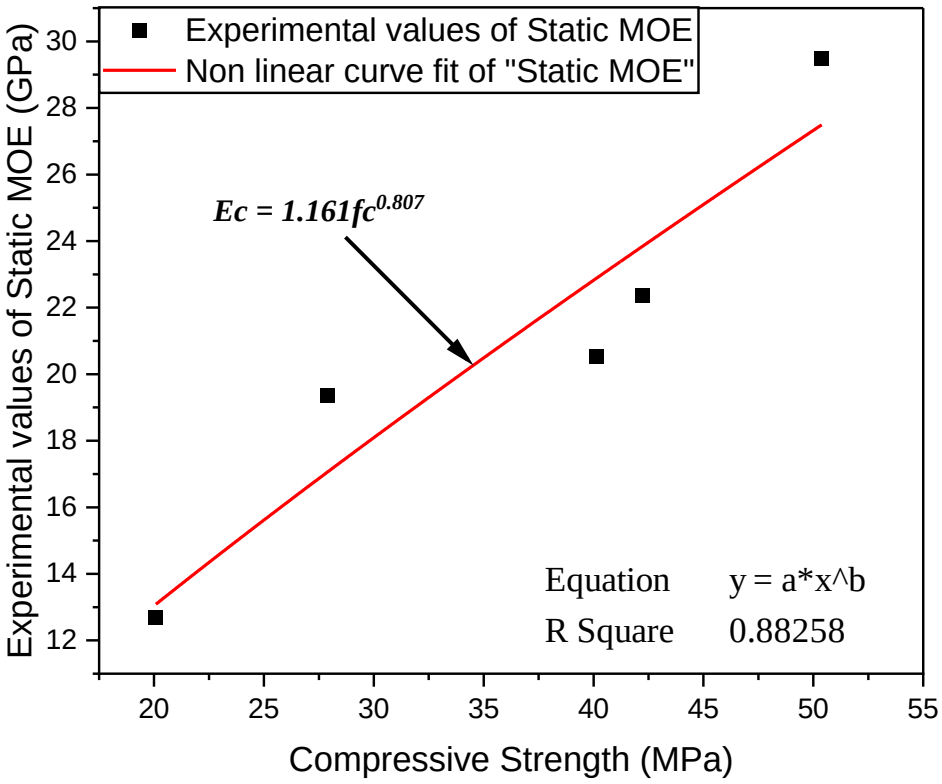

Fig. 5.6 Correlation Eq. generation between MOE and compressive strength

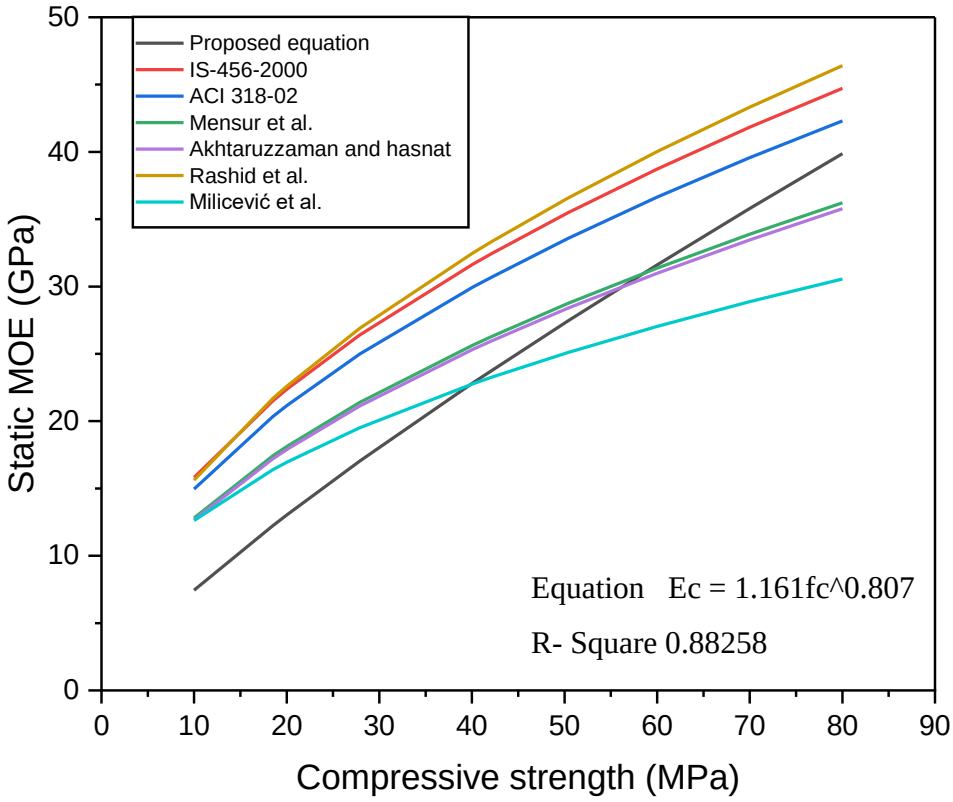

Fig. 5.7 Correlation between MOE and compressive strength comparison graph

Table 5.4 Correlation between compressive strength and Static MOE

fc	Proposed Eq.	IS-456-2000	ACI 318-02	Mensur et al.	Akhtaruzzaman and hasnat	Rashid et al.	Milicević et al.
	Ec = 1.161fc^0.807 (GPa)	Ec = 5000fc^0.5 (MPa)	Ec = 4.70fc^0.5 (GPa)	Ec = 4050fc^0.5 (MPa)	Ec = 40000fc^0.5 (PSi)	Ec = 5324fc^0.5 (MPa)	Ec = 4735.7fc^0.4255 (MPa)
80	39.86813	44.72136	42.30641	36.2243	35.77709	46.4013	30.55969
70	35.79533	41.833	39.57402	33.88473	33.4664	43.32578	28.87177
60	31.60824	38.72983	36.63842	31.37117	30.98387	40.02153	27.03881
50.38	27.45077	35.48944	33.57301	28.74644	28.39155	36.57115	25.10123
42.22	23.80266	32.48846	30.73408	26.31565	25.99077	33.37571	23.28317
40.12	22.84254	31.67018	29.95999	25.65284	25.33614	32.5044	22.78318
27.89	17.03371	26.40549	24.9796	21.38845	21.12439	26.89857	19.51743
20.085	13.06922	22.40815	21.19811	18.1506	17.92652	22.64219	16.9729
18.51	12.23571	21.51162	20.35	17.42442	17.2093	21.68758	16.39327
10	7.44444	15.81139	14.95757	12.80722	12.64911	15.61797	12.61491

CHAPTER 6 CONCLUSIONS

This experimental study is conducted in the concrete laboratory of the civil engineering department at Delhi Technological University, India. After the experimental investigation, the RuC and conventional concrete specimens are tested against various severe conditions for durability. The following conclusions found through this study are as follows:

1. The surface treatment of RC with 15% H_2SO_4 solution minimises the loss of RuC's strength and enhances the interfacial bonding between the RC and cement paste. RC as a partial replacement of FA can be up to 15% without significant compressive strength loss after surface treatment of RC by H_2SO_4 solution. However, if the RC replacement level is greater than 15%, the strength decrease will be high.
2. From the graph of stress vs strain of standard and RuC, the RuC has a satisfactory deformability capability, and it can be considered an optimistic advantage in RuC. This increased ductility and ability to withstand large deformations before failure is due to its low MOE of RuC. In certain applications, such as in earthquake-resistant construction, flexibility is an important property of concrete. At 15% RC replacement Poission ratio of concrete increased from 0.14 to 0.3. Due to the higher value of Poisson's ratio, the RuC has a higher deformable capacity. By incorporating RC in concrete the RuC can deform transversely under stress and can reduce the chance of cracking before failure and enhance the deformation capacity of RuC.
3. The impact resistance and the energy absorption capacity of the RuC improve when the RC is added to the concrete. These are the positive results of RuC, and it can absorb the impact energy by seismic activities. After getting these results, 15% replacement of coarse aggregate by rubber crumb is considered to be the optimum dosage in concrete.
4. When exposed to H_2SO_4, the RuC specimens showed moderate spalling, but they showed only minor spalling of cement paste, RC, and aggregates when exposed to HCl. It is discovered that with the same time of immersion and concentration of H_2SO_4 and HCl, the RuC experience less surface degradation, weight loss, and

compressive strength loss due to HCl. RC, which are acid-resistant, are more durable aggregates than natural FA, resulting in higher performance than conventional concrete.

5. There are no apparent microcracks on the surfaces of the samples exposed to freeze-thaw cycles and no spalling of cement paste, RC, or aggregates in the RuC mix. RuC specimens do not lose much weight throughout the freeze-thaw cycles up to 90 cycles. RuC has a slight percentage loss in compressive strength (0.57%) after 90 freeze-thaw cycles. RuC's design strength remains unaffected after 45 freeze-thaw cycles. After every 15 cycles, it is apparent that the UPV has dropped. RuC's UPV is lowered to a smaller amount throughout 90 freeze-thaw cycles, but it still has good concrete quality.
6. PPC improves the mechanical and durability properties of RuC because pozzolanic material reacts with $Ca(OH)_2$ in the presence of water, forming C-S-H gel and reducing capillary pores, which are beneficial to concrete. The pozzolanic reaction produces a less porous cement matrix, preventing acid ions from penetrating the inner section of RuC and reducing the compressive strength loss of RuC incorporating PPC. As a result, PPC is utilised in this work to make RuC resistant to acid attacks.
7. Four correlation equations are proposed to determine the compressive strength of RuC by the replacement level of RC, and split tensile strength, flexural strength, and MOE of RuC by the compressive strength of RuC, which are $\boldsymbol{f_{cr} = 52.65 - 1.16x}$ **(MPa),** $\boldsymbol{f_{st} = 0.776 f_c^{0.39}}$ **(MPa),** $\boldsymbol{f_{fs} = 0.652 f_c^{0.5}}$ **(MPa)**, and $\mathbf{E_c = 1.161 f_c^{0.807}}$ **(GPa)** respectively.

Future Scope

- To analyze the damping capacity and crack patterns of the reinforced rubberised concrete columns under dynamic load by shaking table.
- Rubber crumb bonding with cement or other concrete constituents is rubberised concrete's main issue. Some other advanced techniques should be developed to enhance the bonding property of rubber crumbs and cement.
- The present work identified many salient parameters that influence rubberised concrete's fresh and hardened properties. A large database should be built on the engineering properties of various mixtures using fly ash and GGBFS. Such a database may identify additional parameters and lead to familiarising the utilisation of this material in many applications.
- Further research should identify possible applications of rubberised concrete technology. This would lead to research areas that are specifically oriented toward applications. The rubberised concrete has the potential to go beyond making concrete; there could be possibilities in other areas of infrastructure needed by the community. So, the following work is needed in the future before application in the construction industry.
- To analyse the structural behaviour of the rubberised concrete with the steel reinforcement and bond properties.
- To analyse the flexural behaviour of reinforced rubberised concrete under-point loadings.
- To analyse the eccentric load behaviour on the reinforced rubberised concrete columns and crack patterns.
- Numerical analysis of reinforced rubberised concrete structural members using a variety of software.

References

1. Tread Carefully: Draft Notification Wants Tyre Companies to Take Charge of Waste, https://thewire.in/environment/environment-ministry-brings-out-draft-notification-on-how-to-deal-with-waste-tyres
2. Tackling the Global Tire Waste Problem with Pretred, https://www.azocleantech.com/article.aspx?ArticleID=1227
3. Global Tire Recycling Market Report - Edition 2020, https://www.goldsteinresearch.com/report/global-tire-recycling-industry-market-trends-analysis
4. Ismail, M.K., Sherir, M.A.A., Siad, H., Hassan, A.A.A., Lachemi, M.: Properties of self-consolidating engineered cementitious composite modified with rubber. J. Mater. Civ. Eng. 30, (2018). https://doi.org/10.1061/(ASCE) MT.1943-5533.0002219
5. Gupta, T., Chaudhary, S., Sharma, R.K.: Mechanical and durability properties of waste rubber fiber concrete with and without silica fume. J. Clean. Prod. 112, 702–711 (2016). https://doi.org/10.1016/j.jclepro.2015.07.081
6. Habib, A., Yildirim, U., Eren, O.: Seismic Behavior and Damping Efficiency of Reinforced Rubberized Concrete Jacketing. Arab. J. Sci. Eng. 46, 4825–4839 (2021). https://doi.org/10.1007/s13369-020-05191-1
7. Murali, G., Poka, L., Parthiban, K., Haridharan, M.K., Siva, A.: Impact Response of Novel Fibre-Reinforced Grouted Aggregate Rubberized Concrete. Arab. J. Sci. Eng. 44, 8451–8463 (2019). https://doi.org/10.1007/s13369-019-03819-5
8. Karunarathna, S., Linforth, S., Kashani, A., Liu, X., Ngo, T.: Effect of recycled rubber aggregate size on fracture and other mechanical properties of structural concrete. J. Clean. Prod. 314, (2021). https://doi.org/10.1016/j.jclepro.2021.128230
9. OH Waste, https://ohwaste.wordpress.com/about-2/
10. World’s Biggest Tire Graveyard in Sulabiya, Kuwait | Amusing Planet, https://www.amusingplanet.com/2015/01/worlds-biggest-tire-graveyard-in.html
11. Waste tire recycling rubber powder production line, https://www.recycle-plant.com/rubber-powder-production-line.html
12. Wang, R., He, X., Li, Y.: Evaluation of microcracks in the interfacial transition zone of recycled rubber concrete. Struct. Concr. 20, 1684–1694 (2019). https://doi.org/10.1002/suco.201900044
13. He, L., Cai, H., Huang, Y., Ma, Y., Van Den Bergh, W., Gaspar, L., Valentin, J., Vasiliev, Y.E., Kowalski, K.J., Zhang, J.: Research on the properties of rubber concrete containing surface-modified rubber powders. J. Build. Eng. 35, 101991 (2021). https://doi.org/10.1016/j.jobe.2020.101991
14. Kashani, A., Ngo, T.D., Hemachandra, P., Hajimohammadi, A.: Effects of surface treatments of recycled tyre crumb on cement-rubber bonding in concrete composite foam. Constr. Build. Mater. 171, 467–473 (2018).

https://doi.org/10.1016/j.conbuildmat.2018.03.163

15. Gupta, T., Chaudhary, S., Sharma, R.K.: Assessment of mechanical and durability properties of concrete containing waste rubber tire as fine aggregate. Constr. Build. Mater. 73, 562–574 (2014). https://doi.org/10.1016/j.conbuildmat.2014.09.102
16. He, L., Ma, Y., Liu, Q., Mu, Y.: Surface modification of crumb rubber and its influence on the mechanical properties of rubber-cement concrete. Constr. Build. Mater. 120, 403–407 (2016). https://doi.org/10.1016/j.conbuildmat.2016.05.025
17. Ganjian, E., Khorami, M., Maghsoudi, A.A.: Scrap-tyre-rubber replacement for aggregate and filler in concrete. Constr. Build. Mater. 23, 1828–1836 (2009). https://doi.org/10.1016/j.conbuildmat.2008.09.020
18. Tian, S., Zhang, T., Li, Y.: Research on modifier and modified process for rubber-particle used in rubberized concrete for road. Adv. Mater. Res. 243–249, 4125–4130 (2011). https://doi.org/10.4028/www.scientific.net/AMR.243-249.4125
19. Li, G., Stubblefield, M.A., Garrick, G., Eggers, J., Abadie, C., Huang, B.: Development of waste tire modified concrete. Cem. Concr. Res. 34, 2283–2289 (2004). https://doi.org/10.1016/j.cemconres.2004.04.013
20. Richardson, A.E., Coventry, K.A., Ward, G.: Freeze/thaw protection of concrete with optimum rubber crumb content. J. Clean. Prod. 23, 96–103 (2012). https://doi.org/10.1016/j.jclepro.2011.10.013
21. Tarry, S.R.: Effect of partial replacement of coarse aggregates in concrete by untreated and treated tyre rubber aggregates. Int. J. Adv. Sci. Res. 3, 65–69 (2018)
22. Najim, K.B., Hall, M.R.: Crumb rubber aggregate coatings/pre-treatments and their effects on interfacial bonding, air entrapment and fracture toughness in self-compacting rubberised concrete (SCRC). Mater. Struct. Constr. 46, 2029–2043 (2013). https://doi.org/10.1617/s11527-013-0034-4
23. Reda Taha, M.M., El-Dieb, A.S., Abd El-Wahab, M.A., Abdel-Hameed, M.E.: Mechanical, Fracture, and Microstructural Investigations of Rubber Concrete. J. Mater. Civ. Eng. 20, 640–649 (2008). https://doi.org/10.1061/(ASCE)0899-1561(2008)20:10(640)
24. Gupta, T., Sharma, R.K., Chaudhary, S.: Impact resistance of concrete containing waste rubber fiber and silica fume. Int. J. Impact Eng. 83, 76–87 (2015). https://doi.org/10.1016/j.ijimpeng.2015.05.002
25. Ozbay, E., Lachemi, M.: Compressive strength, abrasion resistance and energy absorption capacity of rubberized concretes with and without slag. Mater. Struct. 1297–1307 (2011). https://doi.org/10.1617/s11527-010-9701-x
26. Najim, K.B., Hall, M.R.: Mechanical and dynamic properties of self-compacting crumb rubber modified concrete. Constr. Build. Mater. 27, 521–530 (2012). https://doi.org/10.1016/j.conbuildmat.2011.07.013
27. Sukontasukkul, P., Chaikaew, C.: Properties of concrete pedestrian block mixed with crumb rubber. Constr. Build. Mater. 20, 450–457 (2006). https://doi.org/10.1016/j.conbuildmat.2005.01.040
28. Gupta, T., Siddique, S., Sharma, R.K., Chaudhary, S.: Effect of aggressive

environment on durability of concrete containing fibrous rubber shreds and silica fume. Struct. Concr. 22, 2611–2623 (2021). https://doi.org/10.1002/suco.202000043

29. Ayub, T., Khan, S.U., Mahmood, W.: Mechanical Properties of Self-Compacting Rubberised Concrete (SCRC) Containing Polyethylene Terephthalate (PET) Fibres. Iran. J. Sci. Technol. Trans. Civ. Eng. 46, 1073–1085 (2022). https://doi.org/10.1007/s40996-020-00568-6

30. Gupta, T., Siddique, S., Sharma, R.K., Chaudhary, S.: Investigating mechanical properties and durability of concrete containing recycled rubber ash and fibers. J. Mater. Cycles Waste Manag. 23, 1048–1057 (2021). https://doi.org/10.1007/s10163-021-01192-w

31. Khelaifa, H., Boudaoud, Z., Benouis, A.: Effect of adding rubber aggregates on the behaviour of compacted sand concrete. Innov. Infrastruct. Solut. 6, (2021). https://doi.org/10.1007/s41062-021-00513-0

32. Mohammed, B.S., Xian, L.W., Haruna, S., Liew, M.S., Abdulkadir, I., Zawawi, N.A.W.A.: Deformation Properties of Rubberized Engineered Cementitious Composites Using Response Surface Methodology. Iran. J. Sci. Technol. - Trans. Civ. Eng. 45, 729–740 (2021). https://doi.org/10.1007/s40996-020-00444-3

33. Islam, M.T., Islam, M., Siddika, A., Mamun, M.A. Al: Performance of rubberized concrete exposed to chloride solution and continuous wet–dry cycle. Innov. Infrastruct. Solut. 6, 67 (2021). https://doi.org/10.1007/s41062-020-00451-3

34. Amiri, M., Hatami, F., Golafshani, E.M.: Evaluating the synergic effect of waste rubber powder and recycled concrete aggregate on mechanical properties and durability of concrete. Case Stud. Constr. Mater. 15, (2021). https://doi.org/10.1016/j.cscm.2021.e00639

35. Wu, Y.F., Kazmi, S.M.S., Munir, M.J., Zhou, Y., Xing, F.: Effect of compression casting method on the compressive strength, elastic modulus and microstructure of rubber concrete. J. Clean. Prod. 264, 121746 (2020). https://doi.org/10.1016/j.jclepro.2020.121746

36. Nematzadeh, M., Karimi, A., Gholampour, A.: Pre- and post-heating behavior of concrete-filled steel tube stub columns containing steel fiber and tire rubber. Structures. 27, 2346–2364 (2020). https://doi.org/10.1016/j.istruc.2020.07.034

37. Luo, T., Zhang, C., Sun, C., Zheng, X., Ji, Y., Yuan, X.: Experimental Investigation on the Freeze–Thaw Resistance of Steel Fibers Reinforced Rubber Concrete. Materials (Basel). 13, 1260 (2020). https://doi.org/10.3390/ma13051260

38. Chaikaew, C., Sukontasukkul, P., Chaisakulkiet, U., Sata, V., Chindaprasirt, P.: Properties of Concrete Pedestrian Blocks Containing Crumb Rubber from Recycle Waste Tyres Reinforced with Steel Fibres. Case Stud. Constr. Mater. 11, e00304 (2019). https://doi.org/10.1016/j.cscm.2019.e00304

39. Gregori, A., Castoro, C., Marano, G.C., Greco, R.: Strength Reduction Factor of Concrete with Recycled Rubber Aggregates from Tires. J. Mater. Civ. Eng. 31, 04019146 (2019). https://doi.org/10.1061/(ASCE)MT.1943-5533.0002783

40. Fu, C., Ye, H., Wang, K., Zhu, K., He, C.: Evolution of mechanical properties of

steel fiber-reinforced rubberized concrete (FR-RC). Compos. Part B Eng. 160, 158–166 (2019). https://doi.org/10.1016/j.compositesb.2018.10.045

41. Aslani, F., Gedeon, R.: Experimental investigation into the properties of self-compacting rubberised concrete incorporating polypropylene and steel fibers. Struct. Concr. 20, 267–281 (2019). https://doi.org/10.1002/suco.201800182

42. Gurunandan, M., Phalgun, M., Raghavendra, T., Udayashankar, B.C.: Mechanical and damping properties of rubberized concrete containing polyester fibers. J. Mater. Civ. Eng. 31, 1–10 (2019). https://doi.org/10.1061/ (ASCE)MT.1943-5533.0002614

43. Zhu, H., Rong, B., Xie, R., Yang, Z.: Experimental investigation on the floating of rubber particles of crumb rubber concrete. Constr. Build. Mater. 164, 644–654 (2018). https://doi.org/10.1016/j.conbuildmat.2018.01.001

44. Fernández-Ruiz, M.A., Gil-Martín, L.M., Carbonell-Márquez, J.F., Hernández-Montes, E.: Epoxy resin and ground tyre rubber replacement for cement in concrete: Compressive behaviour and durability properties. Constr. Build. Mater. 173, 49–57 (2018). https://doi.org/10.1016/j.conbuildmat.2018.04.004

45. Pham, T.M., Zhang, X., Elchalakani, M., Karrech, A., Hao, H., Ryan, A.: Dynamic response of rubberized concrete columns with and without FRP confinement subjected to lateral impact. Constr. Build. Mater. 186, 207–218 (2018). https://doi.org/10.1016/j.conbuildmat.2018.07.146

46. Li, D., Zhuge, Y., Gravina, R., Mills, J.E.: Compressive stress strain behavior of crumb rubber concrete (CRC) and application in reinforced CRC slab. Constr. Build. Mater. 166, 745–759 (2018). https://doi.org/10.1016/j.conbuildmat.2018.01.142

47. Gerges, N.N., Issa, C.A., Fawaz, S.A.: Rubber concrete: Mechanical and dynamical properties. Case Stud. Constr. Mater. 9, (2018). https://doi.org/10.1016/j.cscm.2018.e00184

48. Raffoul, S., Garcia, R., Escolano-Margarit, D., Guadagnini, M., Hajirasouliha, I., Pilakoutas, K.: Behaviour of unconfined and FRP-confined rubberised concrete in axial compression. Constr. Build. Mater. 147, 388–397 (2017). https://doi.org/10.1016/j.conbuildmat.2017.04.175

49. Gupta, T., Tiwari, A., Siddique, S., Sharma, R.K., Chaudhary, S.: Response assessment under dynamic loading and microstructural investigations of rubberized concrete. J. Mater. Civ. Eng. 29, 1–15 (2017). https://doi.org/10.1061/(ASCE)MT.1943-5533.0001905

50. Duarte, A.P.C., Silva, B.A., Silvestre, N., de Brito, J., Júlio, E., Castro, J.M.: Tests and design of short steel tubes filled with rubberised concrete. Eng. Struct. 112, 274–286 (2016). https://doi.org/10.1016/j.engstruct.2016.01.018

51. Su, H., Yang, J., Ling, T.C., Ghataora, G.S., Dirar, S.: Properties of concrete prepared with waste tyre rubber particles of uniform and varying sizes. J. Clean. Prod. 91, 288–296 (2015). https://doi.org/10.1016/j.jclepro.2014.12.022

52. Youssf, O., ElGawady, M.A., Mills, J.E.: Experimental Investigation of Crumb Rubber Concrete Columns under Seismic Loading. Structures. 3, 13–27 (2015). https://doi.org/10.1016/j.istruc.2015.02.005

53. Jusli, E., Nor, H.M., Jaya, R.P., Zaiton, H.: Chemical Properties of Waste Tyre Rubber Granules. Adv. Mater. Res. 911, 77–81 (2014). https://doi.org/10.4028/www.scientific.net/AMR.911.77

54. Youssf, O., ElGawady, M.A., Mills, J.E., Ma, X.: An experimental investigation of crumb rubber concrete confined by fibre reinforced polymer tubes. Constr. Build. Mater. 53, 522–532 (2014). https://doi.org/10.1016/j.conbuildmat.2013.12.007

55. Xue, J., Shinozuka, M.: Rubberized concrete: A green structural material with enhanced energy-dissipation capability. Constr. Build. Mater. 42, 196–204 (2013). https://doi.org/10.1016/j.conbuildmat.2013.01.005

56. Ma, Q.W., Yue, J.C.: Effect on mechanical properties of rubberized concrete due to pretreatment of waste tire rubber with NaOH. Appl. Mech. Mater. 357–360, 897–904 (2013). https://doi.org/10.4028/www.scientific.net/AMM.357-360.897

57. Son, K.S., Hajirasouliha, I., Pilakoutas, K.: Strength and deformability of waste tyre rubber-filled reinforced concrete columns. Constr. Build. Mater. 25, 218–226 (2011). https://doi.org/10.1016/j.conbuildmat.2010.06.035

58. Uygunoğlu, T., Topçu, I.B.: The role of scrap rubber particles on the drying shrinkage and mechanical properties of self-consolidating mortars. Constr. Build. Mater. 24, 1141–1150 (2010). https://doi.org/10.1016/j.conbuildmat.2009.12.027

59. Yao, X., Zhang, M., Guan, J., Li, L., Bai, W., Liu, Z.: Research on the Corrosion Damage Mechanism of Concrete in Two Freeze–Thaw Environments. Adv. Civ. Eng. 2020, 1–11 (2020). https://doi.org/10.1155/2020/8839386

60. Xue, G., Pei, Z.: Experimental study on axial compressive properties of rubber concrete at low temperature. J. Mater. Civ. Eng. 30, 1–8 (2018). https://doi.org/10.1061/(ASCE)MT.1943-5533.0002178

61. Richardson, A., Coventry, K., Edmondson, V., Dias, E.: Crumb rubber used in concrete to provide freeze–thaw protection (optimal particle size). J. Clean. Prod. 112, 599–606 (2016). https://doi.org/10.1016/j.jclepro.2015.08.028

62. Zhu, X., Miao, C., Liu, J., Hong, J.: Influence of crumb rubber on frost resistance of concrete and effect mechanism. In: Procedia Engineering. pp. 206–213. Elsevier (2012)

63. Bisht, K., Ramana, P.V.: Waste to resource conversion of crumb rubber for production of sulphuric acid resistant concrete. Constr. Build. Mater. 194, 276–286 (2019). https://doi.org/10.1016/j.conbuildmat.2018.11.040

64. Aiello, M.A., Leuzzi, F.: Waste tyre rubberized concrete: Properties at fresh and hardened state. Waste Manag. 30, 1696–1704 (2010). https://doi.org/10.1016/j.wasman.2010.02.005

65. Muñoz-Sánchez, B., Arévalo-Caballero, M.J., Pacheco-Menor, M.C.: Influence of acetic acid and calcium hydroxide treatments of rubber waste on the properties of rubberized mortars. Mater. Struct. Constr. 50, (2017). https://doi.org/10.1617/s11527-016-0912-7

66. Khaloo, A.R., Dehestani, M., Rahmatabadi, P.: Mechanical properties of concrete containing a high volume of tire-rubber particles. Waste Manag. 28, 2472–2482

(2008). https://doi.org/10.1016/j.wasman.2008.01.015

67. Najim, K.B., Hall, M.R.: A review of the fresh/hardened properties and applications for plain- (PRC) and self-compacting rubberised concrete (SCRC), http://dx.doi.org/10.1016/j.conbuildmat.2010.04.056, (2010)

68. Thomas, B.S., Gupta, R.C.: A comprehensive review on the applications of waste tire rubber in cement concrete. Renew. Sustain. Energy Rev. 54, 1323–1333 (2016). https://doi.org/10.1016/j.rser.2015.10.092

69. Strukar, K., Kalman Šipoš, T., Miličević, I., Bušić, R.: Potential use of rubber as aggregate in structural reinforced concrete element – A review. Eng. Struct. 188, 452–468 (2019). https://doi.org/10.1016/j.engstruct.2019.03.031

70. Mutalib, N.A.N.A., Mokhatar, S.N., Budiea, A.M.A., Jaini, Z.M., Kamarudin, A.F., Noh, M.S.M.: A review: Study on waste rubber as construction material. IOP Conf. Ser. Mater. Sci. Eng. 1144, 012003 (2021). https://doi.org/10.1088/1757-899x/1144/1/012003

71. Lo Presti, D.: Recycled Tyre Rubber Modified Bitumens for road asphalt mixtures: A literature review, (2013)

72. Strukar, K., Kalman, T., Miličević, I., Bušić, R.: Potential use of rubber as aggregate in structural reinforced concrete element – A review. Eng. Struct. 188, 452–468 (2019). https://doi.org/10.1016/j.engstruct.2019.03.031

73. Li, Y., Zhang, X., Wang, R., Lei, Y.: Performance enhancement of rubberised concrete via surface modification of rubber : A review. Constr. Build. Mater. 227, 116691 (2019). https://doi.org/10.1016/j.conbuildmat.2019.116691

74. Bureau of Indian Standard: Determination of Initial and Final Setting Time. IS 4031 (Part 5). 4031, 3–6 (2002)

75. Bureau of Indian Standards: Methods of Physical Tests for Hydraulic Cement Methods of Physical Tests for Hydraulic Cement (Part 5). Bur. Indian Stand. 4031, 2–7 (2002)

76. Bureau of Indian Standard: Fineness by dry sieving. IS 4031 (Part I). 4031, (1996)

77. Bureau of Indian Standard: Determination of Soundness. IS 4031 (Part 3). 4031, 2–7 (2002)

78. Bureau of Indian Standard: Determination of Consistency of Standard Cement Paste. IS 4031 (Part 4). 4031, (1997)

79. Bureau of Indian Standard: Determination of False Set. IS 4031 (Part 14). 4931, (1999)

80. Bureau of Indian Standard: Specification for 43 grade Ordinary Portland Cement IS: 8112 – 1989. Bur. Indian Stand. Delhi. 17 (2013)

81. ASTM C1365-18: Standard Test Method for Determination of the Proportion of Phases in Portland Cement and Portland-Cement Clinker Using X-Ray Powder. ASTM Int. 1–11 (1998). https://doi.org/10.1520/C1365-18.2

82. Bureau of Indian Standards: Specification for Coarse and Fine Aggregates From Natural Sources for Concrete IS 383: 1970. IS 383 1970(Reaffirmed 2002). 1–24 (1970)

83. Bureau of Indian Standards (BIS): Method of Test for aggregate for concrete. IS 2386- Part III- 1963 (Reaffirmed 2002) Specific gravity, density, voids, absorption and bulking. Bur. Indian Stand. New Delhi. (1963)

84. Bureau of Indian Standard: Methods of test for aggregates for concrete IS : 2386 (Part IV) – 1963 (Reaffirmed 2002), Mechanical properties. Indian Stand.

85. Bureau of Indian Standard: Methods of test for aggregates for concrete IS-2386-Part II- 1963 (Reaffirmed 2011) Estimation of deleterious materials and organic impurities. Indian Stand. (2011)

86. Bureau of Indian Standards: Specification for Coarse and Fine Aggregates From Natural Sources for Concrete IS:383-1970. Indian Stand. 1–24 (1970)

87. Bureau of Indian Standard: Particle Size and Shape. Is 2386(Part I). 2386, (1997)

88. Bureau of Indian Standard: Specific Gravity, Density, Voids, Absorption and Bulking. IS 2386 (Part III). 2386, (1997)

89. Bureau of Indian Standard: Measuring mortar making properties of fine aggregate IS 2386 (Part VI). 2386, (1997)

90. Bureau of Indian Standard: Methods of Physical Tests for Hydraulic Cement, Part 3: Determination of Soundness IS 4031 - 3 (1988) (Reaffirmed 2005). (1988)

91. Bureau of Indian Standards (BIS): IS : 2386 (Part IV)-1963-Methods of test for Aggregates for Concrete, part 4 : Mechanical properties. Indian Stand. 1–37 (2002)

92. ASTM C117 − 17: Standard Test Method for Materials Finer than 75-µm (No . 200) Sieve in Mineral Aggregates by Washing. ASTM Int. 7–10 (2019). https://doi.org/10.1520/C0117-17.

93. ASTM C70 − 13: Standard Test Method for Surface Moisture in Fine Aggregate. ASTM Int. 1–3 (2019). https://doi.org/10.1520/C0070-13.2

94. ASTM C29/C29M − 17a: Standard Test Method for Bulk Density (“ Unit Weight ”) and Voids in Aggregate. ASTM Int. 1–5 (2019). https://doi.org/10.1520/C0029

95. ASTM C136/C136M − 14: Standard Test Method for Sieve Analysis of Fine and Coarse Aggregates. ASTM Int. 1–5 (2019). https://doi.org/10.1520/C0136

96. ASTM International: Standard Test Method for Relative Density (Specific Gravity) and Absorption of Coarse. C127 − 15. 1–5 (2019). https://doi.org/10.1520/C0127-15.2

97. M.S. Shetty: Concrete Technology: Theory and Practice. S.Chand, New Delhi (2013)

98. RANKEM (A AVANTOR BRAND): Sulphuric Acid, https://in.vwr.com/store/product/27465747/sulphuric-acid-98-00-ar-rankem, (1889)

99. Ma, Q.W., Yue, J.C.: Effect on Mechanical Properties of Rubberized Concrete due to Pretreatment of Waste Tire Rubber with NaOH. Appl. Mech. Mater. 357–360, 897–904 (2013). https://doi.org/10.4028/www.scientific.net/AMM.357-360.897

100. D934-13: Identification of Crystalline Compounds in Water-Formed Deposits by

X-Ray Diffraction. ASTM Int. 11, 1–10 (2014). https://doi.org/10.1520/D0934-13.2

101. ASTM E1131 − 08: Standard Test Method for Compositional Analysis by Thermogravimetry. ASTM Int. 08, 6 (2015). https://doi.org/10.1520/D6370-99R19.2
102. Bureau of Indian Standards: Indian Standard Guidelines for concrete mix design proportioning IS:10262- 2009. Bur. Indian Stand. New Delhi. New Delhi,India (2009)
103. Bureau of Indian Standard: General requirement for pan mixtures for concrete IS : 12119-1987. Bur. Indian Stand. New Delhi. (1999)
104. Bureau of Indian Standard: Methods of sampling and analysis of concrete IS: 1199 - 1959 Reaffirmed 2004. Bur. Indian Stand. Dehli. (2004)
105. Bureau of Indian Standards: Method of Tests for Strength of Concrete IS 516:1959 (Reaffirmed 2004). Bur. Indian Stand. New Delhi. New Delhi,India (2004)
106. Bureau of Indian Standards Delhi: Specification for moulds for use in tests of cement and concrete IS: 10086-1982 Reaffirmed 2008. Bur. Indian Stand. Delhi. (2008)
107. Bureau of Indian Standards: Method of non-destructive testing of concrete, IS 13311-(Part 2) 1992, Reaffirmed 2004, Rebound hammer. Bur. Indian Stand. New Delhi. (2004)
108. Bureau of Indian Standard: Non-destructive testing of concrete methods of test Part 1: Ultrasonic pulse velocity. IS 13311 (Part1) 1992. (1992)
109. Bureau of Indian Standards: Method of Non-destructive testing of concrete, IS 13311 Part 1 - 1992 Reaffirmed: 2004 Ultrasonic pulse velocity. Bur. Indian Stand. Dehli. 1–7 (2004)
110. D7234-19: ASTM D7234-19: Standard Test Method for Pull-off Adhesion Strength of Coatings on Concrete Using Portable Pull-Off Adhesion Testers. ASTM Int. (2019). https://doi.org/10.1520/D7234-19.2
111. Bureau of Indian Standard: Geological exploration by geophysical method (electrical resistivity) IS 15736:2007 (Reaffirmed-2012). Bur. Indian Stand. New Delhi. (2012)
112. ASTM C642: Standard Test Method for Density, Absorption, and Voids in Hardened Concrete, ASTM International, United States. Annu. B. ASTM Stand. 1–3 (1997). https://doi.org/10.1520/C0642-13.5.
113. ASTM C666/C666M: Standard Test Method for Resistance of Concrete to Rapid Freezing and Thawing. ASTM Int. 03, 1–6 (2003). https://doi.org/10.1520/C0666
114. Gupta, T., Sharma, R.K., Chaudhary, S.: Influence of waste tyre fibers on strength, abrasion resistance and carbonation of concrete. Sci. Iran. 22, 1481–1489 (2015)
115. Marie, I.: Thermal conductivity of hybrid recycled aggregate – Rubberized concrete. Constr. Build. Mater. 133, 516–524 (2017). https://doi.org/10.1016/j.conbuildmat.2016.12.113
116. Batayneh, M.K., Marie, I., Asi, I.: Promoting the use of crumb rubber concrete in

developing countries. Waste Manag. 28, 2171–2176 (2008). https://doi.org/10.1016/j.wasman.2007.09.035

117. Bheel, N., Memon, F.A., Meghwar, S.L.: Study of Fresh and Hardened Properties of Concrete Using Cement with Modified Blend of Millet Husk Ash as Secondary Cementitious Material. Silicon. 13, 4641–4652 (2021). https://doi.org/10.1007/s12633-020-00794-7

118. Liu, F., Zheng, W., Li, L., Feng, W., Ning, G.: Mechanical and fatigue performance of rubber concrete. Constr. Build. Mater. 47, 711–719 (2013). https://doi.org/10.1016/j.conbuildmat.2013.05.055

119. Su, H., Yang, J., Ling, T.C., Ghataora, G.S., Dirar, S.: Properties of concrete prepared with waste tyre rubber particles of uniform and varying sizes. J. Clean. Prod. 91, 288–296 (2015). https://doi.org/10.1016/j.jclepro.2014.12.022

120. Toutanji, H.A.: The use of rubber tire particles in concrete to replace mineral aggregates. Cem. Concr. Compos. 18, 135–139 (1996). https://doi.org/10.1016/0958-9465(95)00010-0

121. Al-Tayeb, M.M., Abu Bakar, B.H., Ismail, H., Md Akil, H.: Effect of partial replacement of sand by fine crumb rubber on impact load behavior of concrete beam: Experiment and nonlinear dynamic analysis. Mater. Struct. Constr. 46, 1299–1307 (2013). https://doi.org/10.1617/s11527-012-9974-3

122. Mohammed, B.S., Azmi, N.J.: Strength reduction factors for structural rubbercrete. Front. Struct. Civ. Eng. 8, 270–281 (2014). https://doi.org/10.1007/s11709-014-0265-7

123. Jingfu, K., Chuncui, H., Zhenli, Z.: Strength and shrinkage behaviors of roller-compacted concrete with rubber additives. Mater. Struct. Constr. 42, 1117–1124 (2009). https://doi.org/10.1617/s11527-008-9447-x

124. Najim, K.B., Hall, M.R.: Mechanical and dynamic properties of self-compacting crumb rubber modified concrete. Constr. Build. Mater. 27, 521–530 (2012). https://doi.org/10.1016/j.conbuildmat.2011.07.013

125. Flores-Medina, D., Flores Medina, N., Hernández-Olivares, F.: Static mechanical properties of waste rests of recycled rubber and high quality recycled rubber from crumbed tyres used as aggregate in dry consistency concretes. Mater. Struct. Constr. 47, 1185–1193 (2014). https://doi.org/10.1617/s11527-013-0121-6

126. Oikonomou, N., Mavridou, S.: Improvement of chloride ion penetration resistance in cement mortars modified with rubber from worn automobile tires. Cem. Concr. Compos. 31, 403–407 (2009). https://doi.org/10.1016/j.cemconcomp.2009.04.004

127. Mavroulidou, M.: Discarded tyre rubber as concrete aggregate: A possible outlet for used tyres. Glob. NEST J. 12, 359–367 (2010). https://doi.org/10.1109/ICCTET.2013.66759046

128. Mohammadi, I., Khabbaz, H., Vessalas, K.: Enhancing mechanical performance of rubberised concrete pavements with sodium hydroxide treatment. Mater. Struct. Constr. 49, 813–827 (2016). https://doi.org/10.1617/s11527-015-0540-7

129. Goulias, D.G., Ali, A.H.: Evaluation of Rubber-Filled Concrete and Correlation between Destructive and Nondestructive Testing Results. Cem. Concr.

Aggregates. 20, 140–144 (1998). https://doi.org/10.1520/cca10447j

130. Bureau of Indian Standards: Indian Standard Plain and Reinforced Concrete - Code of Practice, IS-456:2000. Bur. Indian Stand. New Delhi. New Delhi,India (2000)

131. Abdelmonem, A., El-Feky, M.S., Nasr, E.S.A.R., Kohail, M.: Performance of high strength concrete containing recycled rubber. Constr. Build. Mater. 227, 116660 (2019). https://doi.org/10.1016/j.conbuildmat.2019.08.041

132. ASTM C267-20: Standard Test Methods for Chemical Resistance of Mortars , Grouts , and Monolithic. ASTM. 04, 1–6 (2020). https://doi.org/10.1520/C0267-20.2

133. Sadaka, F., Campistron, I., Laguerre, A., Pilard, J.: Controlled chemical degradation of natural rubber using periodic acid : Application for recycling waste tyre rubber. Polym. Degrad. Stab. 97, 816–828 (2012). https://doi.org/10.1016/j.polymdegradstab.2012.01.019

134. Mwiti, M.J., Karanja, J., Muthengia, W.J.: Properties of activated blended cement containing high content of calcined clay. Heliyon. 4, 742 (2018). https://doi.org/10.1016/j.heliyon.2018

135. Marangu, J.M.: Effects of sulfuric acid attack on hydrated calcined clay–limestone cement mortars. J. Sustain. Cem. Mater. 0, 1–15 (2020). https://doi.org/10.1080/21650373.2020.1810168

136. Alnahhal, M.F., Alengaram, U.J., Jumaat, M.Z., Alsubari, B., Alqedra, M.A., Mo, K.H.: Effect of aggressive chemicals on durability and microstructure properties of concrete containing crushed new concrete aggregate and non-traditional supplementary cementitious materials. Constr. Build. Mater. 163, 482–495 (2018). https://doi.org/10.1016/j.conbuildmat.2017.12.106

137. Donatello, S., Palomo, A., Fernández-Jiménez, A.: Durability of very high volume fly ash cement pastes and mortars in aggressive solutions. Cem. Concr. Compos. 38, 12–20 (2013). https://doi.org/10.1016/j.cemconcomp.2013.03.001

138. Alsubari, B., Shafigh, P., Jumaat, M.Z.: Utilization of high-volume treated palm oil fuel ash to produce sustainable self-compacting concrete. J. Clean. Prod. 137, 982–996 (2016). https://doi.org/10.1016/j.jclepro.2016.07.133

139. Chatveera, B., Lertwattanaruk, P.: Evaluation of nitric and acetic acid resistance of cement mortars containing high-volume black rice husk ash. J. Environ. Manage. 133, 365–373 (2014). https://doi.org/10.1016/j.jenvman.2013.12.010

140. Ranjbar, N., Behnia, A., Alsubari, B., Moradi Birgani, P., Jumaat, M.Z.: Durability and mechanical properties of self-compacting concrete incorporating palm oil fuel ash. J. Clean. Prod. 112, 723–730 (2016). https://doi.org/10.1016/j.jclepro.2015.07.033

141. Wang, Z., Zeng, Q., Wang, L., Li, K., Xu, S., Yao, Y.: Characterizing frost damages of concrete with flatbed scanner. Constr. Build. Mater. 102, 872–883 (2016). https://doi.org/10.1016/j.conbuildmat.2015.11.029

142. Setzer, M.J.: Micro-ice-lens formation in porous solid. J. Colloid Interface Sci. 243, 193–201 (2001). https://doi.org/10.1006/jcis.2001.7828

143. Fu, Y., Cai, L., Yonggen, W.: Freeze-thaw cycle test and damage mechanics models of alkali-activated slag concrete. Constr. Build. Mater. 25, 3144–3148 (2011). https://doi.org/10.1016/j.conbuildmat.2010.12.006

144. Bumanis, G., Dembovska, L., Korjakins, A., Bajare, D.: Applicability of freeze-thaw resistance testing methods for high strength concrete at extreme −52.5 °C and standard −18 °C testing conditions. Case Stud. Constr. Mater. 8, 139–149 (2018). https://doi.org/10.1016/j.cscm.2018.01.003

145. ACI Committee 363: State-of-the-Art Report on High-Strength Concrete ACI363R-92 Reapproved 1997. Am. Concr. Inst. 92, 55 (1997)

146. CEB-FIB 1990: Design code for concrete structure. Euro-International Comm. 1 & 2, 105 (1990)

147. ACI 318-14: ACI 318-14 - Building Code Requirements for Structural Concrete. (2014)

148. Ahmed, M., El Hadi, K.M., Hasan, M.A., Mallick, J., Ahmed, A.: Evaluating the co-relationship between concrete flexural tensile strength and compressive strength. Int. J. Struct. Eng. 5, 115–131 (2014). https://doi.org/10.1504/IJSTRUCTE.2014.060902

149. Ryu, G.S., Lee, Y.B., Koh, K.T., Chung, Y.S.: The mechanical properties of fly ash-based geopolymer concrete with alkaline activators. Constr. Build. Mater. 47, 409–418 (2013). https://doi.org/10.1016/j.conbuildmat.2013.05.069

150. AS3600-2009: Reinforced Concrete Design : in accordance with AS 3600-2009. Cem. Concr. Aggregates Aust. Stand. Aust. (2011)

151. Bellum, R.R., Muniraj, K., Madduru, S.R.C.: Empirical relationships on mechanical properties of class-F fly ash and GGBS based geopolymer concrete. Ann. Chim. Sci. des Mater. 43, 189–197 (2019). https://doi.org/10.18280/acsm.430308

152. Neville, A.M., Brooks, J.J.: concrete technology. Pearson Education Limited, London (2013)

153. Mansur, M.A., Wee, T.H., Cheran, L.S.: Crushed bricks as coarse aggregate for concrete. ACI Mater. J. 96, 478–484 (1999). https://doi.org/10.14359/649

154. Akhtaruzzaman, A.A. and hasnat A.: Properties of concrete using crushed brick as aggregate. Concr. Int. 5, 58–63 (1983). https://doi.org/NA

155. Rashid, M.A., Salam, M.A., Kumar Shill, S., Hasan, M.K.: Effect of replacing natural coarse aggregate by brick aggregate on the properties of concrete. Dhaka Univ. Eng. Technol. Gazipur. 1, (2012). https://doi.org/NA

156. Miličević, I., Štirmer, N., Bjegović, D.: Relation between the compressive strength and modulus of elasticity of concrete with crushed brick and roof tile aggregates. Struct. Concr. 18, 366–375 (2017). https://doi.org/10.1002/suco.201500207